In presenting the dissertation as a partial fulfillment of the requirements for an advanced degree from the Georgia Institute of Technology, I agree that the Library of the Institute shall make it available for inspection and circulation in accordance with its regulations governing materials of this type. I agree that permission to copy from, or to publish from, this dissertation may be granted by the professor under whose direction it was written, or, in his absence, by the Dean of the Graduate Division when such copying or publication is solely for scholarly purposes and does not involve potential financial gain. It is understood that any copying from, or publication of, this dissertation which involves potential financial gain will not be allowed without written permission.

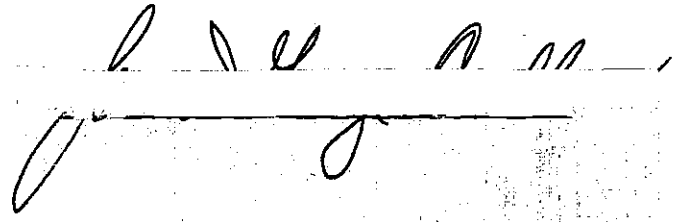

3/17/65
b

MODEL STUDIES IN THE ELASTIC BUCKLING OF BEAMS

A THESIS

Presented to

The Faculty of the Graduate Division

by

James George Carellas

In Partial Fulfillment

of the Requirements for the Degree

Master of Science in Civil Engineering

Georgia Institute of Technology

September, 1966

MODEL STUDIES IN THE ELASTIC

BUCKLING OF BEAMS

Approved:

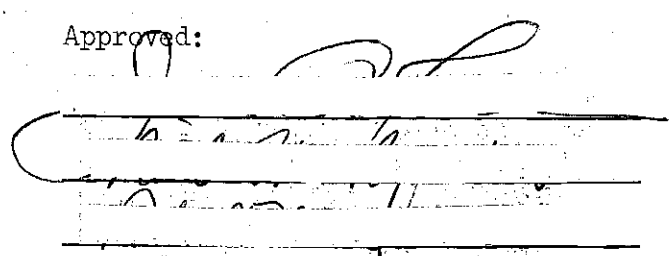

Date Approved by Chairman 2 JUNE 1967

ACKNOWLEDGMENTS

The writer is very grateful to Professor James R. Fincher for his inspiration in model studies and for his guidance and encouragement throughout this investigation.

Thanks are due Professor R. M. Dinnat and Dr. P. H. Sanders, members of the reading committee, for their assistance and recommendations.

I wish to thank Mr. C. M. Pavey and Mr. H. Bates of the Civil Engineering Department and Mr. J. Dameron of the Engineering Experiment Station for their generous assistance in fabricating the test equipment. Thanks are also due Mr. T. Mackrovitch of the School of Ceramic Engineering for assisting in the annealing of the model beams.

I would also like to thank Mr. G. Sanchez for his assistance in recording test results and Miss Pat Ward for typing the initial thesis drafts.

TABLE OF CONTENTS

LIST OF FIGURES

LIST OF FIGURES (Continued)

LIST OF FIGURES (Continued)

LIST OF FIGURES (Continued)

Page missing from thesis

LIST OF TABLES

LIST OF SYMBOLS

$A^{(*)}$ = cross sectional area of the restraint

A, B, C = constants which depend upon the distribution and point of application of the load as well as the location of restraints along the beam

E = Young's modulus of elasticity

G = shear modulus of elasticity

I_{xx} = moment of inertia about the x-x axis

I_{yy} = moment of inertia about the y-y axis

J = torsion constant

K_B = stiffness of intermediate lateral restraint in equation (3)

L = length of beam between end supports

P_{cr} = critical buckling load

a = (see Appendix A)

b = width of flange

c = critical stress factor

d = depth of web

e = eccentricity

f_{cr} = critical buckling stress

h = distance above or below the shear center at which the restraint is attached to the beam

k = stiffness of the intermediate lateral restraint in equation (1)

β = angle of twist

ζ_v = vertical centerline deflection (before apply end plate correction)

ζ_{vl} = end plate deflection, north end of beam

LIST OF SYMBOLS (Continued)

ζ_{V2} = end plate deflection, south end of beam

ζ_{HT} = lateral centerline deflection of top flange (phosphorus bronze models)

ζ_{HB} = lateral centerline deflection of bottom flange (phosphorus bronze models)

ζ_{H1} = lateral centerline deflection, top of aluminum beam

ζ_{H2} = lateral centerline deflection, bottom of aluminum beam

ϵ = unit strain

SUMMARY

Since 1955, many experiments have been performed in the field of lateral stability. Various conditions have been studied, such as the effect of end restraints on bisymmetrical and monosymmetrical wide flange sections, the effect of axial load, and the influence of the point of application of the load, however, an extensive review of numerous references on the topic of lateral stability has uncovered very little experimental work on the subject of intermediate elastic restraints.

The primary purpose of this thesis was to investigate the effects of elastic lateral restraints upon the buckling load of simply supported WF beams by a model analysis. Various magnitudes of restraint stiffnesses were to be employed so as to obtain a relationship between these stiffnesses and the rotational tendencies of the cross section. Phosphorus bronze was selected as the beam material for it was believed that the performance of this material in its annealed state was similar to that of structural steel. Each beam was simultaneously annealed and silver soldered within a steel form. A detailed explanation of this beam-making process is presented.

Due to an imperfection within the testing apparatus and/or beam, the results of the tests performed were quite erratic and no clear relationship could be developed between theoretical and experimental buckling loads. Thus, no definite conclusions could be drawn with regard to the effect of the elastic restraints. Several possible causes

ef these inconsistent results were investigated, and it was concluded that the anomalies were a result of eccentric loading and initial imperfections within the beam. Additional tests were performed on rectangular aluminum beams, the results of which reinforce the above conclusion. Twist curves plotted for every test appear to indicate the presence of the initial imperfections.

In addition to the twist curves, lateral deflection curves (for both the tension and compression flanges) and vertical deflection curves are presented for all tests. Detailed drawings of the components of the testing apparatus as well as photographs taken during certain tests are also presented.

CHAPTER I

INTRODUCTION

Prior to 1950, the majority of the investigations performed in the field of lateral stability of beams were of a theoretical nature (1,2,3,4,5,6).* In the past ten years, many experimental analyses have been performed to compliment these theoretical results (11, 12). Several variations in loading and end restraint conditions have been studied. However, it appears that only a few experiments have been concerned with the effects of intermediate elastic restraints upon the critical buckling load. Flint (7) investigated the case of a slender I beam model which was freely supported at the ends and both loaded and elastically restrained at midspan. Sergev and Moore (8) studied the effects of elastic lateral supports applied at midspan by using very small rectangular beam models. Schmidt (9) performed a computer analysis to determine the effect of the interaction between an elastic end torsional restraint and an elastic lateral restraint on the critical buckling load.

The primary objective of this thesis was to provide experimental verification with regard to both the feasibility of employing models in elastic buckling analyses and the influence of elastic lateral support upon the critical buckling load. A secondary purpose was to determine

---

* Numbers appearing in parenthesis refer to references which appear in the literature cited section of the Bibliography.

the practicability of using phosphorus bronze models to simulate the action of steel structures. Initially, the investigation was to determine the effect of elastic restraint employed at third point as well as centerline locations on the model beams. Concentrated loadings acting through the beam shear center were to be applied at third point and centerline positions. The stiffnesses of the intermediate lateral restraints were to have been varied so as to obtain a relationship between the rotational tendencies of the beam cross section and these restraint stiffnesses.

If the results of the preceding tests had been favorable, then an additional study would have been performed to examine the action of two simply supported WF beams which are interconnected by means of intermediate elastic restraints. No experimental analysis of the preceding subject was discovered in the literature reviewed.

Due to the peculiar nature of the results obtained from the phosphorus bronze tests, an investigation was performed to determine the primary cause of these anomalies. Several components of the testing apparatus were examined and the effect of initial curvature and eccentric loading were also considered.

In order to support conclusions drawn from the preceding investigation, a series of buckling tests was performed on rectangular aluminum models.

CHAPTER II

EQUIPMENT AND INSTRUMENTATION

The equipment and instrumentation used in this thesis consist of the following items, each of which will be discussed separately: 1) the model beam; 2) the model beam form; 3) the primary table; 4) the loading device; 5) the intermediate lateral restraints; 6) the intermediate lateral restraints connections; and 7) the measuring table and attachments.

The Model Beam

Phosphorus bronze was chosen as the model beam material because of its favorable chemical and physical properties (Table 4). In addition, it was believed that phosphorus bronze, in its annealed state, performed very much like steel. If this factor were true then phosphorus bronze would be an excellent material for use in constructing models to simulate steel structures.

For example, in the case of experiments involving the lateral buckling of beams, the critical buckling load for a model beam constructed of phosphorus bronze would be nearly half of the critical buckling load for a steel beam of the same cross-section. This is true because

$$E_{\text{Phosphorus bronze}} = 0.54E_{\text{steel}}$$

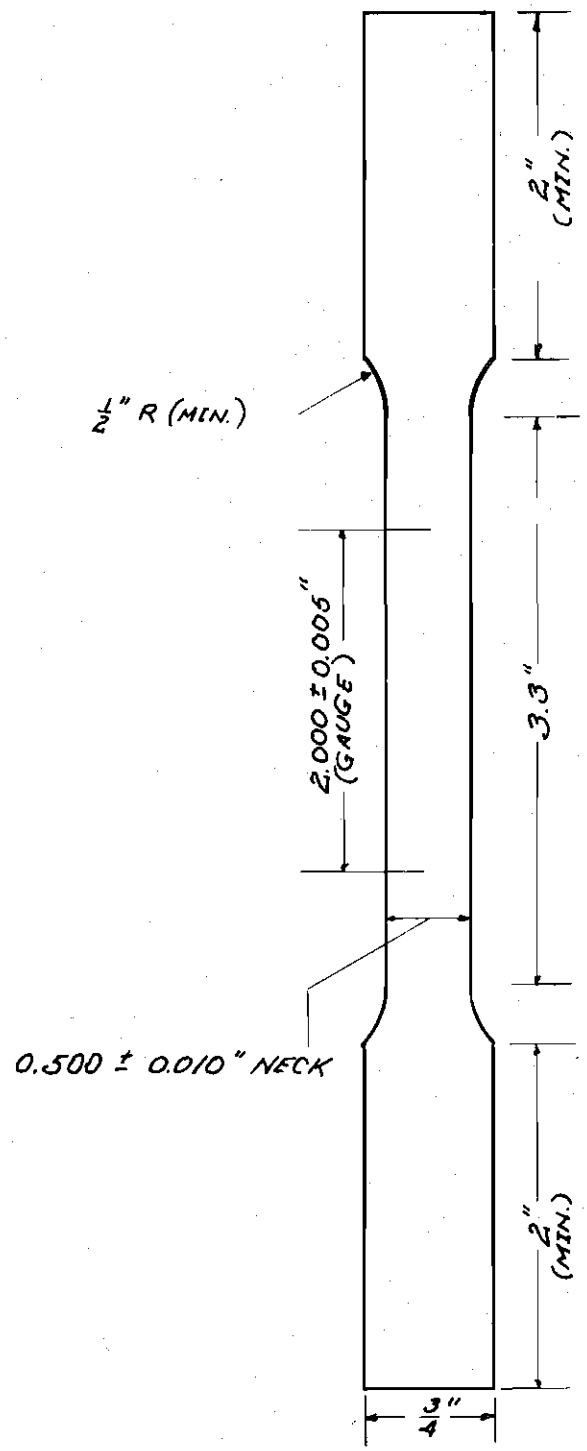

Figure 1. ASTM Standard Tensile Coupon

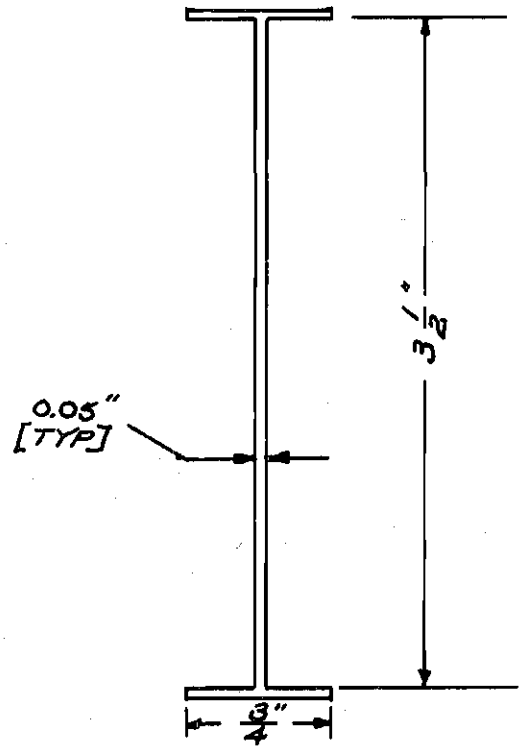

E	= 16,000,000 psi	b	= 0.75 in
G	= 6,000,000 psi	t_w	= 0.05 in
I_{xx}	= 0.409 in^4	t_f	= 0.05 in
I_{yy}	= 0.00352 in^4	d	= 3.5 in

Annealing Temperature 900°-1250°F

Figure 2. Cross Section and Properties of Phosphorus Bronze

In order to determine the effect of annealing on the tensile strength as well as the properties of phosphorus bronze, three ASTM standard tensile coupons were prepared (see Figure 1). The coupons were first annealed in the same manner employed for the model beam as described on page 7.

As a result of these three tests, the following information was obtained:

a) The yield strength of annealed phosphorus bronze was approximately 17 per cent of the original value.

b) Phosphorus bronze is quite ductile in its annealed state.

c) The stress strain curve for annealed phosphorus bronze is very similar to that of steel.

d) Anneal phosphorus bronze undergoes strain hardening. Verification of the above statements can be found in Table 4.

A deep beam was preferred since this type is more susceptible to lateral instability. Figure 2 illustrates the dimensions of the beam cross section.

For a simply supported beam with a concentrated load at midspan, a critical buckling stress of approximately 7,000 psi was sought. Primarily, the reason for selecting this magnitude of stress was to insure that the tests remained within the elastic range, based on the results of the tensile tests which were discussed earlier in Chapter II. The method used to obtain the above critical stress will be discussed in Chapter III beginning on page 20.

The Model Beam Form

After investigating the advantages and disadvantages of certain methods of making and annealing the model beams, it was decided to employ the form described herein. The beam form was machined from two bars of cold rolled steel, each having dimensions of 5/8" x 6' x 36".

Before the machining process, the two bars were annealed at 1125° F to remove residule stresses. The annealing process consisted of raising the temperature in the kiln at an average rate of 20° per minute up to 1125°F. The bars were held at this temperature for three hours to insure a complete "soaking," and then the temperature was lowered at an average rate of 4° per minute until 400°F was reached. At this time, the kiln was opened, thus allowing the bars to air cool from 400°F to room temperature.

The bars were then cut as shown in Figure 3. An additional picture of the beam form can be found in the Appendix on page 113.

The primary advantage of this apparatus is that it allows one to simultaneously anneal and form a model beam. Silver solder ribbon, 1/2" x 0.003", was used as the welding material.

Since the flow temperature of the silver solder ribbon was 1145° F, and the annealing temperature of phosphorus bronze between 900° and 1250°F, it was decided that 1250°F would be the soaking temperature for the first beam. After completion of the heating process, the beam was removed from the form and it was discovered that no bond existed for the first six inches from both ends of the beam. However, the middle 22 inches of the beam contained a uniform bond between the flanges and web.

In order to get a rough idea of the strength of the silver solder bond, this first beam was restrained at the ends and quarter-points and

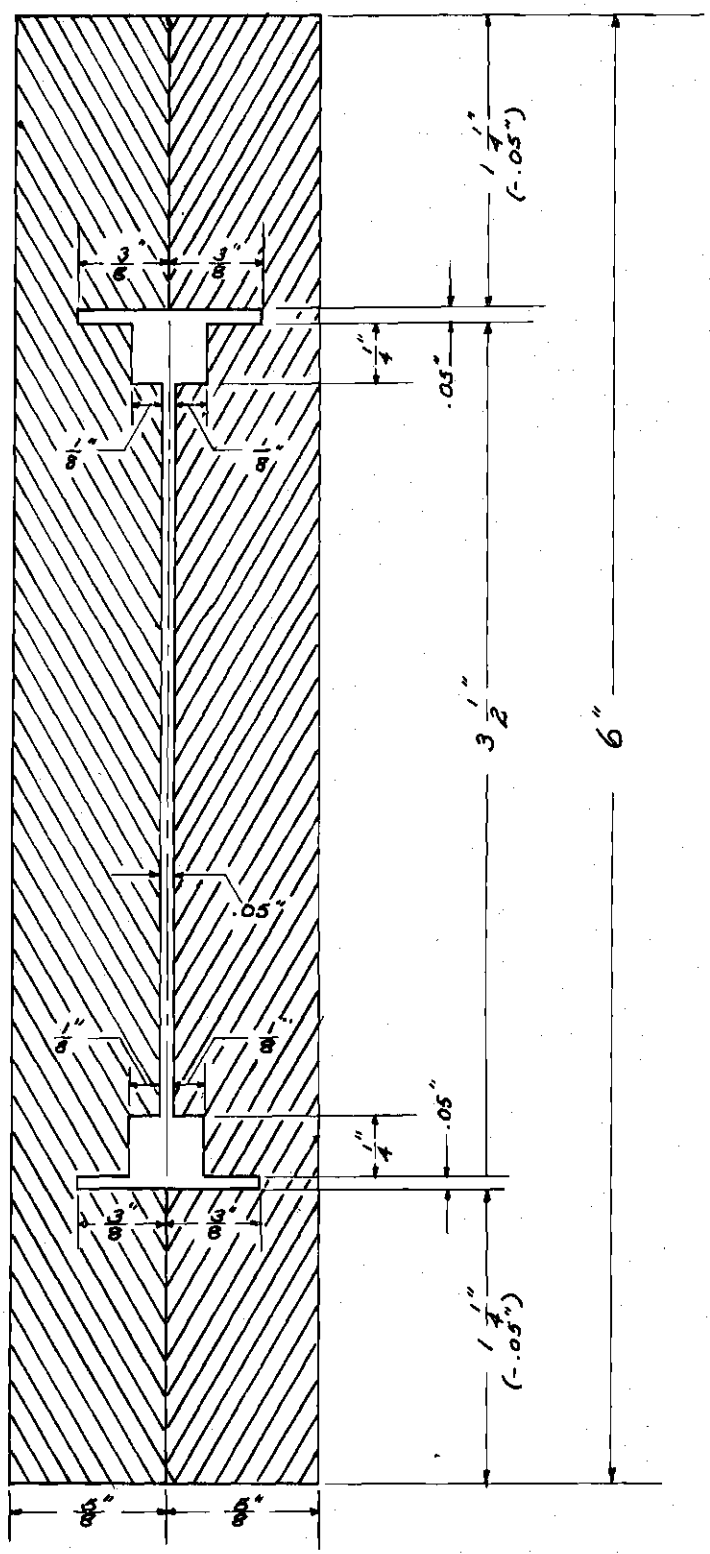

Figure 3. Crossection of Model Beam Form

loaded at midspan. Since the beam easily withstood a load of 300 lbs. it was concluded that the strength of the bond was adequate.

There are at least four reasons why a complete bond of 35 inches may not have been obtained in the first beam:

1) The beam form was resting on refractory bricks which could have caused a temperature differential within the thickness of the steel bars.

2) The silver solder flow temperature was incorrect.

3) The temperature control mechanism was not working properly.

4) The soaking time was too short.

In order to correct for reasons 1), 3), and 4), the beam form was suspended from a "swing" device as shown in Figure 4; in addition, the soaking time and temperature were raised to two hours and 1400°F respectively.

Three sample beams, each six inches long, were used (one placed at the form centerline, the other two at the ends) and a perfect bond was obtained in all three samples. Thus, a second beam was placed into the form for annealing and welding at 1400°F. Unfortunately, the temperature indicator underwent a malfunction, and although 1400° was being indicated during the soaking period, the temperature continued to rise up to approximately 2000°F. This resulted in the complete ruin of the beam form and necessitated the making of a new form, thereby causing a delay in starting the tests.

A new beam form was constructed and annealed as previously described. In order to insure that the temperature indicator would not give a faulty reading, standard pyrometric cones were used to check the

kiln temperature. The annealing temperature was changed from 1400° to 1350°F since an earlier test revealed that the temperature within the kiln was about 30° more than indicated. With the exception of changing the soaking time from three hours to two hours, the annealing procedure is as described on page 4. This attempt was a success and a picture of the beam which was produced can be found on page 17.

The Primary Table

The purpose of this apparatus was to support the model beam as illustrated in Figure 8. The dimensions of the table were 24" x 36" in the horizontal plane and 45" in the vertical plane. Equipto angle was used to construct the table.

The Loading Device

This equipment can be divided into two parts each of which will be discussed separately:

a) The loading discs

b) The weight pan

The Loading Discs

This device is a very effective means of applying the load in that it causes the line of action of the load to be vertically downwards at all times, regardless of the buckled shape of the beam. Therefore, the problem of an eccentric moment due to the applied load when the beam is in a buckled configuration is nonexistent (except that due to inaccurate fabrication).

The general idea for the use of such a loading apparatus was obtained from A. R. Flint. However, the loading discs used in this thesis

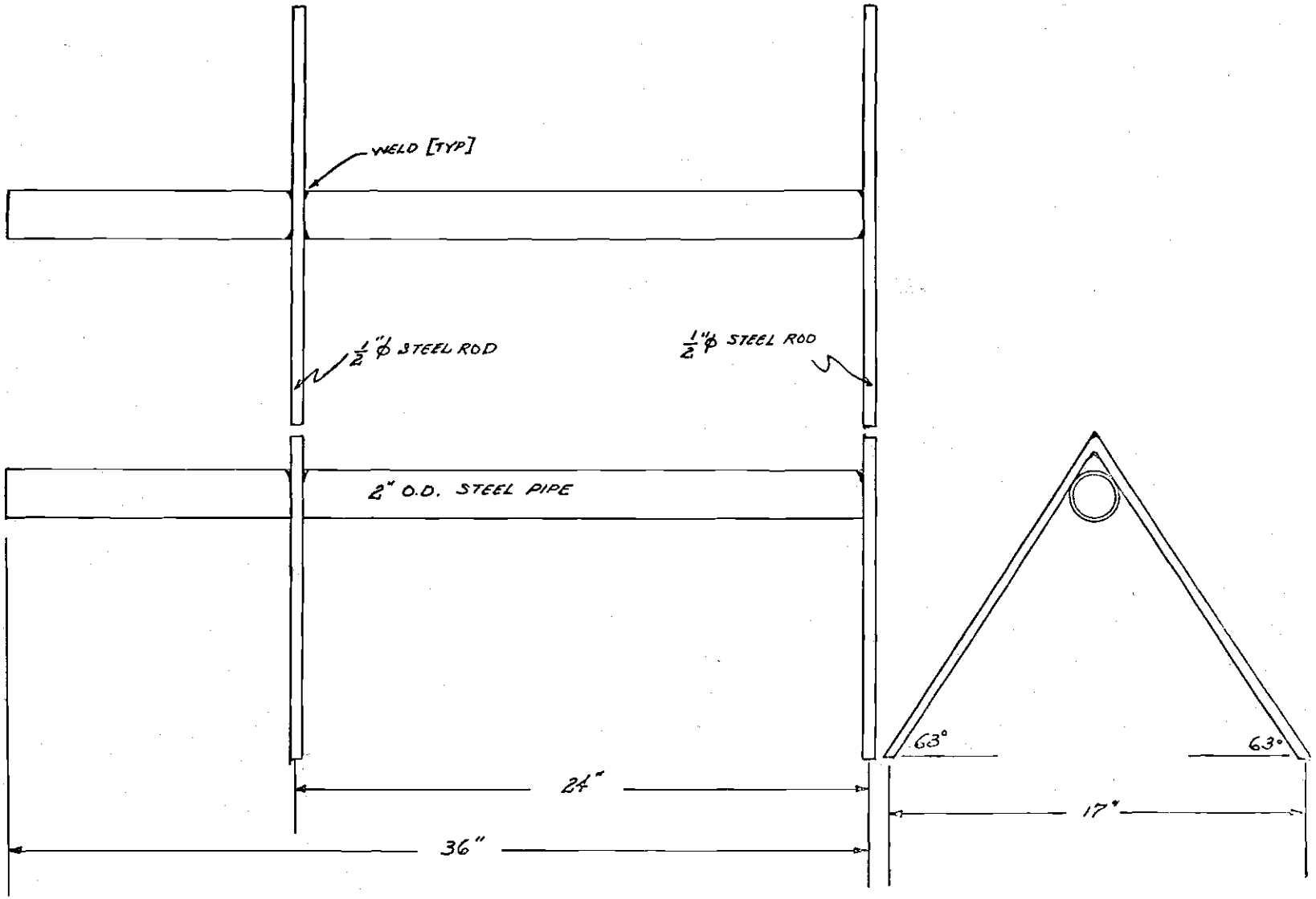

Figure 4. Swing Drvice for Model Beam Form

carry an additional advantage. The intermediate lateral restraints are attached to the discs in such a way that they remain in the same positions, irrespective of the rotation of the beam cross section.

Each loading disc system consists of two plastic discs (R = 1 inch and R = 3 inches) and a piece of steel cable 1/8 inch in diameter. Figures 5,6 and 8 illustrate the loading discs in detail.

The Weight Pan

This device was made up of a series of 1" x 1" x 1/4" angles welded together to form the configuration shown in Figure 7. A sheet of galvanized steel 1/32 inch thick was fitted into the angle skeleton for the purpose of keeping the lead weights from falling out. The two 1/4 inch rods are held together by means of a "U" bolt suspended from the small loading disc (Figure 6). Before making the weight pan, an analysis was made to determine its load capacity. Calculations showed that the pan should be able to support 800 pounds without excess deflection, thus giving the form a minimum safety factor of two.

The Intermediate Lateral Restraints

Aluminum welding wire was selected for use as intermediate lateral restraints. Fabrication of springs from wire has two distinct advantages over all others considered. First, the restraints are very easy to make and second, a high degree of flexibility existed in that the spring constant of the restraint could be varied by merely using various lengths of wires. Furthermore, the modulus of elasticity for aluminum is only 1/3 that of steel and thus the restraint lengths are kept as short as possible for various k values.

The method of connecting restraints to the east and west walls of the test room combined with the limited space (84") between these walls, necessitated the use of a very fine wire to keep the lengths of the restraints below 30". The smallest wire available had a diameter of 0.03". Using the formula:

$$k = \frac{AE}{L}, \qquad (1)$$

several combinations of k and L were obtained.

The Intermediate Lateral Restraint Connections

Each intermediate lateral restraint connection consists of the following items:

1) The disc to restraint section

2) The restraint to turnbuckle section

3) The turnbuckle to wall section

Figures 9 and 11 illustrate the above items. In order to prevent the weight of the connection apparatus from affecting the lateral restraints, the entire system was supported by means of wires suspended from a rigid overhead support.

The Measuring Table and Attachments

The measuring table was constructed from Equipto steel angles. Its dimensions were 53" in the vertical plane and 33" x 33" in the horizontal plane.

A "Z" shaped apparatus was designed to support the dial gages employed to read the horizontal deflection of the top and bottom flanges. The configuration of this apparatus is such that it permits adjustment

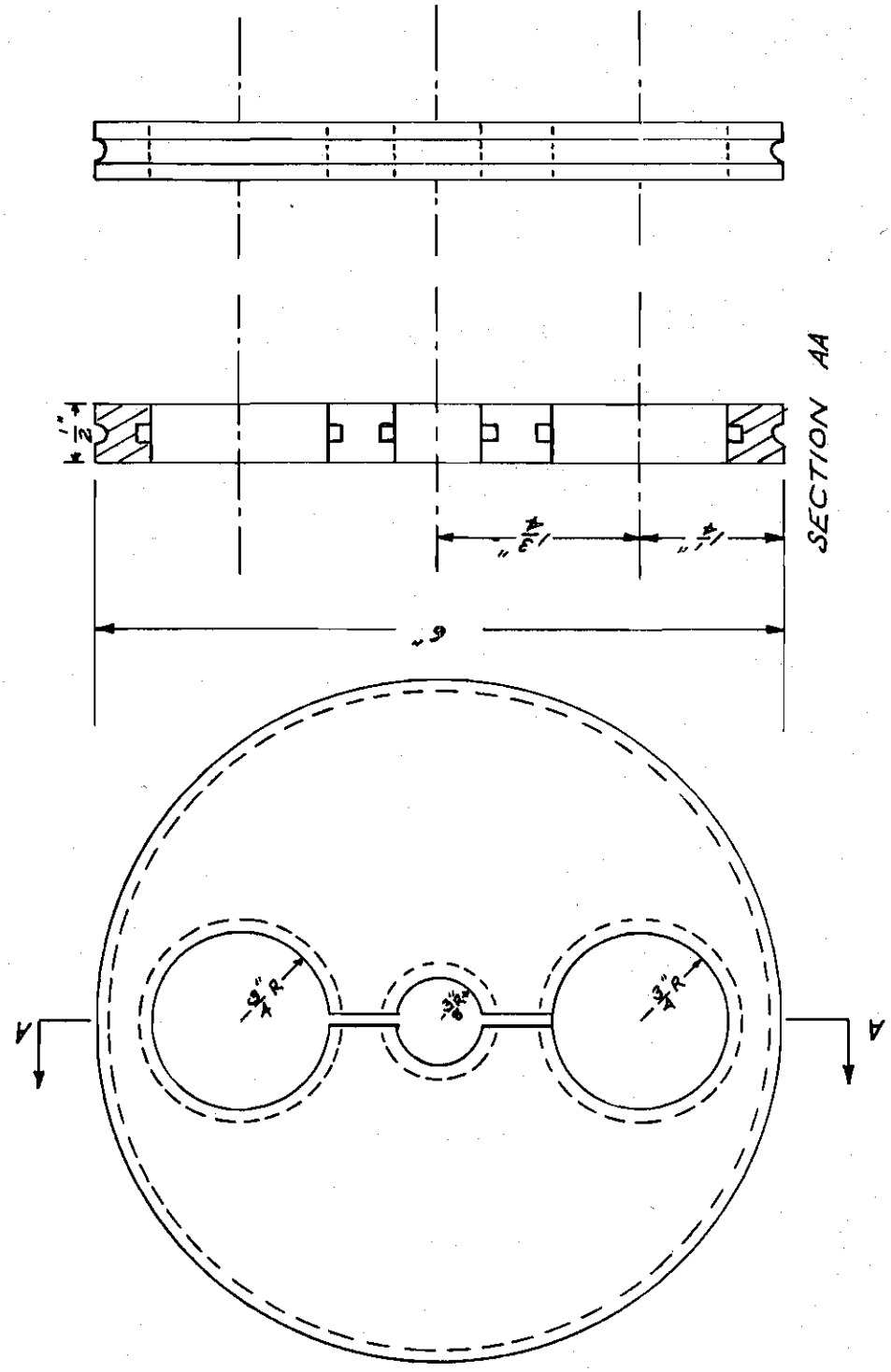

Figure 5. Detail of Large Loading Disc

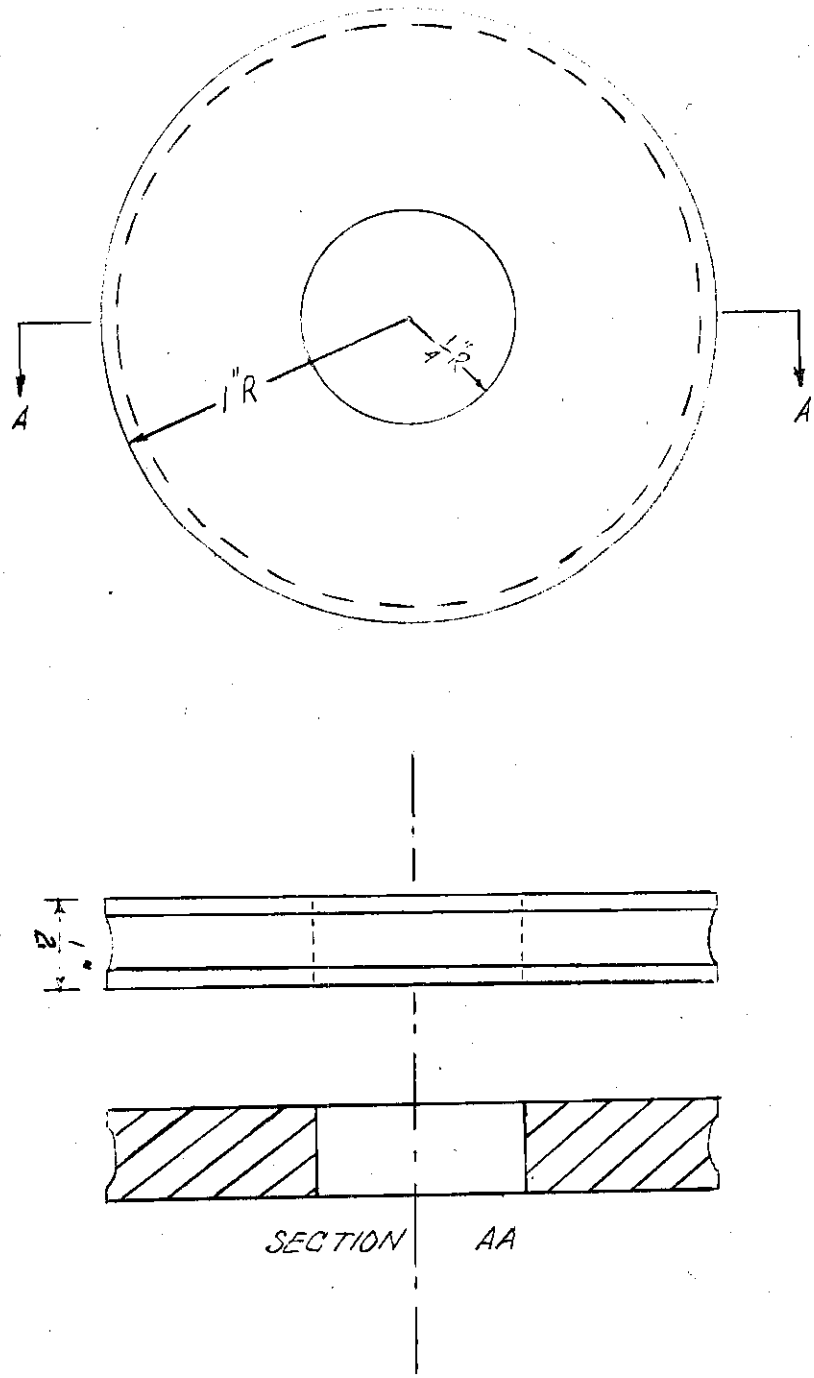

Figure 6. Detail of Small Loading Disc

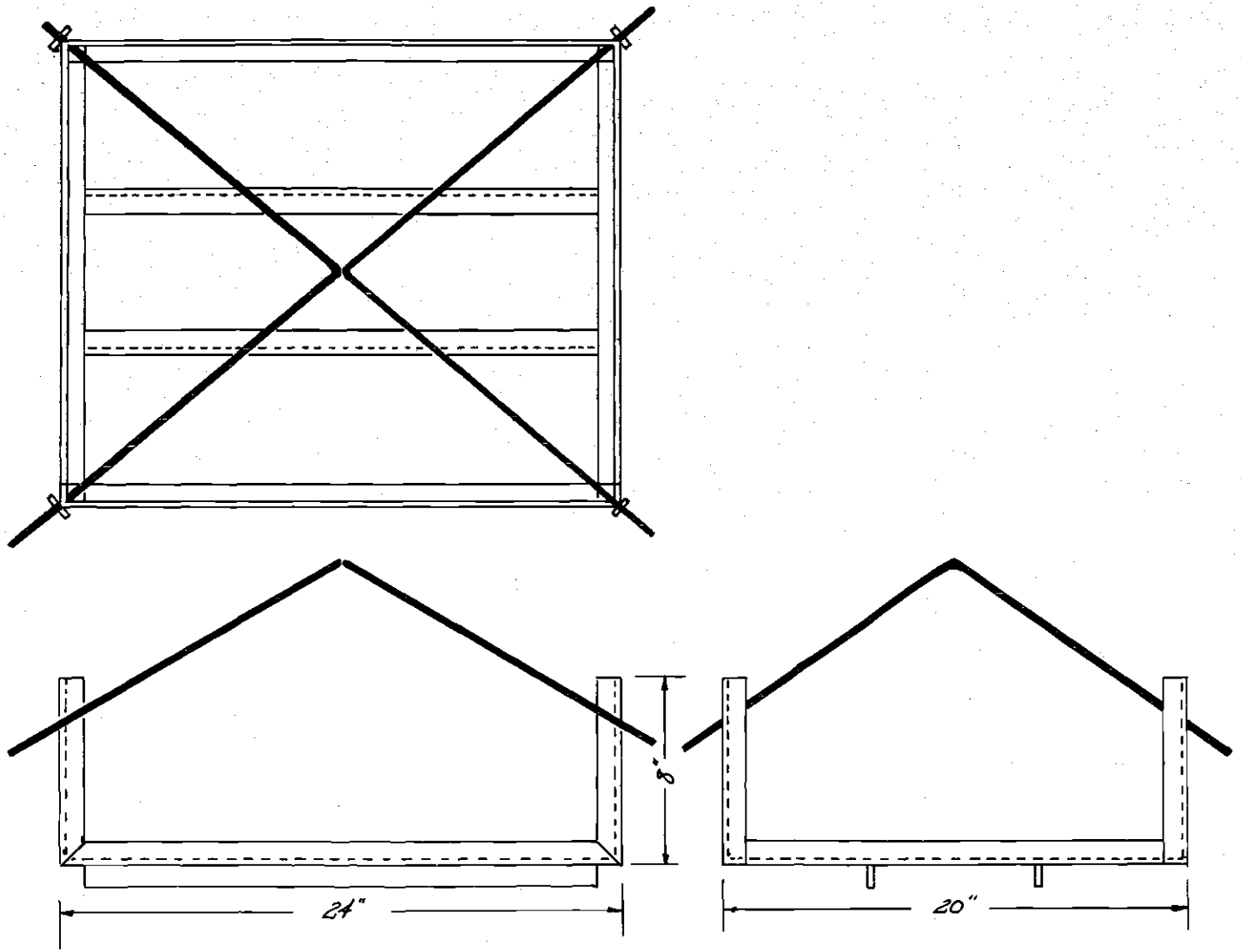

Figure 7. Load Pan

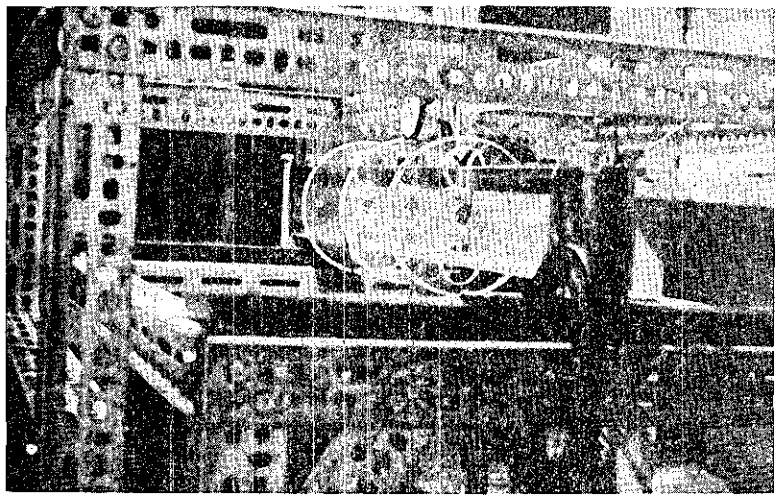

(a)

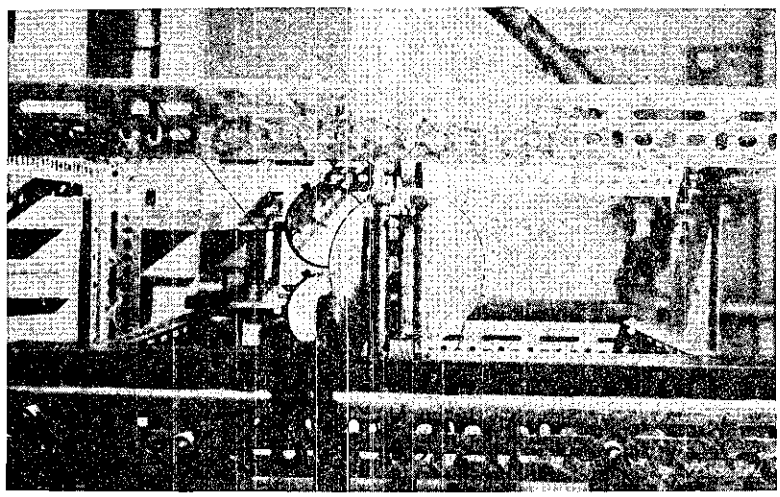

(b)

Figure 8. Test Arrangement and Instrumentation for Tests I(e), III(a), III(b), III(c), III(d) and III(e).

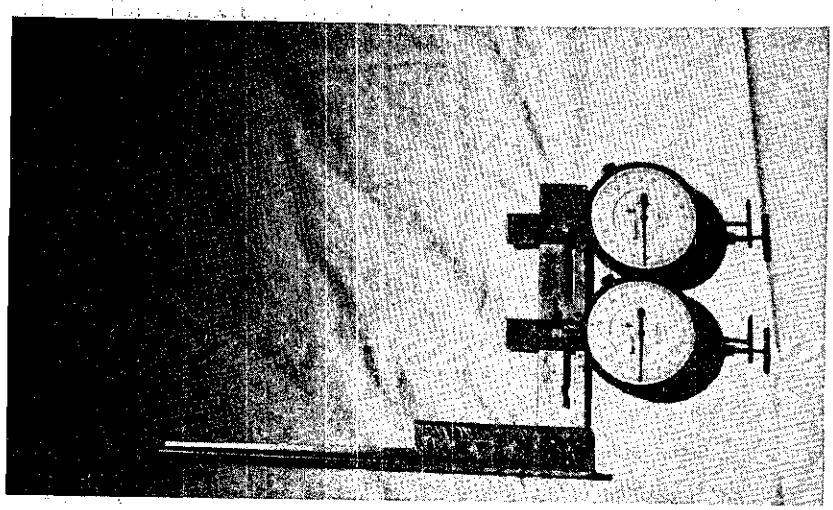

Figure 9(a). Support for Lateral Dial Guages

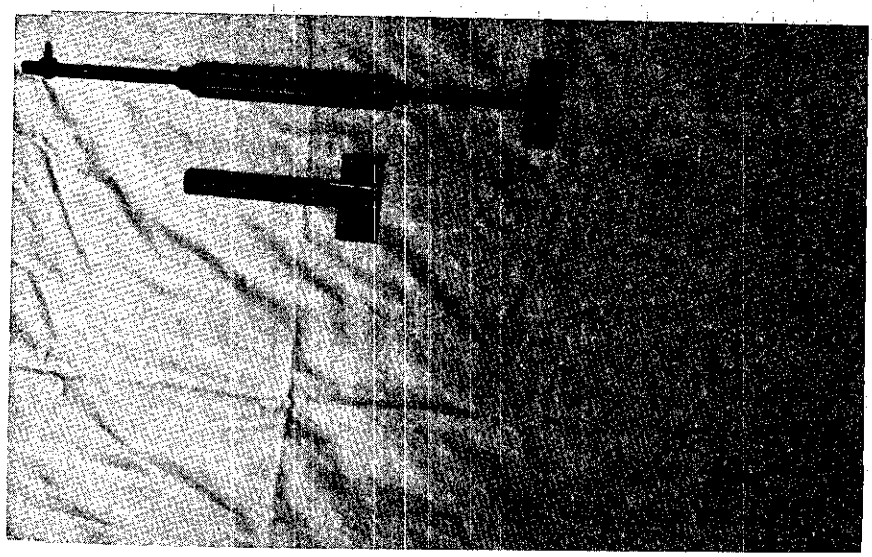

Figure 9(b). Intermediate Restraint Connections

in three directions (see Figure 9a).

Figure 8, illustrates the measuring table and its attachments as they were used in the testing procedures.

CHAPTER III

PROCEDURE

Theoretical and Mathematical Considerations

In this thesis, theoretical and experimental values of P_{cr} were compared. The theoretical critical buckling load was determined for an I beam restrained against rotation at the ends only, as well as the case involving intermediate lateral restraints along the span. The approach used to determine P_{cr} for the case of a simply supported I beam without intermediate restraints (Case I), was taken from an article by J. M. Biggs (10). In order to determine P_{cr} for the case involving an intermediate restraint at midspan (Case II), the method of A. R. Flint (7) was employed.

Both Flint and Briggs utilized the strain energy approach of Timoshenko (1) to obtain their respective solutions. When the beam begins to buckle, there is an increase in the internal strain energy due to both the torsional stresses and the lateral bending of the flanges. At the same instant, external work is being produced as a result of the descending load. In applying the strain energy method, both the internal strain energy and the external work are computed in terms of the load P, the beam constants, and the intermediate restraint stiffness (if applicable). A detailed analysis of the strain energy method can be found in the Theory of Elastic Stability by Timoshenko (1).

CASE I: Simply supported beam without intermediate lateral re-

straints.

Equation (2) was used to determine the critical buckling stress, for f_{cr}, for this case.

$$f_{cr} = AE \frac{Ixx}{Iyy} \frac{d^2}{L^2} \left[\frac{L}{a} \sqrt{1 + B \frac{a^2}{L^2}} + C \right] \qquad (2)$$

A, B, and C are constants which depend upon the distribution and point of application of the load, and the location of lateral restraints. For the case of a concentrated load at midspan and applied at the shear center

$$A = 1.071$$

$$B = \pi^2$$

$$C = 0$$

The value for f_{cr} obtained from equation (2) is:

$$f_{cr} = 6,880 \text{ psi},$$

and therefore,

$$P_{cr} = 187 \text{ lb.}$$

For third point loading,

$$f_{cr} = 10,060 \text{ psi}$$

and

$$P_{cr} = 284 \text{ lb.}$$

Calculations for the above values can be found in Appendix A.

CASE II: Simply supported I beam loaded at midspan through the shear center, and stayed at midspan due to an elastic support.

This case was employed by Flint as an example of the effect of lateral restraint on the span. Equation (3) is the final result of his theoretical derivation. Since no other reference was found to contain both an experimental and theoretical analysis of the influence of intermediate restraints on simply supported I beams, the derivation is given by Flint (7).

$$P_{cr} = \frac{17.2}{L^2}\sqrt{EI_{yy}GJ(1+\lambda)\left(1 + \frac{10\lambda}{1+\lambda}\,\frac{EI_{yy}}{L}\cdot\frac{h^2}{L}\right)} \qquad (3)$$

where

$$\lambda = \frac{K_B L^3}{48EI_{yy}} \quad ,$$

representing the ratio between the stiffness of the intermediate restraint and the lateral bending stiffness of the beam. The value of λ was obtained from a graph (9) relating λ to the critical stress factor, C. The critical stress factor is the ratio of f_{cr} with the presence of elastic lateral supports to f_{cr} without these supports.

Based on the lowest value for yield stress obtained in the tensile tests, the value of C must not exceed 2. Although this value is lower than desired, it must be employed to prevent the occurrence of inelastic buckling.

Since the load is applied at the shear center,

$$d' = 0,$$

and therefore equation (3) reduces to

$$P_{cr} = \frac{17.2}{L^2}\sqrt{EI_{yy}\, GJ(1 + \lambda)} \qquad (5)$$

In equation (5), the effect of warping is ignored thereby inducing an error of 41 per cent for this particular beam cross section. Since warping is considered in equation (2), it is necessary to multiply equation (5) by a factor of 1.41 in order to effectively determine the influence of restraints on the theoretical buckling load.

Experimental Procedure and Results

The experimental procedure was modified during testing as a consequence of the results obtained. In order to maintain coherency, it therefore became necessary to conjugate test procedures and results within this subdivision of Chapter III.

Test I(a), I(b), I(c) - Concentrated Load at the Centerline, No Intermediate Restraints

In general, the same procedure was followed for each test in this series. The large loading discs were fastened with screws to each beam at the centerline and third points by means of small aluminum angles as shown in Figure 8. The location of the holes in the beam are such that they will have negligible effect on the buckling of the model beam.

Each model was placed into position with a span of 34 inches between end supports. For several loading increments, vertical deflec-

tion was measured at the beam centerline and horizontal deflection was measured at the centerline (and in some tests at the third points as well) for both the tension and compression flanges. Since small deflection theory is assumed, the effects of vertical deflections of the flanges are disregarded and the angle of rotations, β, was determined from the knowledge of the horizontal deflection of both flanges. In accordance with the application of the elastic line theory, it is further assumed that the beam cross section does not deform under load.

Test I(a). The primary purpose of this test was to establish a base for comparing the effects of intermediate lateral restraints on the lateral stability of WF beams. The load was increased in small increments by means of lead weights until a substantial increase in the lateral deflection of the compression flange was observed with no increase in load. A value of 186 pounds was observed as the buckling load. This value is within 1 per cent of the theoretical buckling load of 187 pounds. All pertinent data for Test I(a) can be found in the Appendix beginning with Figure 24.

Test I(b). Analysis of Test I(a) data revealed a definite change in slope in the pre-buckling portion of the load versus horizontal deflection curve for the compression flange. It was believed that this slope change could have been the result of improper rotational restraint at the ends of the beam, thus allowing the beam to "slip" laterally once a great enough load was applied. After readjusting the end restraints, Test I(b) was performed. The observed buckling load was 153 pounds or 18 per cent below the theoretical value. This test indicated an apparent loss in elasticity in the lateral direction as can be seen

in Figures 25 and 29. All data related to Test I(b) can be found in Appendix C beginning with Figure 28.

Test I(c). This test appeared to support the hypothesis of permanent set in the lateral direction. The apparent buckling load was 149 pounds or 20 per cent less than the theoretical value (see Figure 33, Appendix C).

Shortly, after completion of the preceding test, a shear failure was observed between the web and the tension flange. The failure extended for approximately eight inches along the beam length measured from the north end. A smaller shear failure may have been present during all or part of the first three tests.

Test I(d). A new beam was prepared for this test. The shear failure in the first beam which occurred during the Test I Series was probably caused by a lack of bond at the ends of the beam as shown below.

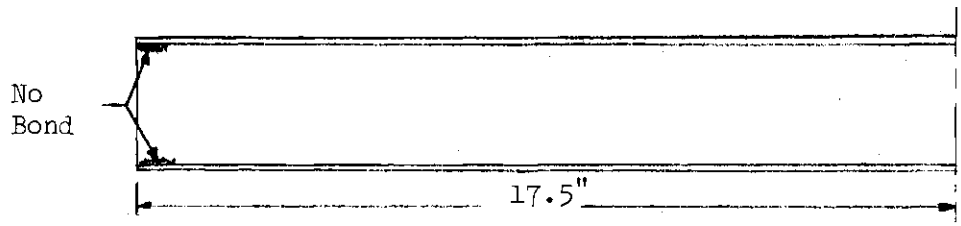

Figure 10. Illustration of Lack of Bond at Beam Ends

Since the second beam also lacked bond at its ends, the ends were cleaned and soft soldered.

Before the test was performed certain changes were made in the testing apparatus. First the 1/4" diameter steel rods in the load pan was replaced with 3/8" rods. These new rods were attached rigidly at the corners of the pan to prevent slippage. Furthermore, the U-bolt which joined the load pan to the small loading disc was replaced by the

cable connection illustrated in operation in Figure (81a). In this way, the line of action of the load in the pan will always be vertical, regardless of the orientation of the weight within the pan. The end restraint rods were replaced by 1/2" x 6" bolts. Once the beam was in position, the adjustable restraint was held firmly against the beam by means of a steel angle clamped to the end restraint bar, (see Figure 81b).

The purpose of Test I(d) was to check the accuracy of the measuring system. The beam was loaded in ten pound increments up to a value of 130 pounds (or approximately 70 per cent of the theoretical buckling load), and then unloaded in ten pound increments. The initial reading and intermediate gauge readings for each load increment coincided with a maximum error of 6 per cent.

Test I(e). The purpose of this test was the same as that of Test I(a) (see page 24). The apparent buckling load was 186.85 pounds or 1 per cent less than the theoretical buckling load. All data pertaining to this test can be found in the Appendix beginning on page 67.

Tests II(a) and II(b) Concentrated Load at the Centerline, Intermediate Restraints at Centerline Acting Through the Shear Center

The initial procedure for the restraint tests is described on page 23. Once the beam was in its proper position, the intermediate lateral restraint connectors were fastened into place. Because the direction of buckling is unknown before commencing a test, the restraints must be employed on both sides of the beam and parallel to the beam axis. In order to obtain approximately the same initial tension in the restraints for each side of the beam, the following procedure was employed:

The two restraints, one on each side, were plucked at their midpoints, thus producing two musical notes. By means of the turnbuckle connection, the wires were then tightened or loosened as required to obtain the same accoustical frequency for both wires. Figure 11 illustrates in detail the assembled restraint apparatus.

Test II(a). A 19 inch wire fastened through the beam shear center was employed as the intermediate restraint. Using equation (1), the stiffness of this wire was found to be 370 pounds/inch. Theoretical calculations revealed that this restraint should increase the critical buckling load to approximately 500 pounds. Since this value exceeds the yield load for bending (see Appendix D, Table 4), it was decided to increase the load up to 300 pounds only. However, apparent lateral buckling was observed at 257 pounds. All graphs related to this test appear in Appendix C beginning with Figure 41.

Test II(b). The length of the wire was changed to 12.5 inches thus giving an increase in stiffness to 550 pounds/inch. Lateral buckling occurred at 267 pounds. Although the stiffness of the restraint was increased for this test, the amount of lateral deflection of the compression flange per load was greater than in Test I(a). Graphs and data sheets for Test II(b) can be found in Appendix C and D respectively.

Tests III(a), III(b), III(c), III(d), III(e) - Concentrated Load at the Centerline, No Intermediate Restraints

Due to the unfavorable agreement between the theoretical and experimental results of Tests II, a series of five additional tests was performed. The general procedure for each test is as described on page 23.

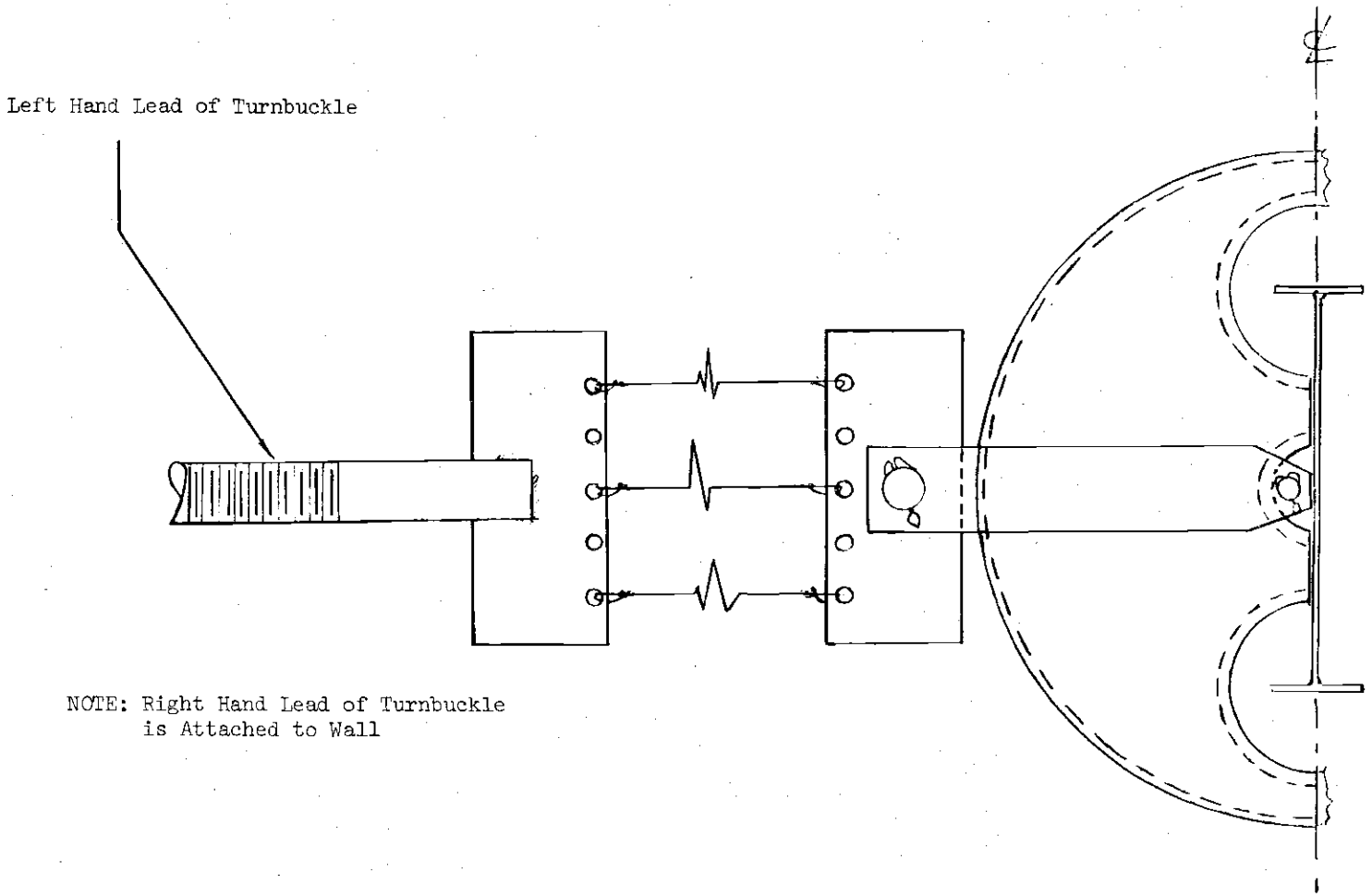

Figure 11. Detail of Intermediate Restraint Apparatus in Operation

Test III(a). The load was increased in 5 and 10 pound increments up to a value of 257 pounds. No lateral buckling was observed. (See Appendix C, Figure 49).

Test III(b). The total load applied was 326 pounds. A study of Figure 52 reveals a definite similarity to the performance of Test III (a).

Test III(c). The beam was loaded to a value of 228 pounds and then unloaded in ten pound increments. Dial readings were taken at each increment for the purpose of plotting unload curves. No permanent set was observed. In addition, a lateral buckling was not detected. Before the unloading process, dial guages were also placed at each end of the beam for the purpose of recording the vertical deflection of the end plates (see Figure 8). It was discovered that the end plate deflection comprised approximately 30 per cent of the deflection recorded at the centerline of the beam. Thus absolute E values were determined for Test III(c) - III(e).

Test III(d). The purpose of this test was to see if the rotational restraints were acting as moment restraints as well. The end restraints were released so as to allow a very small opening between the beam flange and one of the restraint rods.

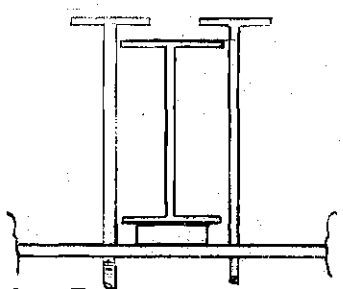

Figure 12. End View of Rotational Restraints

The load was increased to a value of 278 pounds and then unloaded in the same manner as described in Test III(c). A negligible amount of permanent set was observed in the vertical direction. (See Figure 54, 55 and 56). Lateral buckling did not occur in this test.

Test III(e). The purpose of this test was to load the beam until the occurrence of lateral instability. A buckling load of 477 pounds was observed. (Two hundred and fifty per cent greater than the theoretical value) Figure 60 and 61 indicate that permanent set occurred in both the horizontal and vertical directions. The ends were also "released" in this test.

CHAPTER IV

DISCUSSION OF RESULTS AND CONCLUSIONS FOR PHOSPHORUS BRONZE MODEL TESTS

The results of the tests performed on the phosphorus bronze models are quite diverse with respect to relating experimental and theoretical buckling loads. In Tests I(a) and I(e) for example, the apparent buckling loads were within 1 per cent of the theoretical value determined in equation (2). However, in other tests performed on the same beam used in Test I(a), apparent experimental buckling loads varied from 50 (+) to 250 per cent of the appropriate theoretical value. In order to formulate a reasonable explanation for the serious lack of compatibility between calculated and observed values of P_{cr}, several items which may have influenced the magnitude of the experimental value were investigated; each will be discussed separately:

1). The simultaneous process of annealing and forming the model beams (page 7) could have produced a change in the physical properties of phosphorus bronze. Such a change could be detected in the vertical deflection curves (see Appendix C) as well as the horizontal deflection curves. Due to the erratic nature of the horizontal deflection curves, the vertical deflection curves were studied. In the nine tests performed, only one curve revealed a nominal amount of permanent set, but this particular curve was elastic up to a value exceeding 450 pounds.

+ For tests involving intermediate restraints.

The modulus of elasticity was determined from the ζ_v curve for each test, and a comparison of these quantities revealed a differential of only 12 per cent between the maximum and minimum values. E was also determined for various loads in Test III(d) and III(e) after subtracting end plate deflections from the ζ_v values. Maximum variation between these corrected values of E was less than 10 per cent.

2). The restraints at the ends of the beam may have induced a moment as well as torsional restraint thereby resulting in an increased value for P_{cr}. In Test III(c), the end restraints were "released" as described on page 29, and the results obtained were quite similar to those of Test III(a) and III(b). Verification of the preceding statement can be obtained by comparing the graphs in Figures 49 and 51.

3). An improper set up of the horizontal dial gauges could have produced a misconception as to the occurrence of lateral buckling. For example, if the dial gauge extention plate (see Figure 9) was not perpendicular to the beam flange, it would be possible for the gauge to record within one loading increment, a large increase in lateral motion at loads below the value of P_{cr}. The result of Test I(d) (page 25) appears to cancel this hypothesis.

4). If the location of the large loading disc upon the beam is not through the shear center, then a variation will occur in the theoretical as well as experimental values of the buckling load. In order to arrive at an estimate of the magnitude of the error produced, equation (2) was solved assuming that the loading disc has been placed $\pm$ 0.1 inch off the beam shear center. A variation of only $\pm$ 4 per cent was obtained in the theoretical value of P_{cr}.

5). If the geometric center and the point of application of the load induced by the large discs are not in exact agreement, torque is applied to the beam cross section (Figure 13). Therefore, it is conceivable that this eccentric loading could have a positive or negative

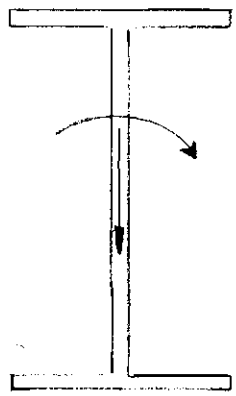

Figure 13. Cross Section of Phorphorus Bronze Model Illustrating the Effect of Eccentric Loading

effect on the buckling load. If the eccentricity is opposed to the direction of lateral motion (Figure 14a), there may be an increase in the buckling load as well as a decrease in the amount of lateral deflection. If the eccentricity compliments the direction of lateral motion (Figure 14b), the exact opposite results may be obtained.

6). The initial deflected shape of the beam has a significant effect on the path of lateral motion up to buckling. If the plane of the load acting on the beam coincides with plane of symmetry, then the effect of an initial lateral deformation becomes evident; for as soon as the load is applied, the beam is deflected into a lateral position and undergoes twisting as well. A large deflection for a small amount of load replaces the stability problem when the beam is initially deflected. Stresses are produced in this case on account of torsion and

lateral bending.

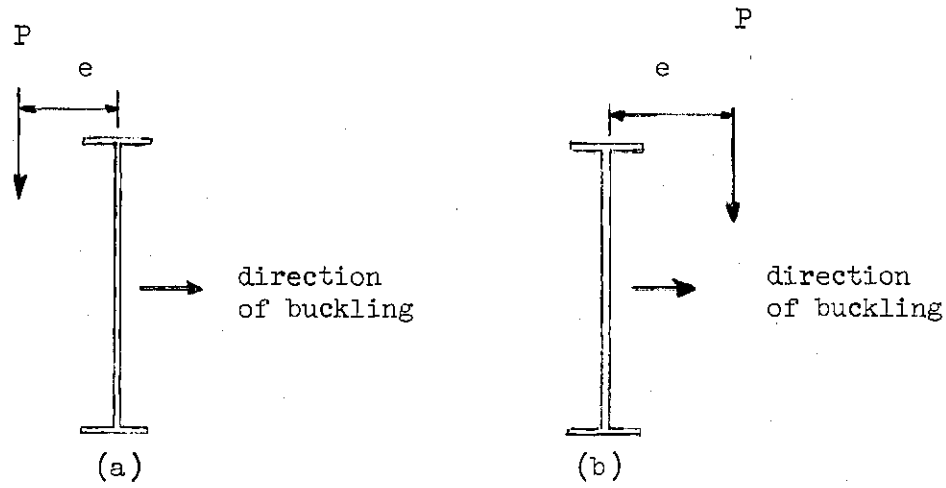

Figure 14. Effects of Eccentric Loading

From the information in the preceding six paragraphs, it appears that the primary source of divergency in the experimental values of P_{cr} is a result of eccentricity within the loading disc combined, perhaps, with the effects of initial curvature. Since the above two items may have resulted in a misconception as to the occurrence of lateral buckling, twist curves were plotted for each test. The following conclu-

sions may be drawn from these curves:

1). Lateral buckling did not occur in Test II(a) and (b) (see Figures 43 and 47). The increased lateral motion may have been a result of eccentric loading and/or initial curvature of the beam.

2). Lateral buckling appears to have occurred in Tests I(b) I(c), but not in Test I(a) (see Figures 31, 35, and 27). However, since beam 1 failed in shear sometime during the Test I series, (see page 22), no definite conclusions should be drawn from these tests.

3). Lateral buckling seems to exist in Test I(e) (see Figure 39).

4). Lateral buckling definitely occurred in Test III(e) but not before reaching the observed buckling load of 477 pounds (see Figure 63).

CHAPTER V

PROCEDURE FOR RECTANGULAR ALUMINUM BEAMS

In order to give support to the belief that eccentricity within the loading disc was largely responsible for the erratic test results of the phosphorus bronze beams, rectangular aluminum beams were tested. Aluminum was chosen as the beam material in order to eliminate peculiarities within the model material as a possible cause of experimental error.

Theoretical Procedure

Equation (4) was used to determine the theoretical buckling load of a simply supported rectangular beam having no intermediate restraints (1). In deriving this equation, it was assumed that a small lateral buckling had occurred; the magnitude of the smallest load required to keep the beam in this slightly buckled form was determined from the differential equations of equilibrium and the end conditions.

$$P_{cr} = \frac{16.94_{(*)}\sqrt{EI_{yy}GJ}}{L^2} \qquad (4)$$

Substituting the appropriate values into equation (4),

$$P_{cr} = 115.5 \text{ pounds}$$

(*) There is a variation in the value of the numerical constant for equations (4) and (2).

Experimental Procedure

Test IV(a), IV(b), IV(c), IV(d) - Concentrated Load at the Centerline, No Intermediate Restraints

Two beams of identical dimensions were prepared for testing (see Figure 15). In general, the test procedure described on page 23 was followed. The only change required in the testing apparatus was a modification of the rotational restraints as illustrated in Figure 81b. Before proceeding with the tests, a rough estimate of the maximum elastic lateral deflection was determined. Because this analysis revealed that the beam could deflect seven inches laterally without inducing permanent set, the stops were placed so as to allow approximately two inches of lateral motion.

Test IV(a). Beam 1 was placed into position with a span of 32.25 inches between supports. A tracing of both the top and bottom beam surfaces was made prior to testing. Double ordinates were obtained by reversing the beam and a slight initial curvature was observed. Lateral buckling occurred at a load of 177 pounds or 35 per cent greater than the theoretical value.

Test IV(b). Beam 1 was rotated about the longitudinal axis 180° without reversing the end positions. The same test procedure was followed and lateral buckling was observed at 124 pounds or 7 per cent greater than the calculated value.

Test IV(c). Beam 2 was placed into position with an unbraced length of 32.25 inches. The critical buckling load for this test was 120.5 pounds or 4.5 per cent greater than the theoretical value.

Test IV(d). Beam 2 was rotated about the longitudinal axis 180°

Type of Aluminum -6061-T6

E = 10,000,000 psi	b = 1/8"
G = 3,750,000 psi	d = $3\frac{1}{2}$"
I_{xx} = 0,448 in^4	I_{yy} = 0,000,569 in^4

Figure 15. Cross Section and Properties of Aluminum Models

without reversing the end positions. Lateral buckling was observed at 173 pounds or 33 per cent greater than the theoretical value.

Graphical results of above tests can be found in Appendix C (see list of illustrations).

Test V - Concentrated Load at the Centerline; Intermediate Restraint at Centerline Acting Through Shear Center

The purpose of this test was to obtain a secondary mode of failure ($\lambda \geq 15$) in order to test the effectiveness of the intermediate restraint apparatus. A nineteen inch restraint was attached to the beam center as described on page 27 and illustrated in Figure 81b. The beam failed in double curvature at a load of 312 pounds. Graphical results of this test as well as a photograph of the beam at failure can be found in the Appendix C beginning with Figure 76.

CHAPTER VI

DISCUSSION OF RESULTS AND CONCLUSIONS FOR ALUMINUM MODEL TESTS

The results of Test IV(a), (b), (c), and (d) appear to confirm the idea of eccentricity in the loading disc. Examination of the chart below reveals that each beam buckled very close to the theoretical value in one test and 30 per cent higher than the theoretical value in the other test.

TEST	BEAM	BUCKLING LOAD
IV(a)	1	177 pounds
IV(b)	1	123 pounds
IV(c)	2	120 pounds
IV(d)	2	172 pounds

In Tests IV(a), and (d), it is possible that the eccentricity opposed the direction of buckling, thus allowing the beam to take a greater load before failure. See page 37 and Figures 65, 67, 73 and 75. In like manner, the eccentricity could have been in the direction of buckling for Tests IV(b) and (c) and although the beams actually reached the theoretical buckling load, the amount of lateral deflection and twist was nearly twice that obtained in Tests IV(a) and (d). An examination of Figures 16 and 17 reveals that each beam appeared to buckle at loads of 30 per cent to 40 per cent below the theoretical value. The twist curves in Figures 18 and 19 further confirm the apparent tendency

of the beams to buckle at a lower load. Thus, a possible explanation for the "restiffening" process in Figures 16 and 17 is that an initial deformation acted to counteract the effect of eccentric loading.

The results of Test V verify that the restraint connection used in this thesis are capable of producing second mode buckling.

CHAPTER VII

RECOMMENDATIONS

1. A computer analysis should be performed to determine the effect of initial curvature and misalignment on the lateral stability of beams.

2. Due to the erratic nature of the test results, no definite conclusions could be drawn as to the effectiveness of phosphorus bronze in model analysis. Several tensile tests should be performed on coupon annealed at various temperatures and soaking periods in order to obtain conclusive information as to the effect of annealing on the yield strength of phosphorus bronze.

3. In future tests which use similar loading discs, it is recommended that the center of gravity of each disc be located by accurate methods. Adjustment of the center of gravity position can then be made by removing small amounts of the material from the unbalanced side of the disc.

4. A series of tests similar to those mentioned in the Introduction should be performed. The effect of varying the position and type of loading, (concentrated, uniform or a combination of both) as well as a variation in the positioning of the restraints along the beam need experimental verifications. Furthermore, the influence of restraints which interconnect two simply supported beams should be investigated.

5. The lead weights used to apply load to the beam could be replaced by a fluid such as water. In this way, not only would the load be applied in a more uniform matter but also the magnitude of the load increment could be varied without difficulty.

6. A more sophisticated method of determining the existence of equal tension in two opposing restraints should be employed. (See page 13).

7. It is suggested that a friction reducing apparatus (such as roller bearings) be employed at the end restraints in order that horizontal curvature can increase without the influence of friction resistance from the end support.

8. In order to enhance the effectiveness of the beam making process employed in this thesis, an induction coil furnace should be used.

APPENDIX A

SAMPLE CALCULATIONS

DETERMINATION OF f_{cr} AND P_{cr}

FOR CASE I (SEE PAGE 20)

$E = 16 \times 10^6$ psi

$G = 6 \times 10^6$ psi

$L = 34"$

1. $I_{xx} = \frac{(0.05)(3.5)^3}{12} + 2(3/4)(0.05)(1.75)^2$

$$\underline{I_{xx} = 0.409 \text{ in}^4}$$

2. $I_{yy} = \frac{2(0.05)(3/4)^3}{12} + \frac{(0.05)^3(3.5)}{12}$

$$\underline{I_{yy} = 0.00352 \text{ in}^4}$$

3. $J = 1.1(2/3bt_t^3 + 1/3\ dt_w^3)$

$$\underline{J = 0.000229 \text{ in}^4}$$

4. $a^2 = \frac{EI_{yy}\ d^2}{4GJ}$

$$a^2 = \frac{(16\text{x}10^6)(352\text{x}10^{-5})(3.5)^2}{(4)(6\text{x}10^6)(229\text{x}10^{-6})}$$

$$a^2 = 129.5 \text{ in}^2$$

therefore,

$$\underline{a = 11.38 \text{ in}}$$

$$f_{cr} = AE \frac{I_{yy}}{I_{xx}} \frac{d^2}{L^2} \left(\frac{L}{a} \sqrt{1 + B \frac{a^2}{L^2}} + C\right)$$

$$f_{cr} = (1.071)(16\text{x}10^6) \left(\frac{352\text{x}10^{-5}}{0.409}\right)\left(\frac{12.25}{1.156\text{x}10^3}\right)\left(\frac{34}{11.38} \sqrt{1 + 9.875 \frac{129.5}{1156}} + 0\right)$$

$$\underline{\underline{f_{cr} = 6{,}780 \text{ psi}}}$$

$$P_{cr} = \frac{4 f_{cr} I_{xx}}{Lc'}$$

$$P_{cr} = \frac{4(6{,}780)(.409)}{34(1.75)}$$

$$\underline{\underline{P_{cr} = 187 \text{ pounds}}}$$

APPENDIX B

FIGURES (16 - 82)

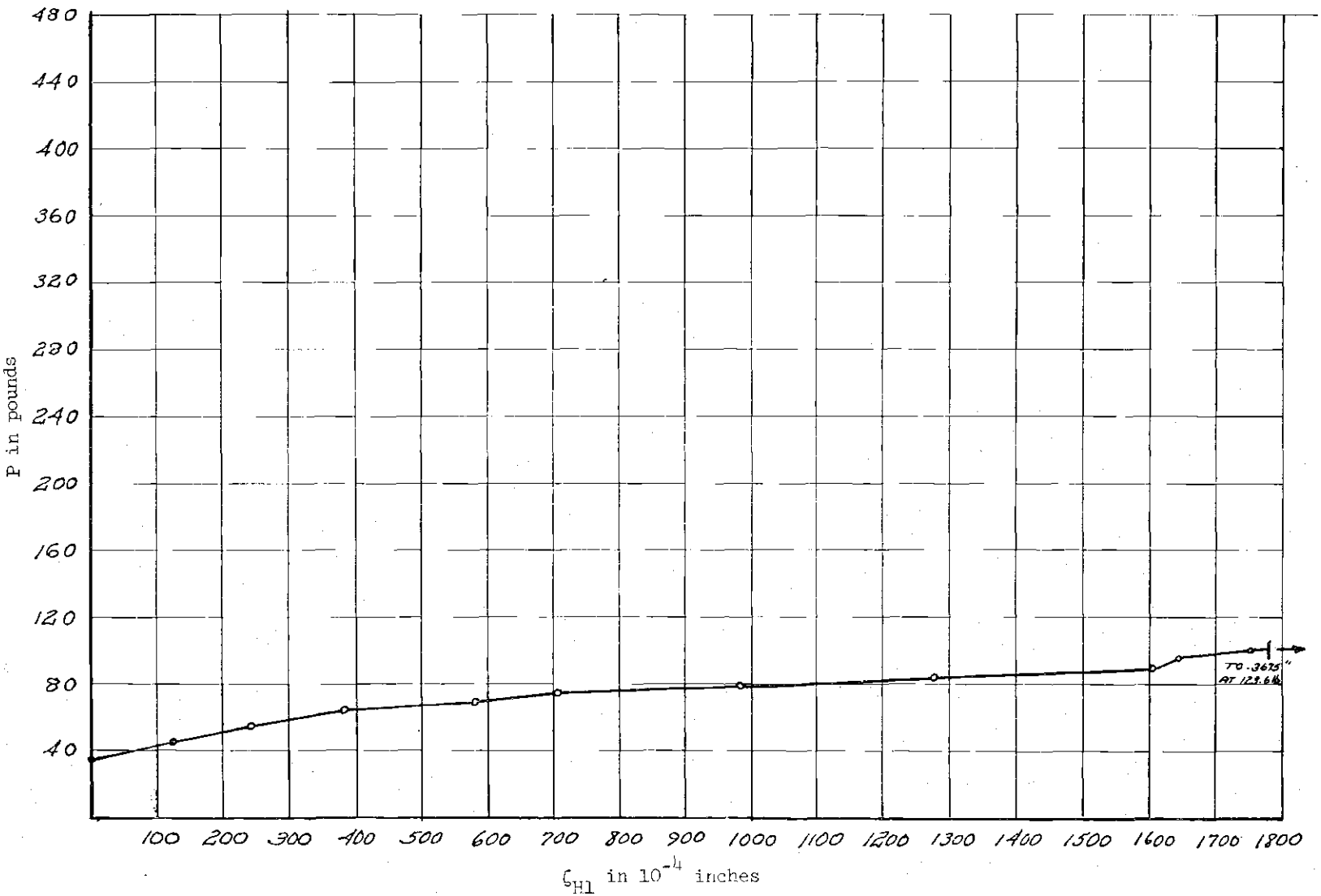

Figure 16. P versus ζ_{H1} Curve for Test IV(b)

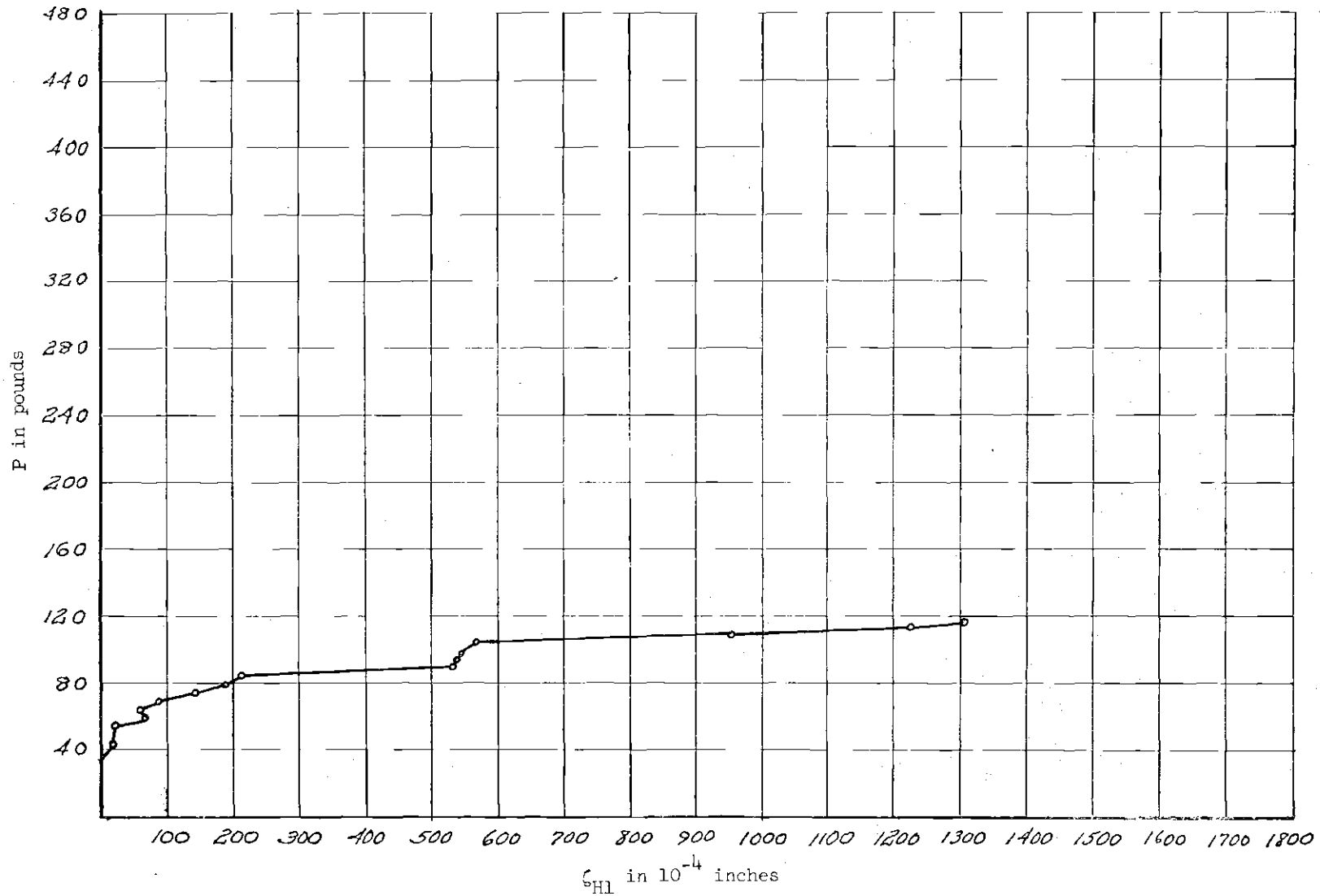

Figure 17. P versus ζ_{H1} Curve for Test IV(c)

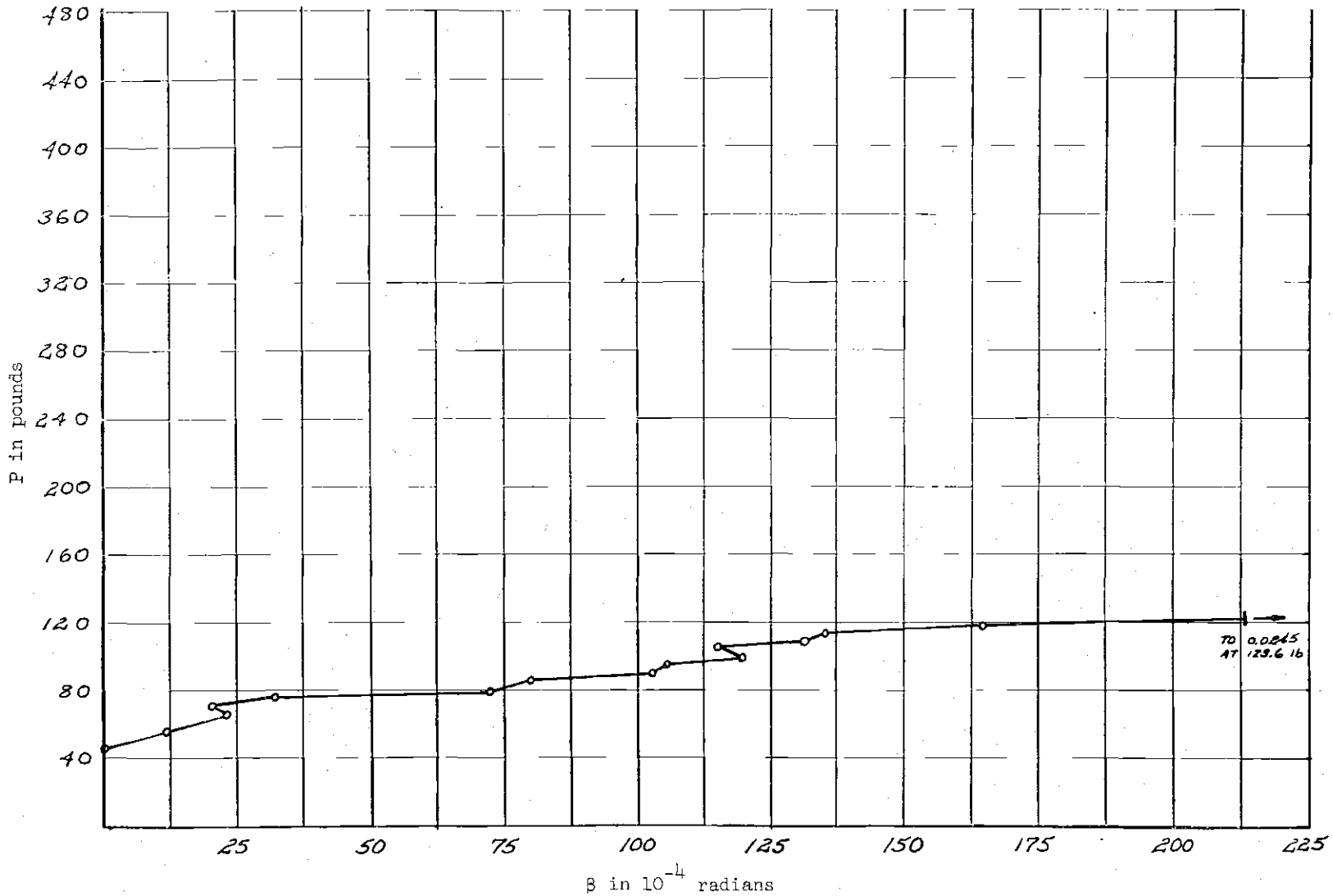

Figure 18. Twist Curve for Test IV(b)

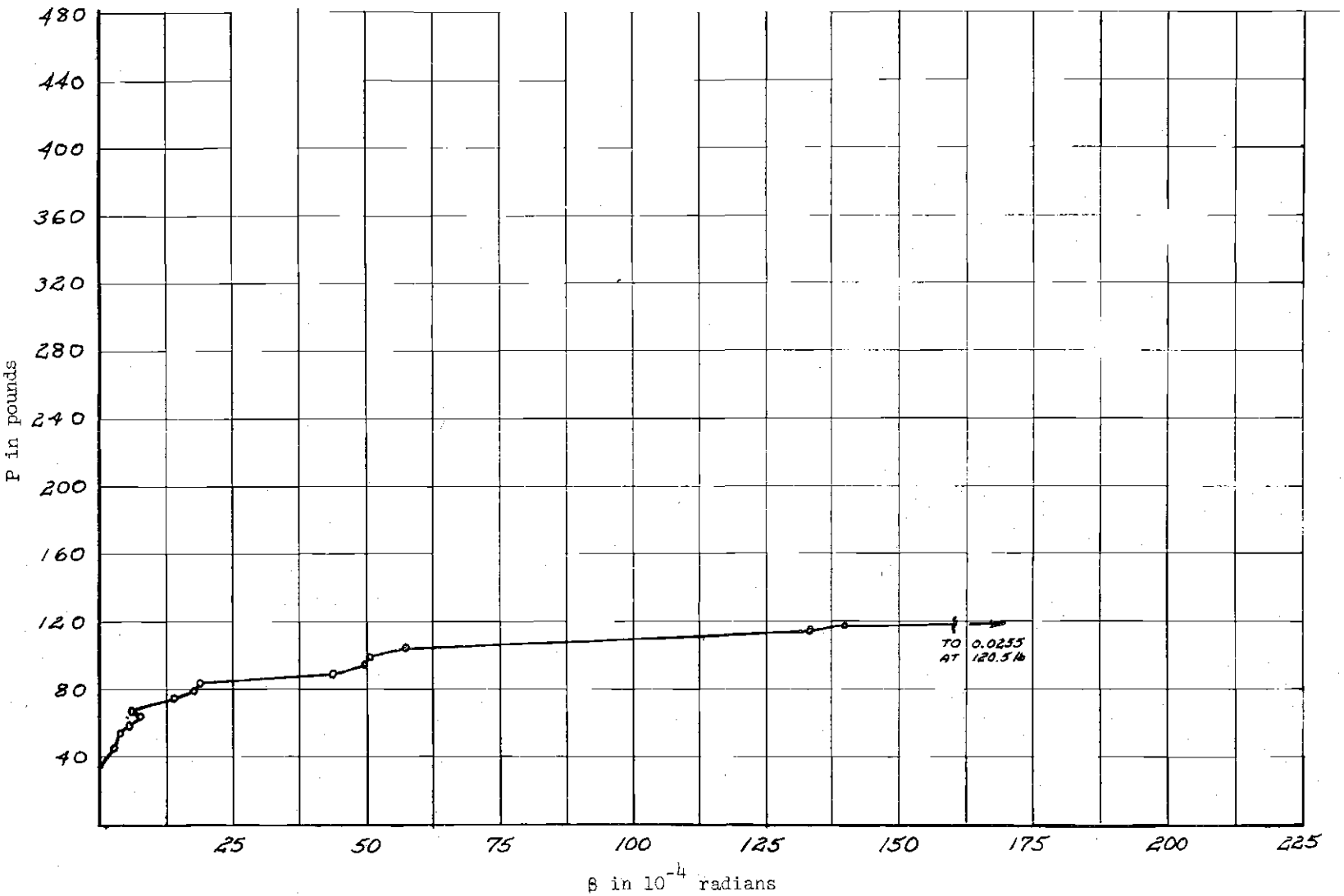

Figure 19. Twist Curve for Test IV(c)

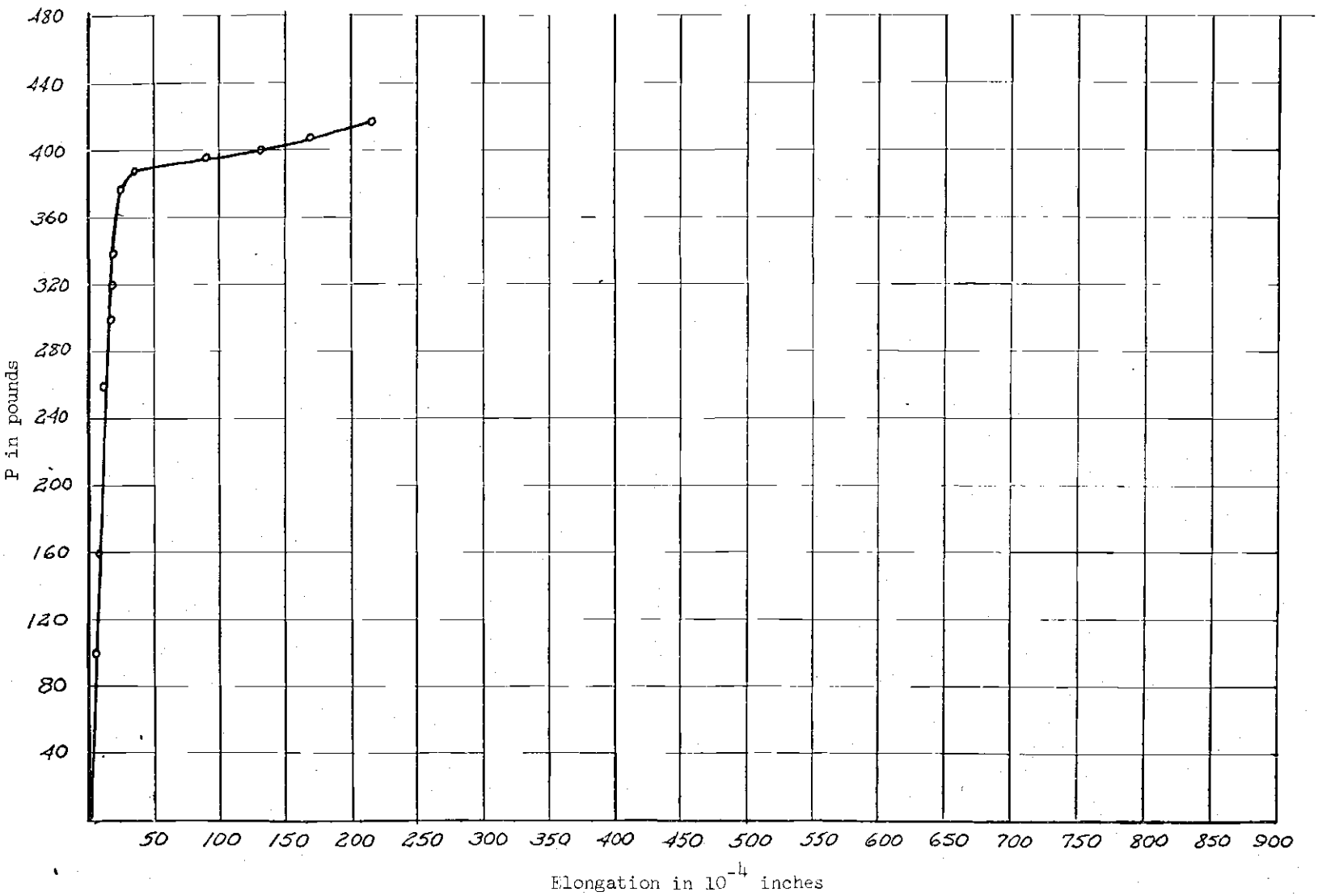

Figure 20. Load vs. Elongation Curve for Tensile Test I

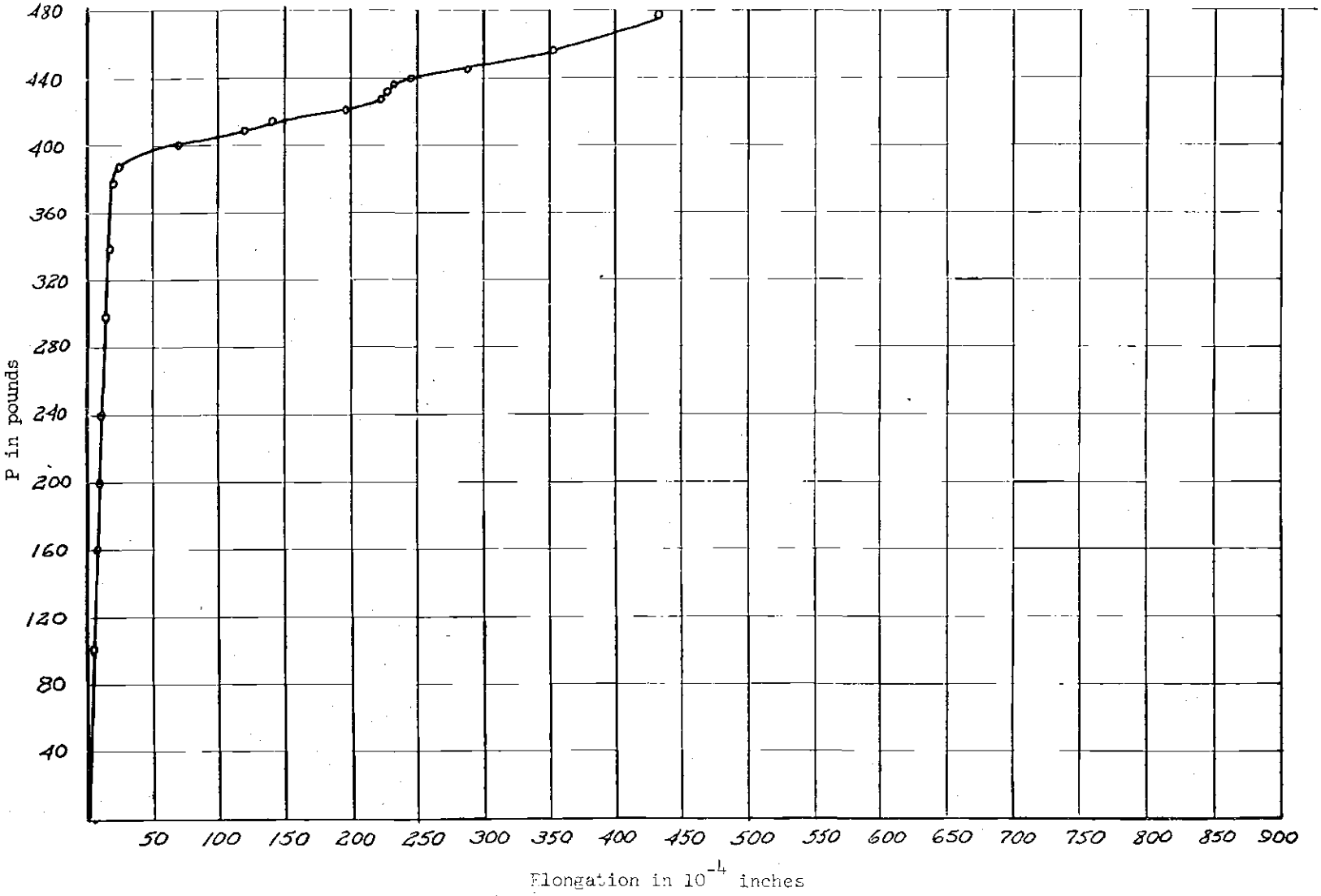

Figure 21. Load vs. Elongation Curve for Tensile Test II

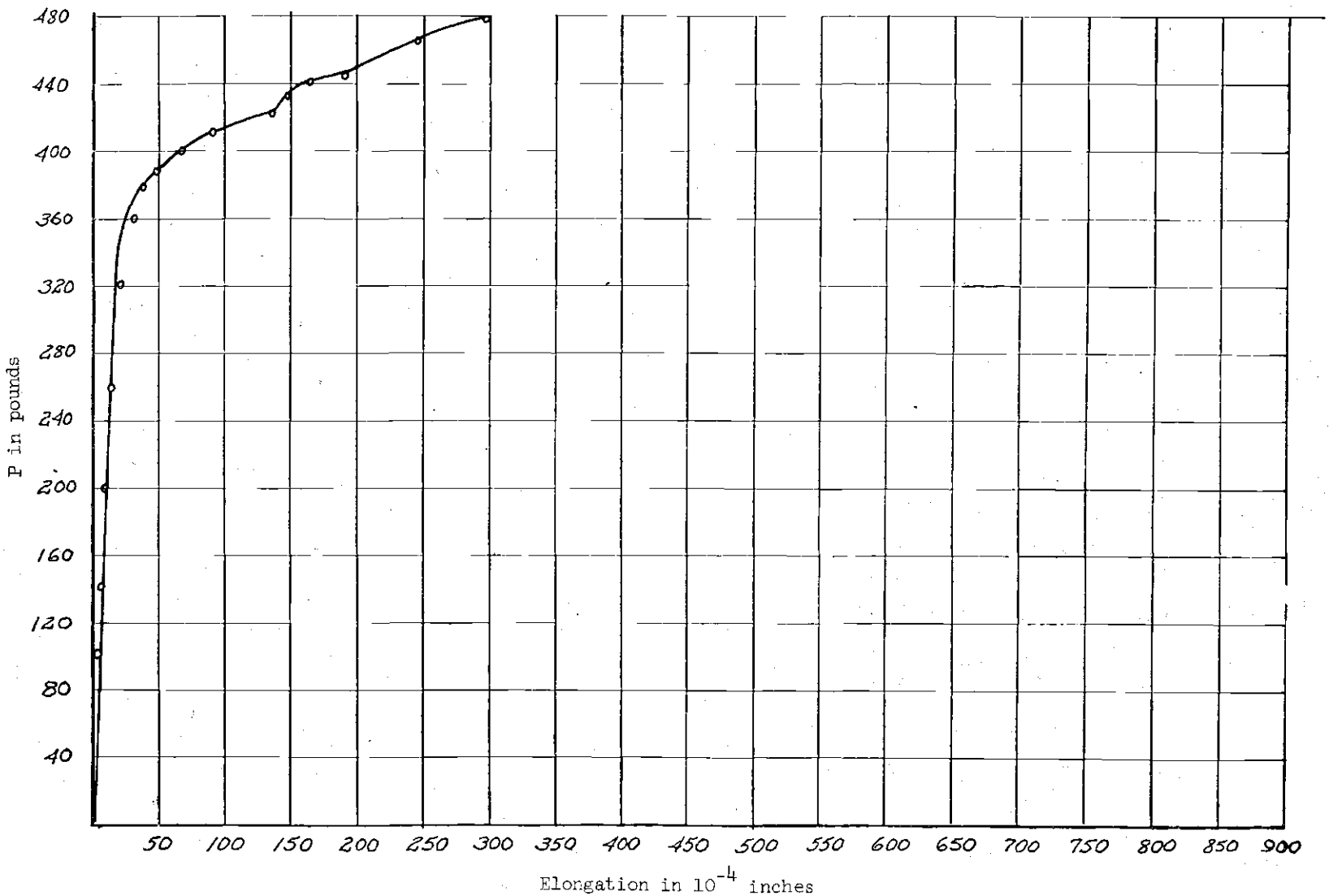

Figure 23. Load versus Elongation Curve for Tensile Test III

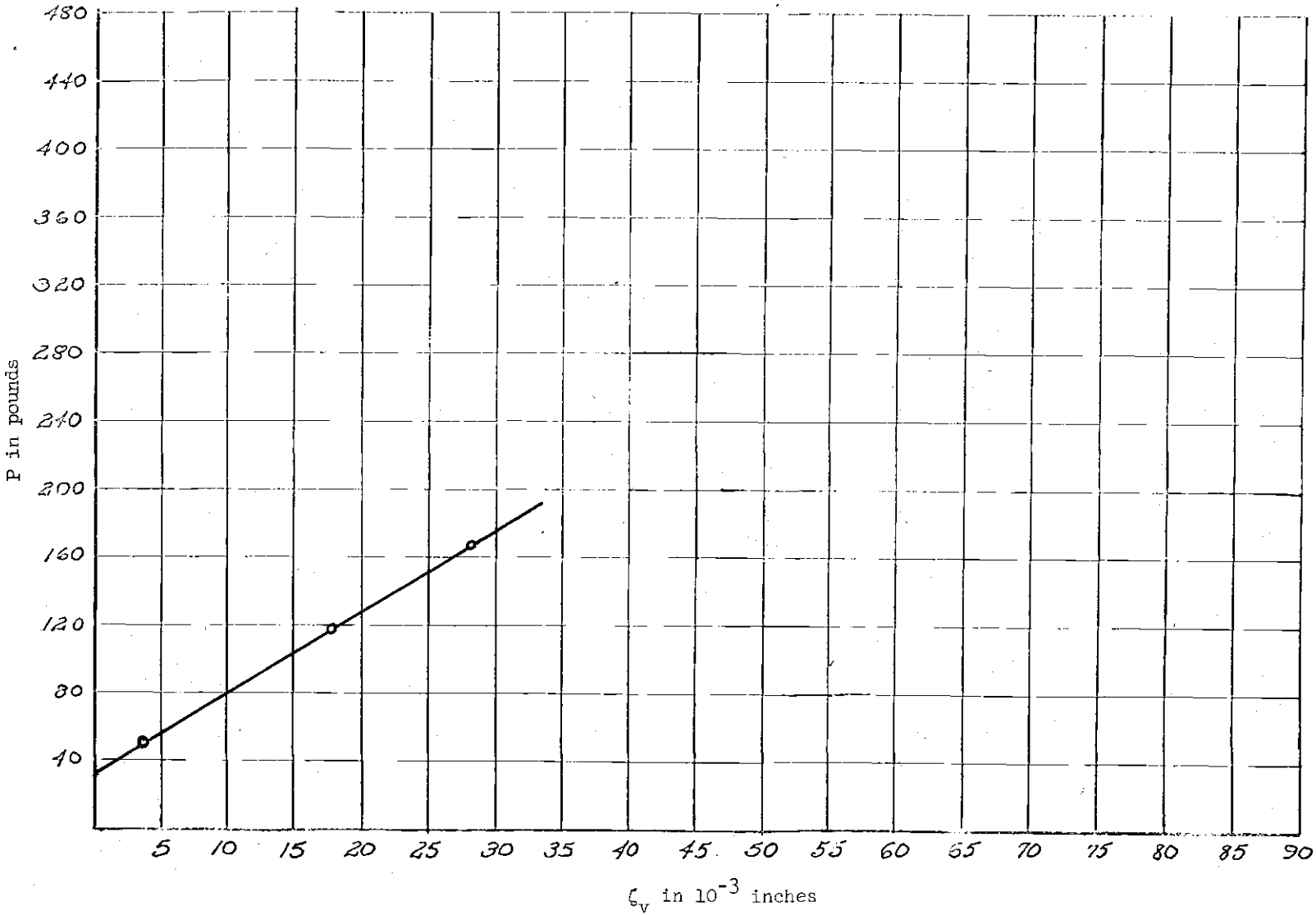

Figure 24. P versus ζ_v Curve for Test I(a)

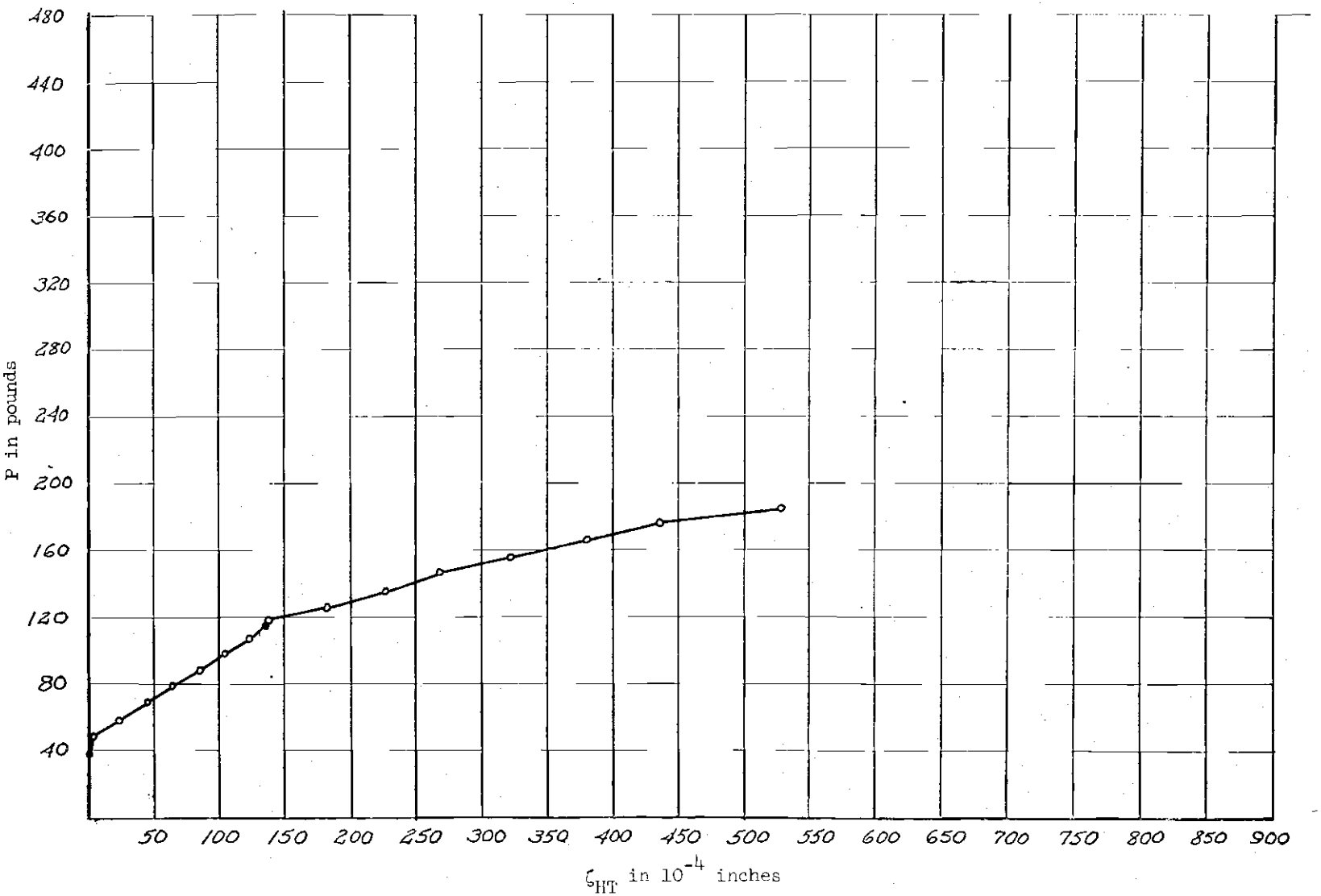

Figure 25. P versus ζ_{HT} Curve for Test I(a)

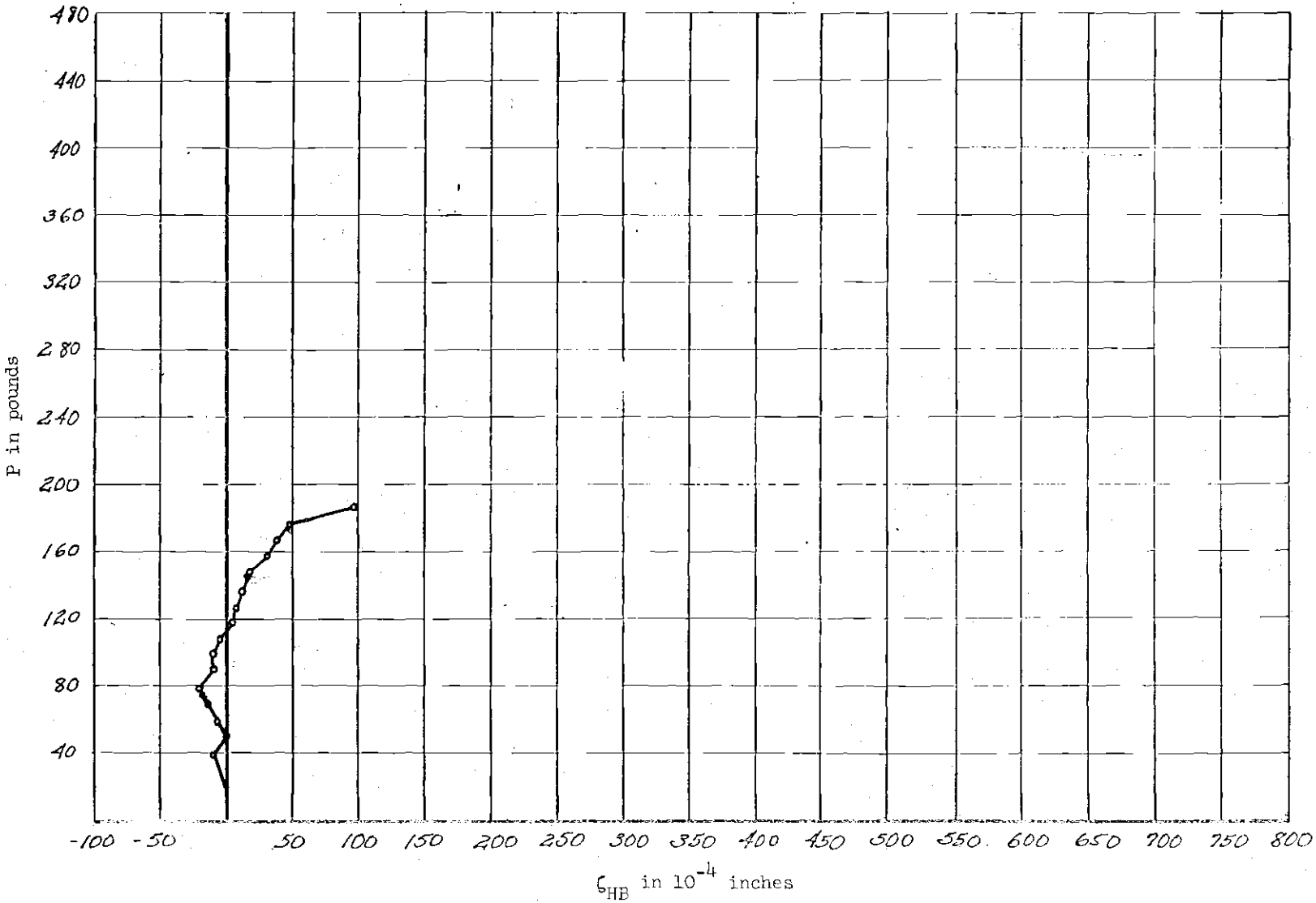

Figure 26. P versus ζ_{HB} Curve for Test I(a)

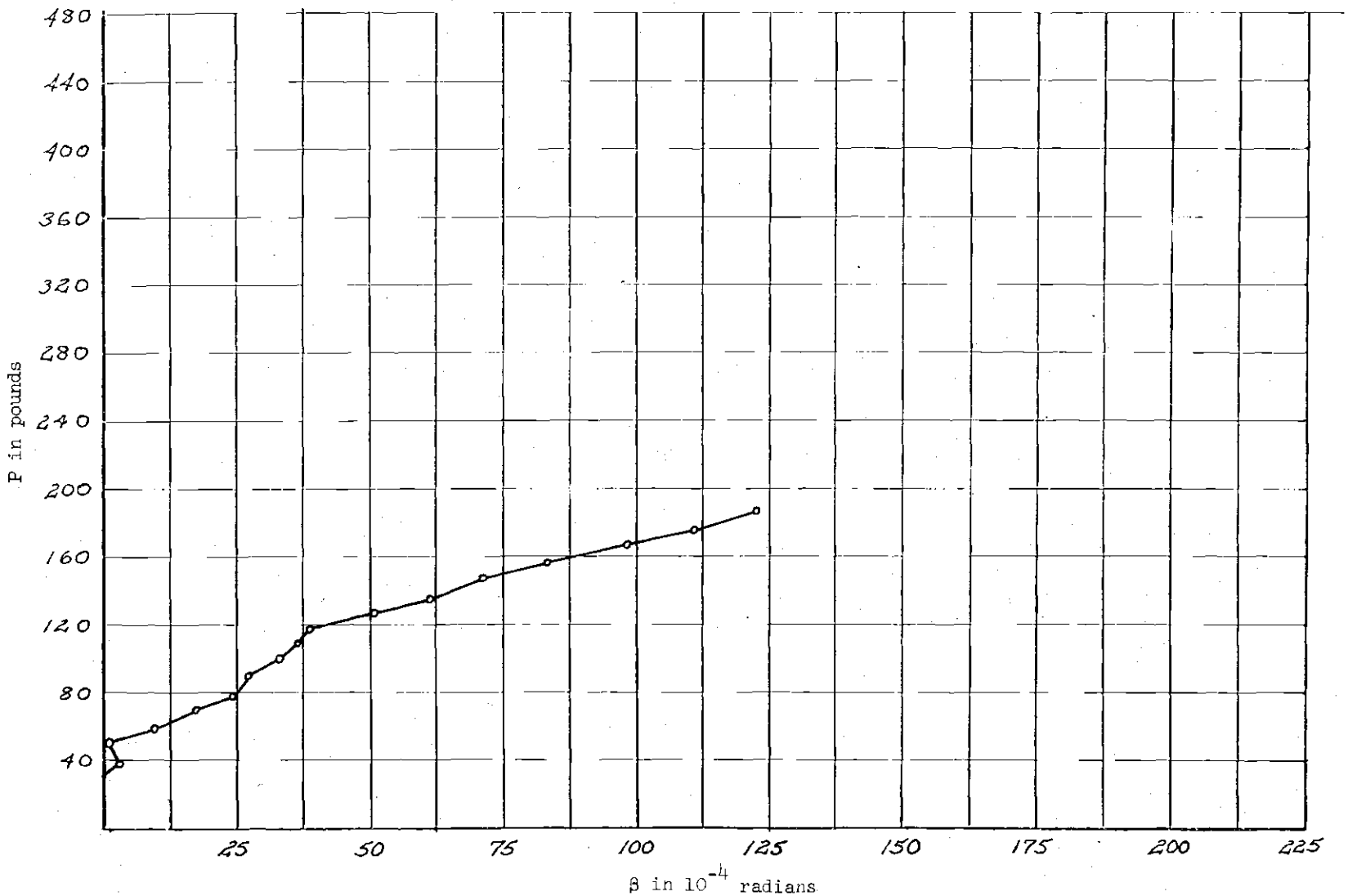

Figure 27. Twist Curve for Test I(a)

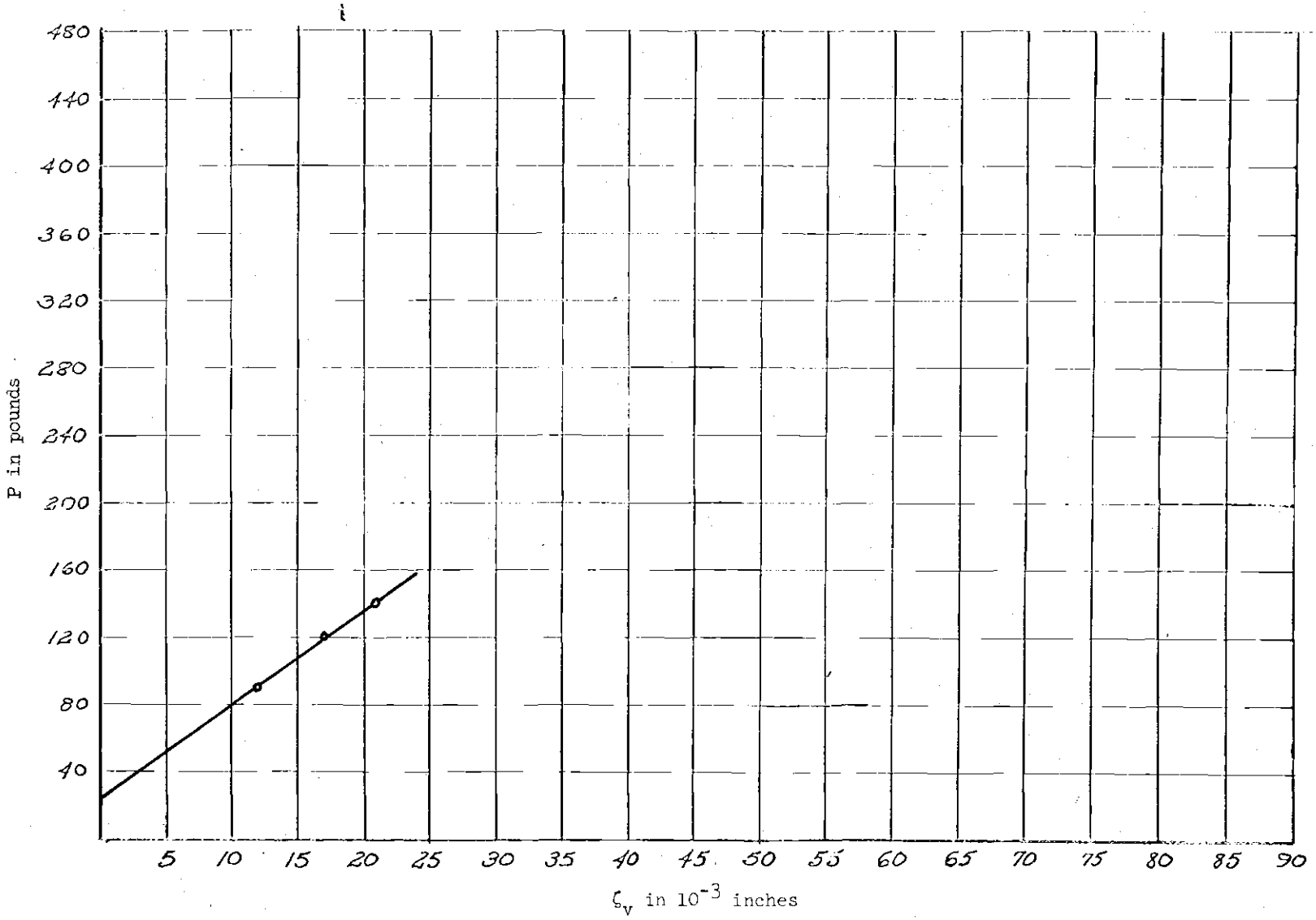

Figure 28. P versus ζ_v Curve for Test I(b)

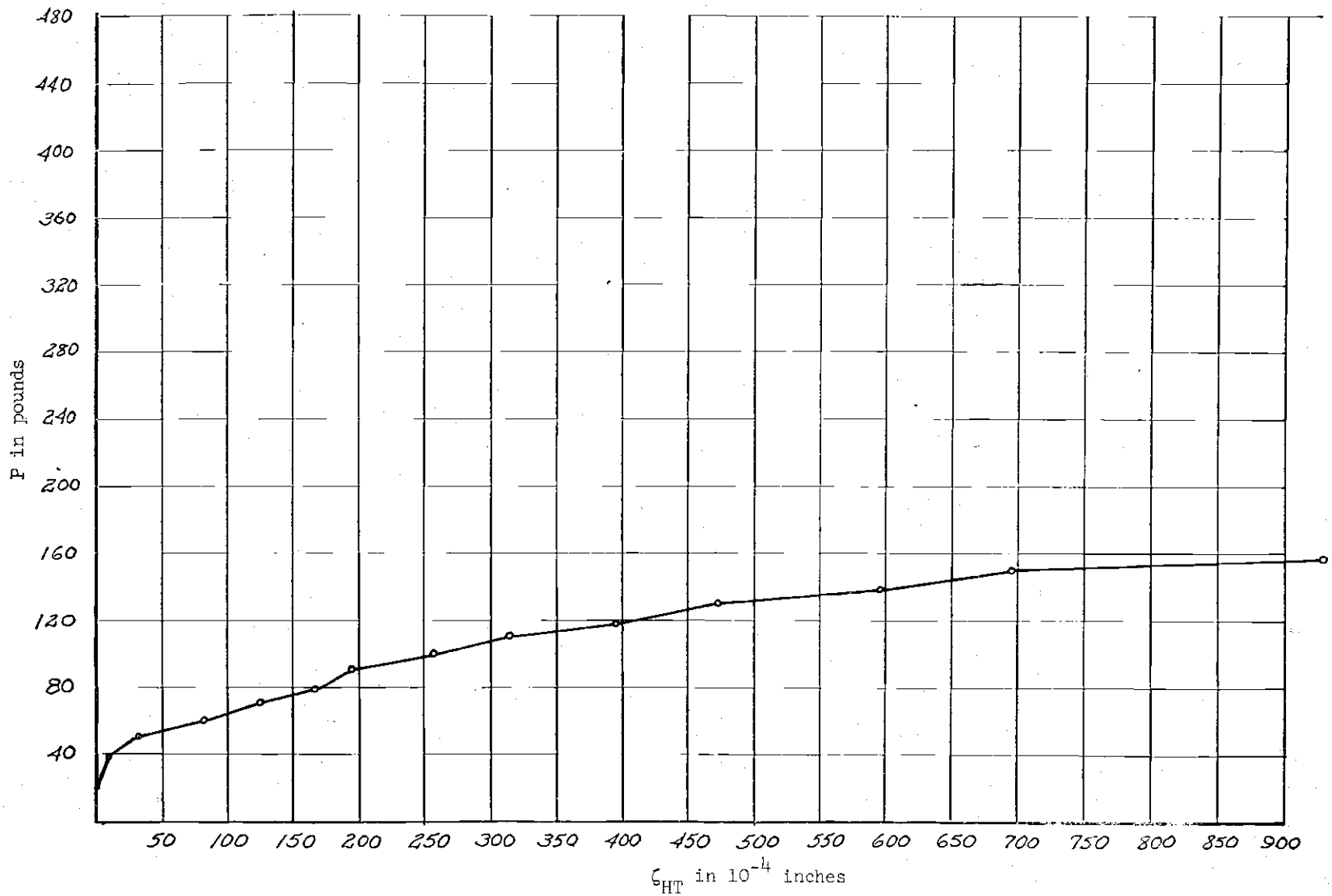

Figure 29. P versus ζ_{HT} Curve for Test I(b)

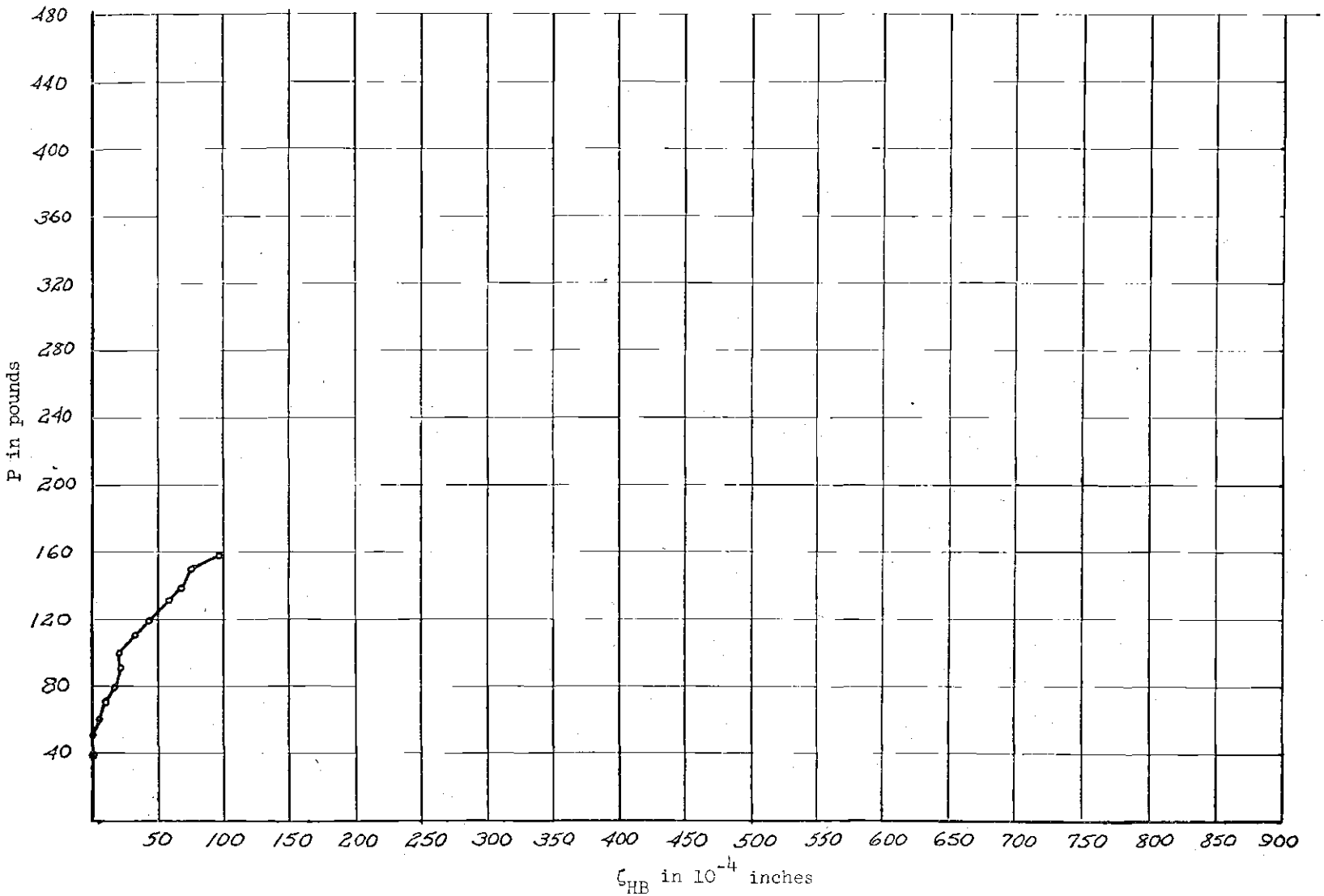

Figure 30. P versus ζ_{HB} Curve for Test I(b)

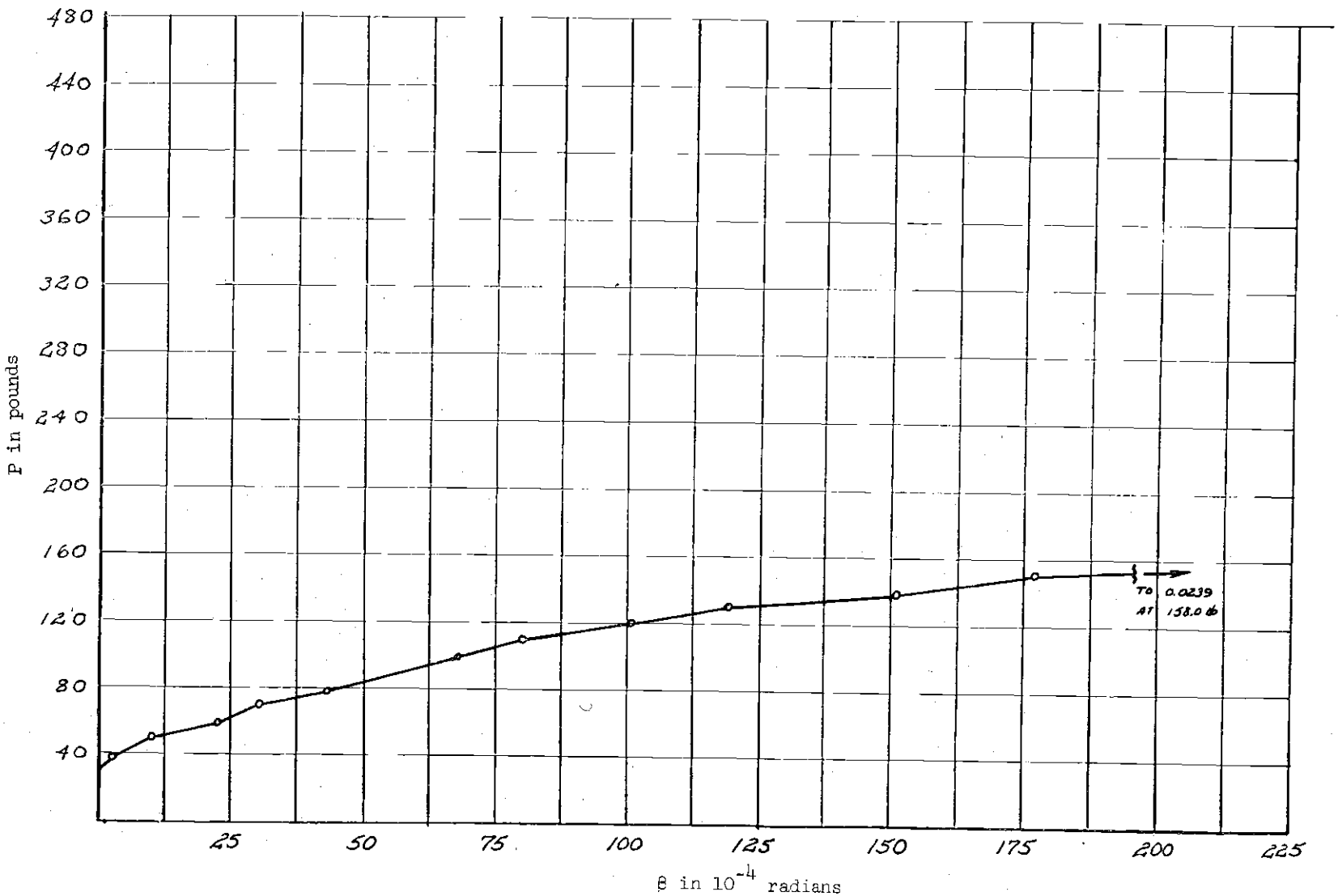

Figure 31. Twist Curve for Test I(b)

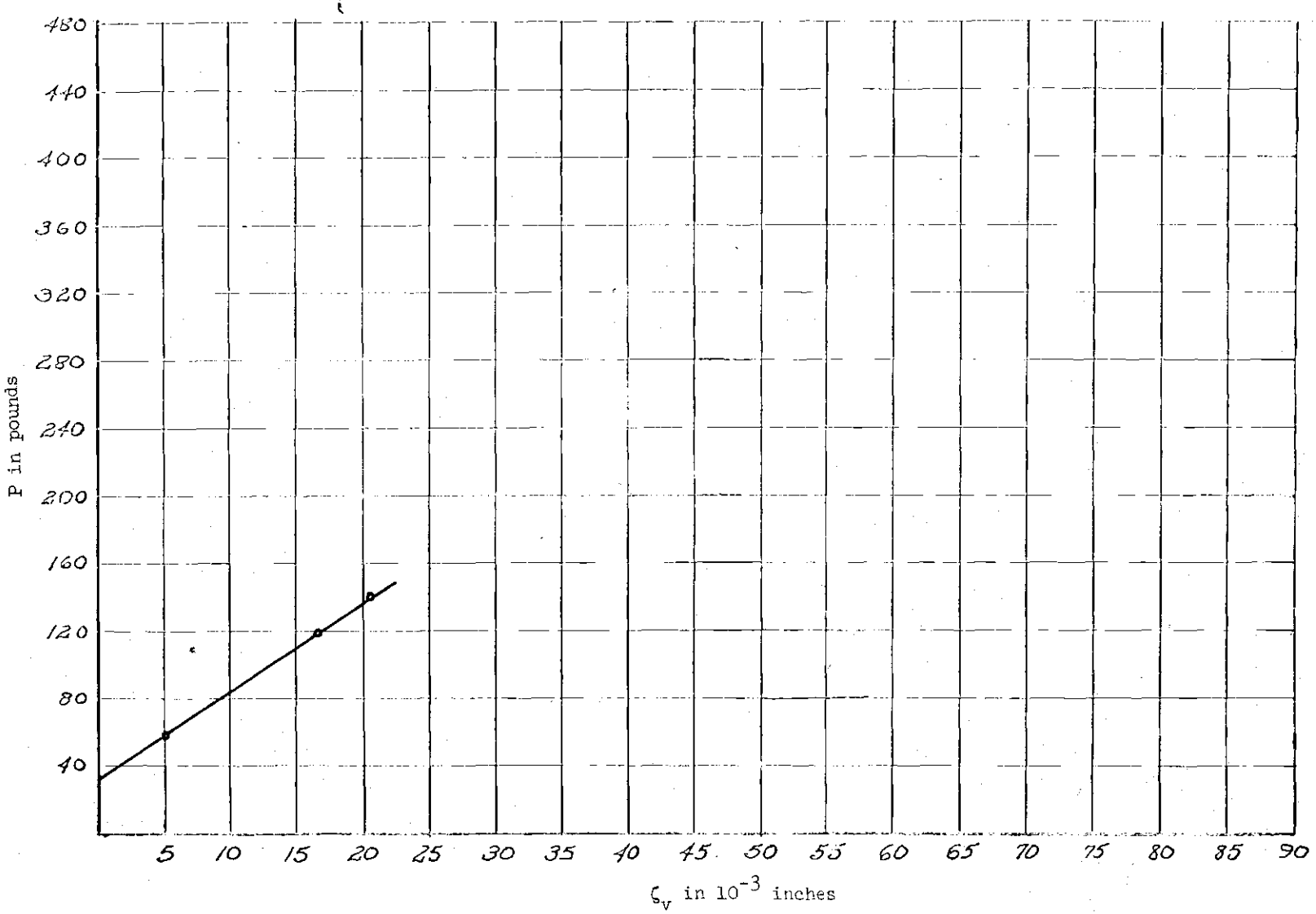

Figure 32. P versus ζ_v Curve for Test I(c)

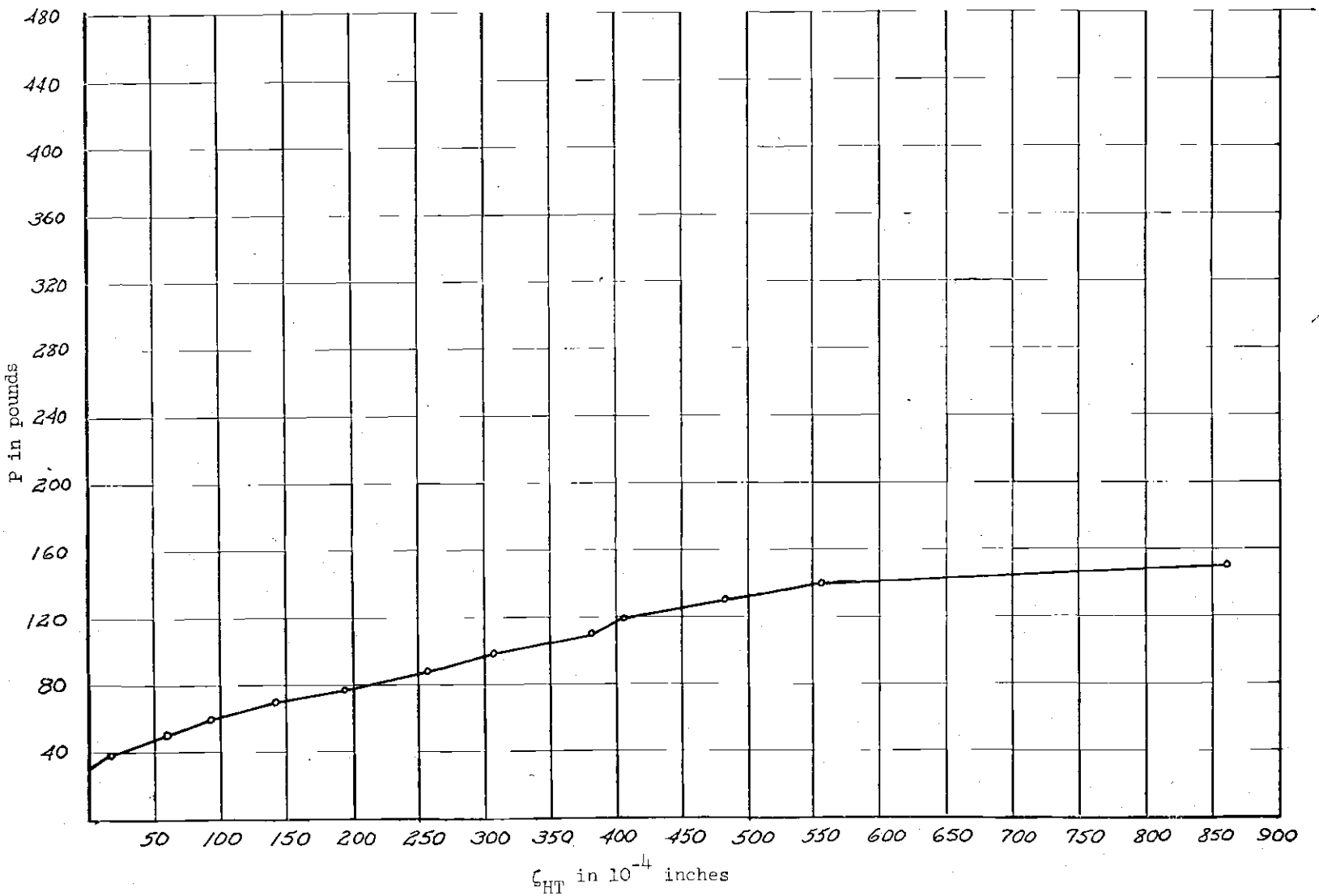

Figure 33. P versus ζ_{HT} Curve for Test I(c)

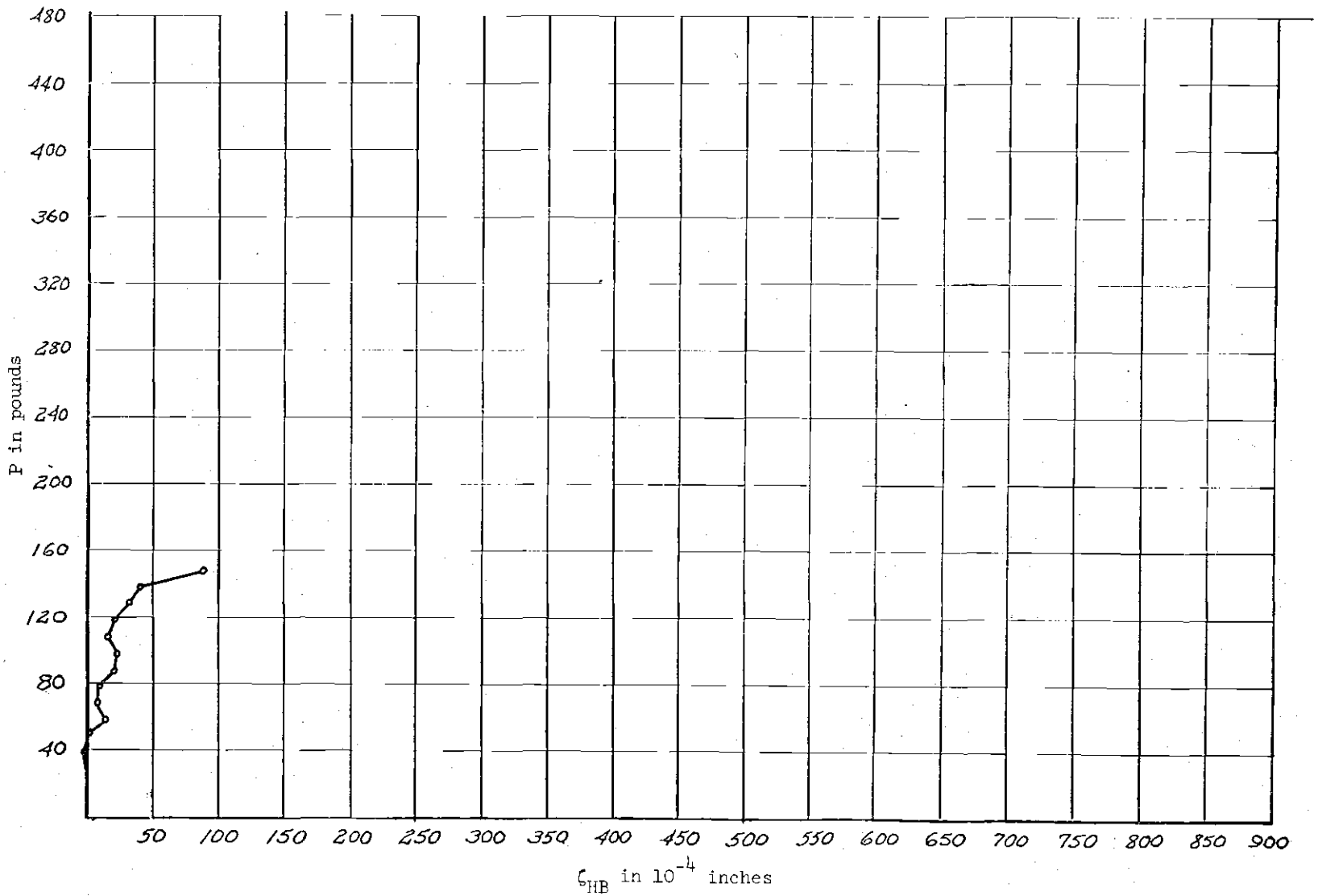

Figure 34. P versus ζ_{HB} Curve for Test I(c)

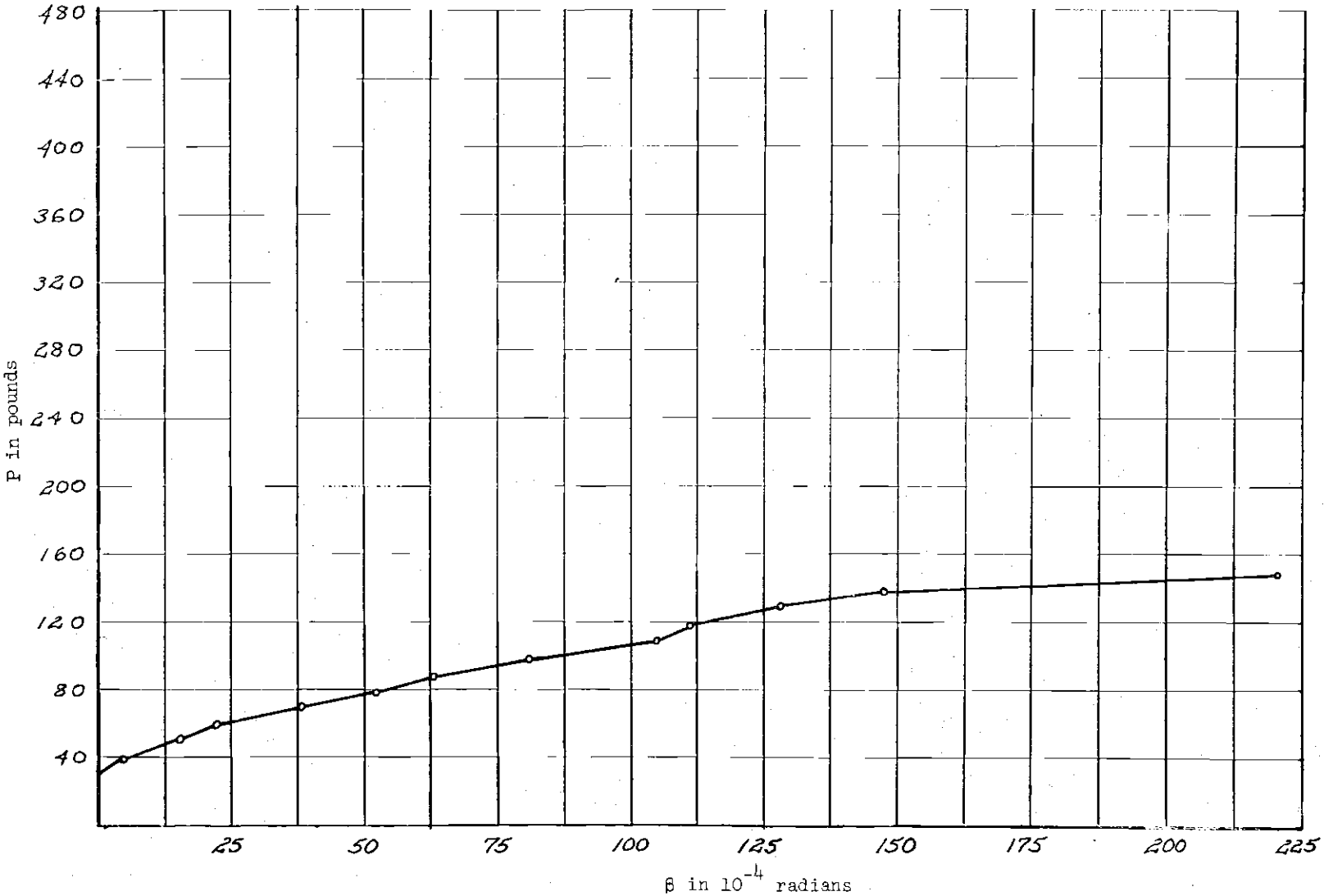

Figure 35. Twist Curve for Test I(c)

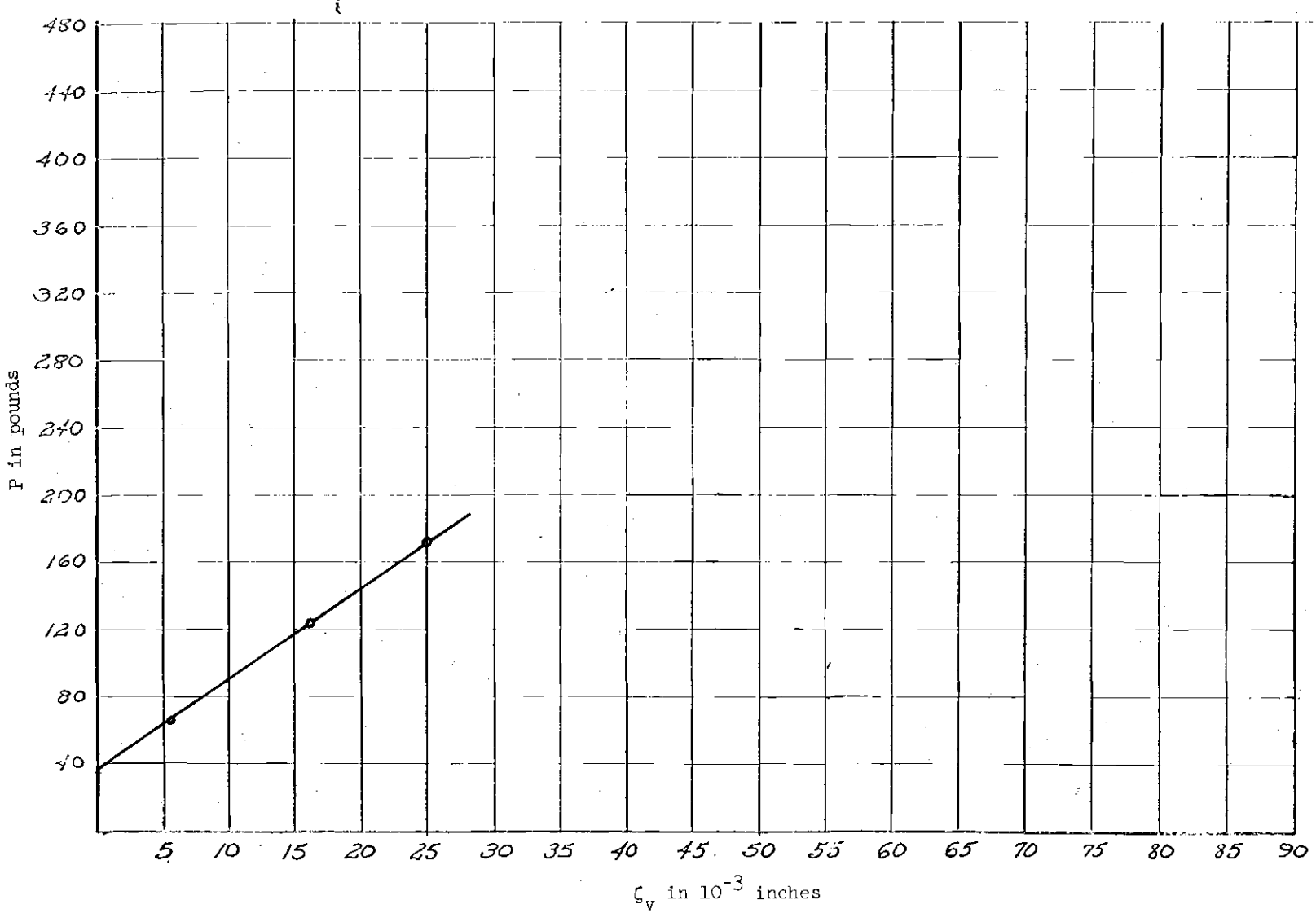

Figure 36. P versus ζ_v Curve for Test I(e)

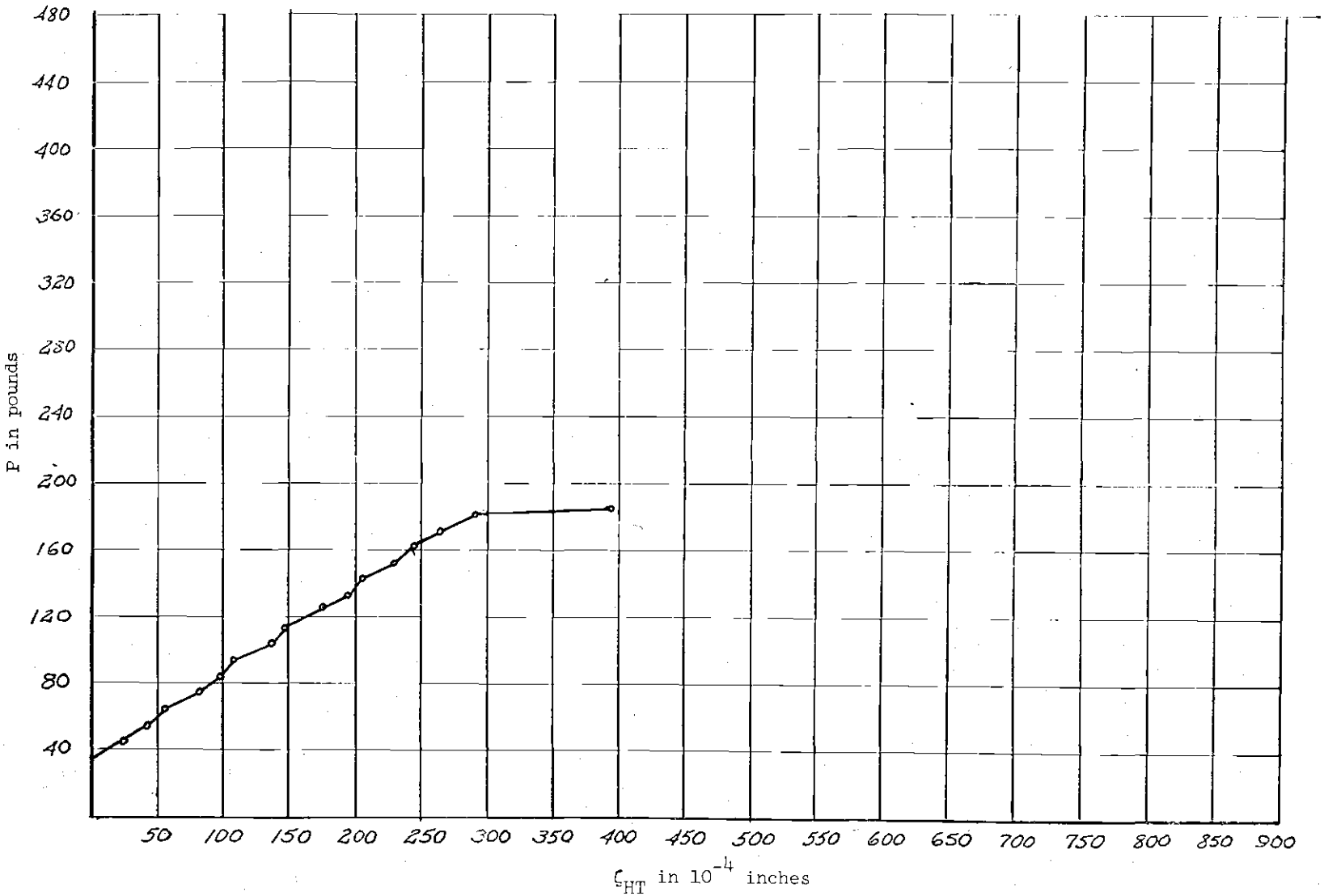

Figure 37. P versus ζ_{HT} Curve for Test I(e)

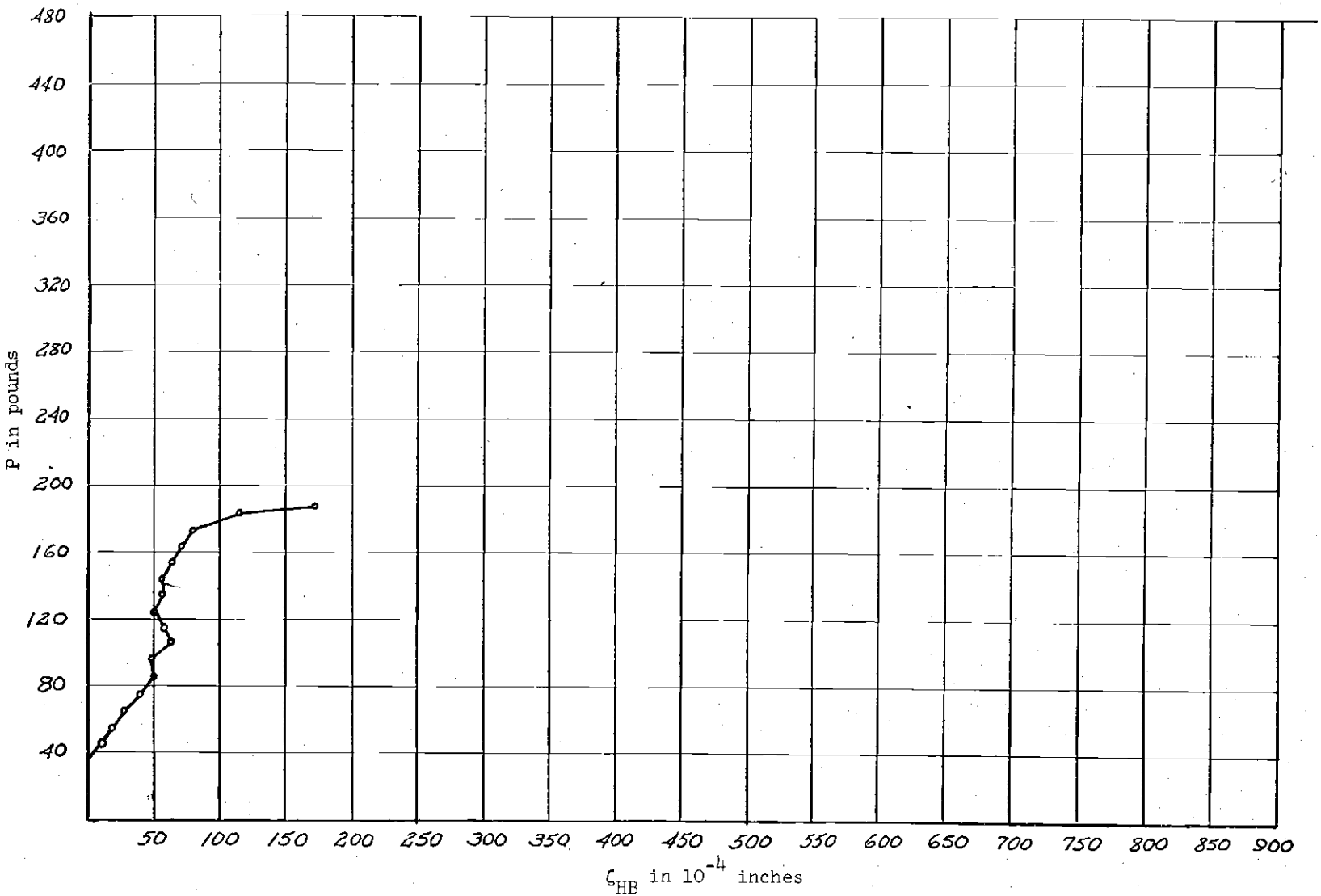

Figure 38. P versus ζ_{HB} Curve for Test I(e)

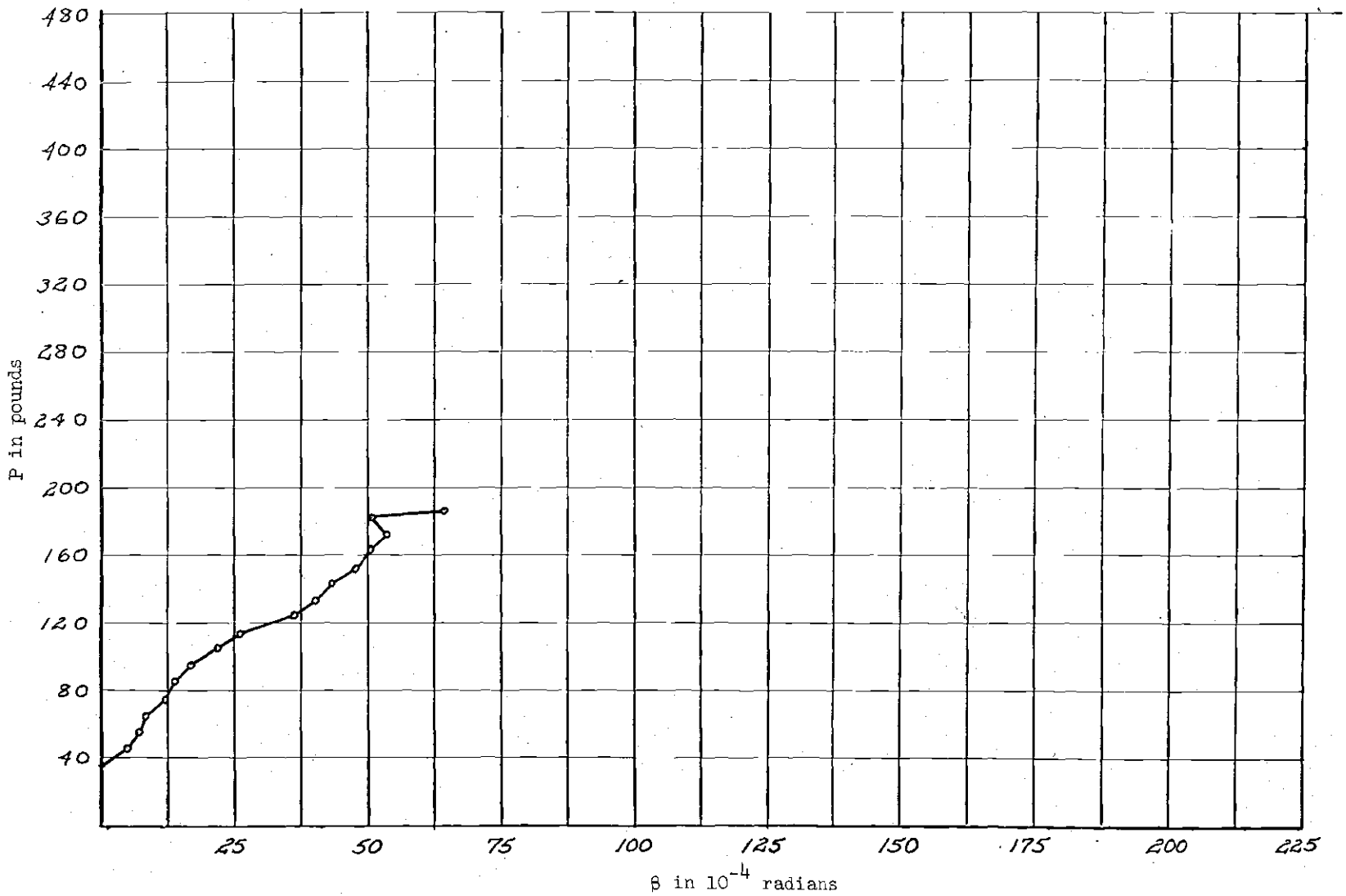

Figure 39. Twist Curve for Test I(e)

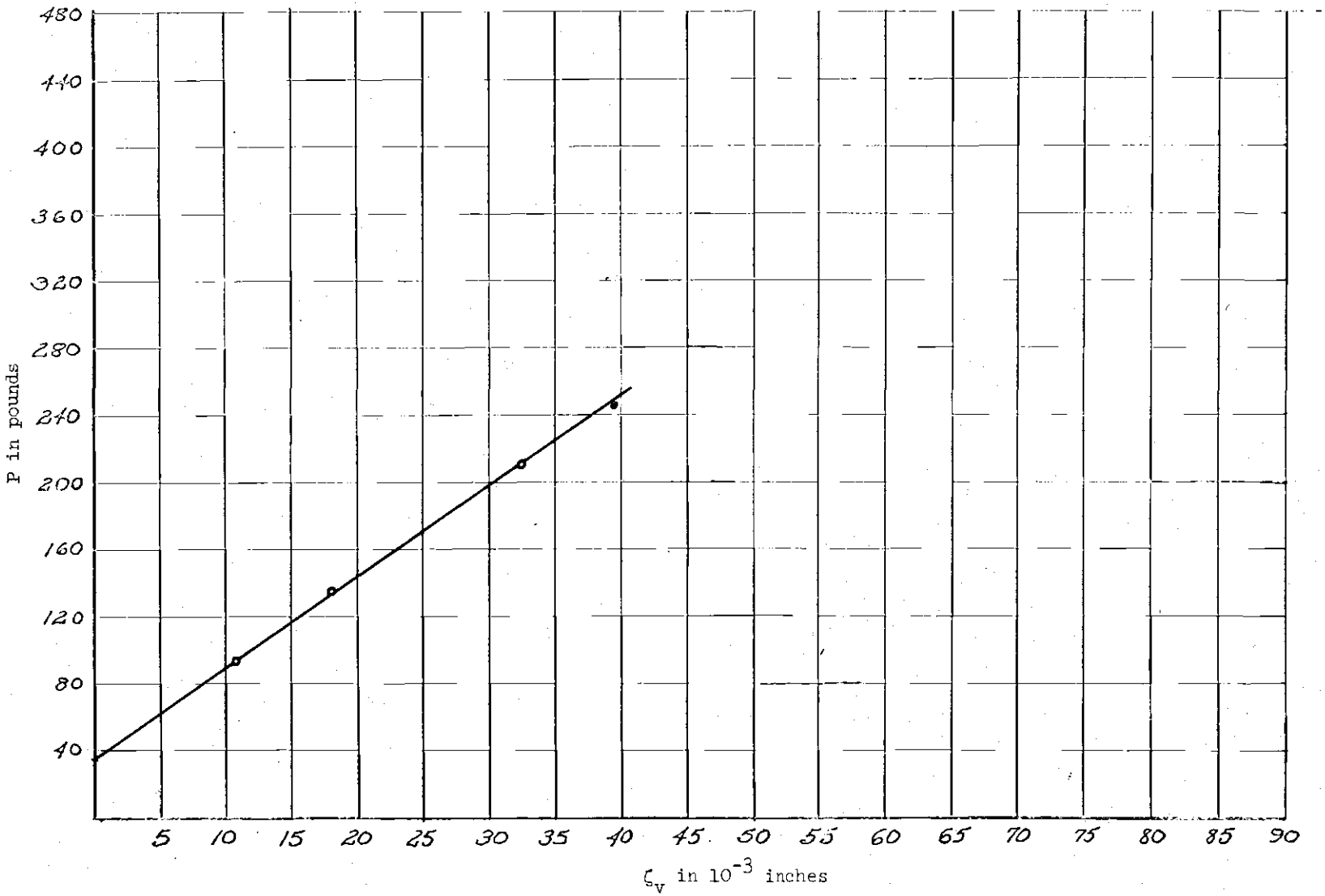

Figure 40. P versus ζ_v Curve for Test II(a)

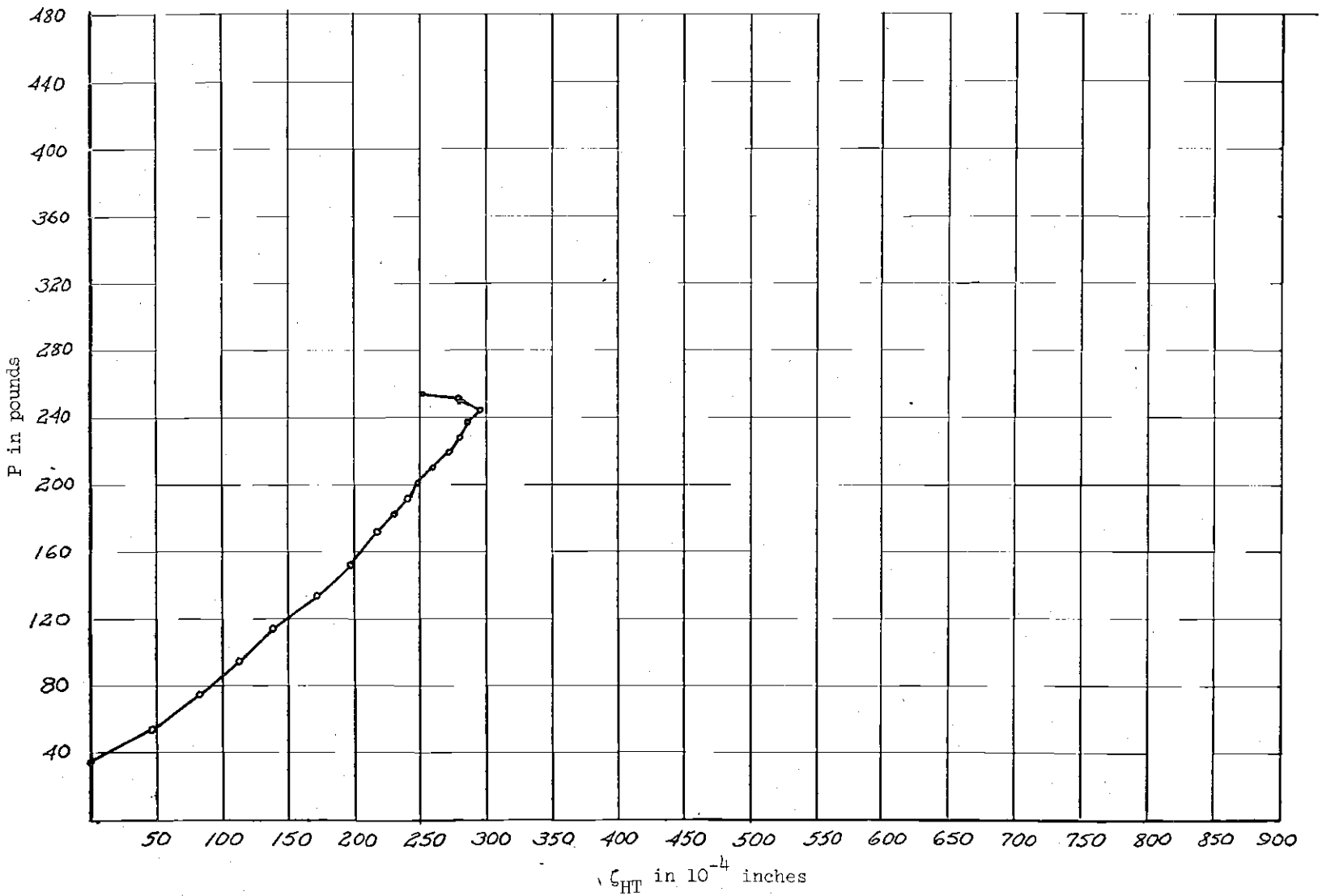

Figure 41. P versus ζ_{HT} Curve for Test II(a)

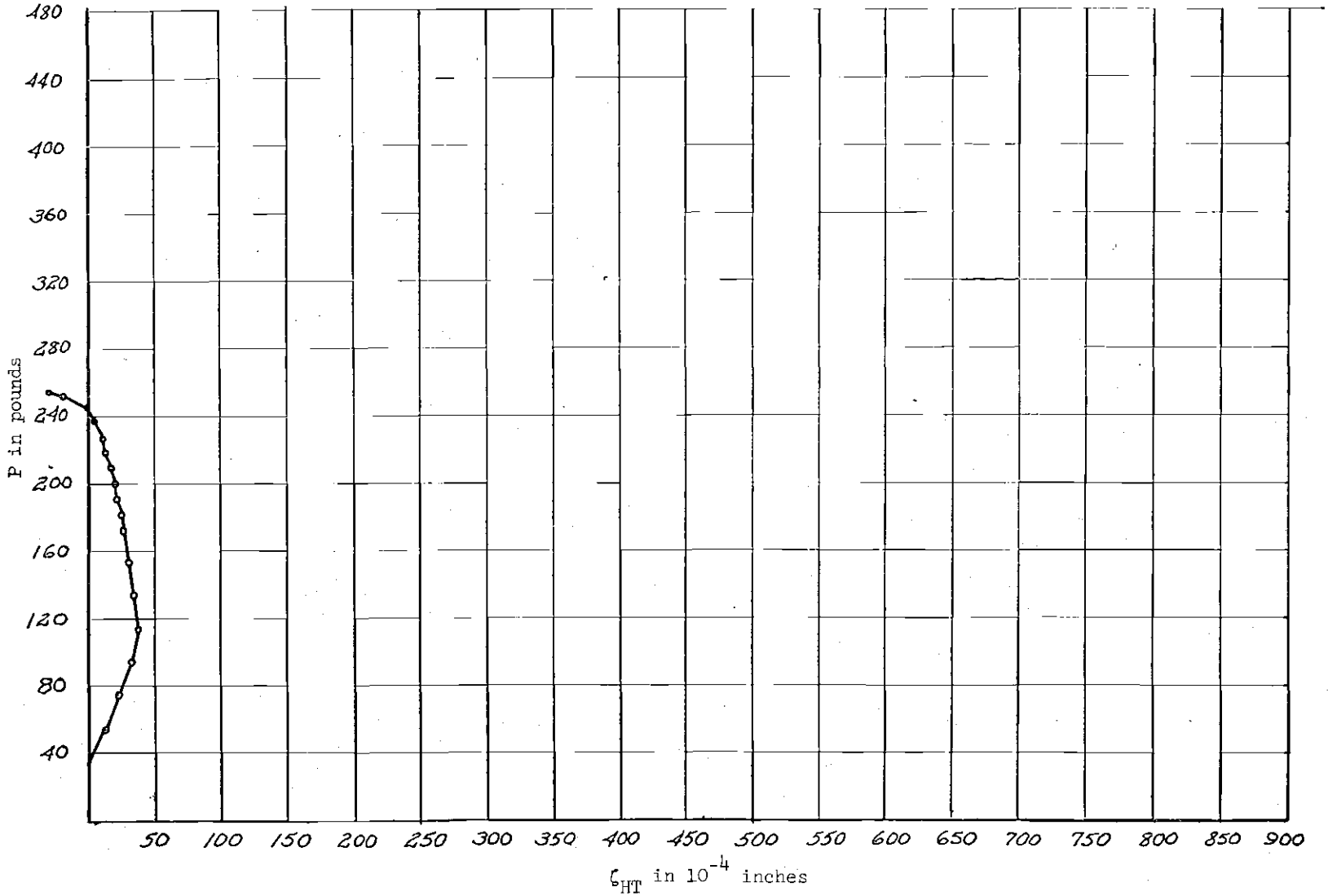

Figure 42. P versus ζ_{HB} Curve for Test II(a)

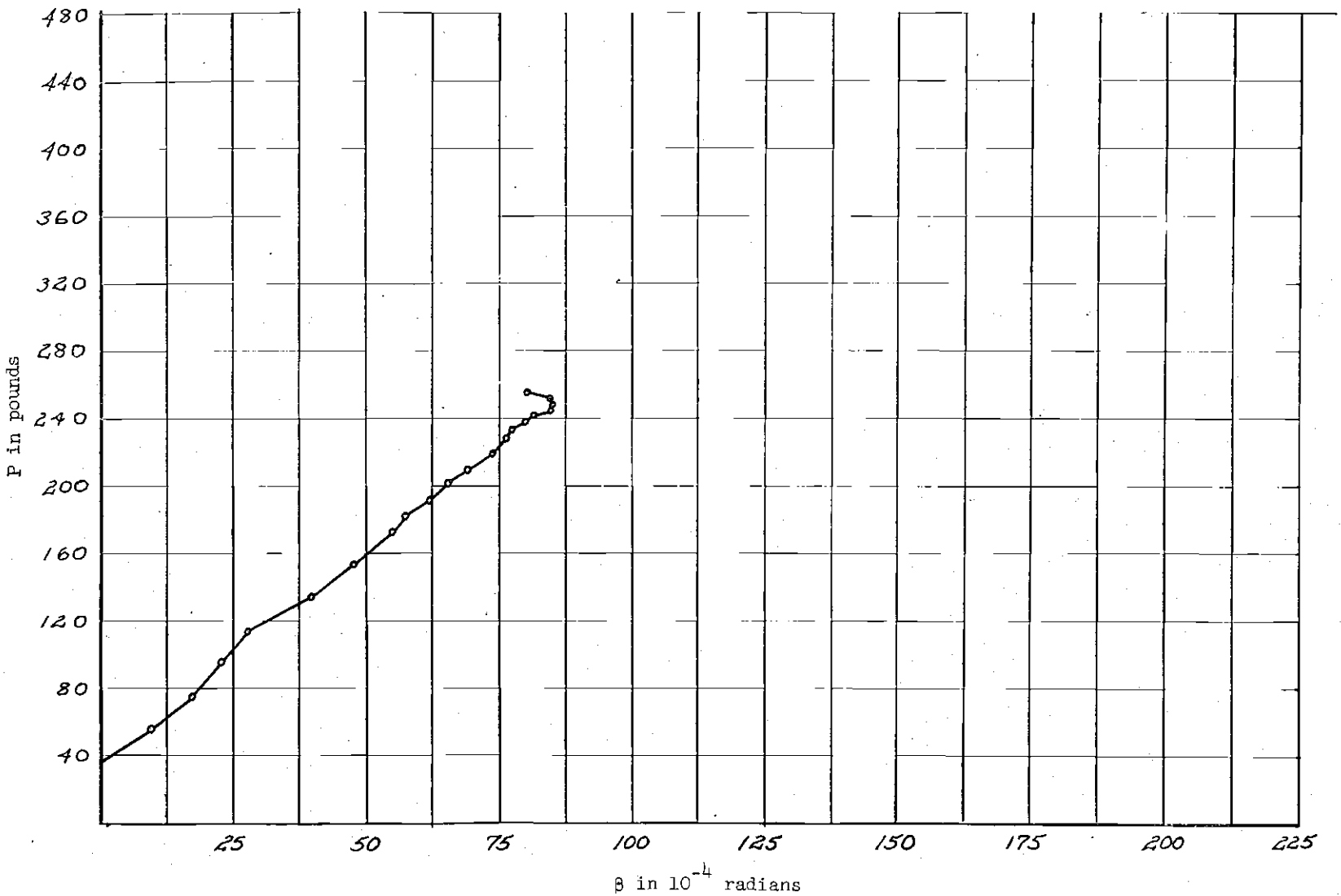

Figure 43. Twist Curve for Test II(a)

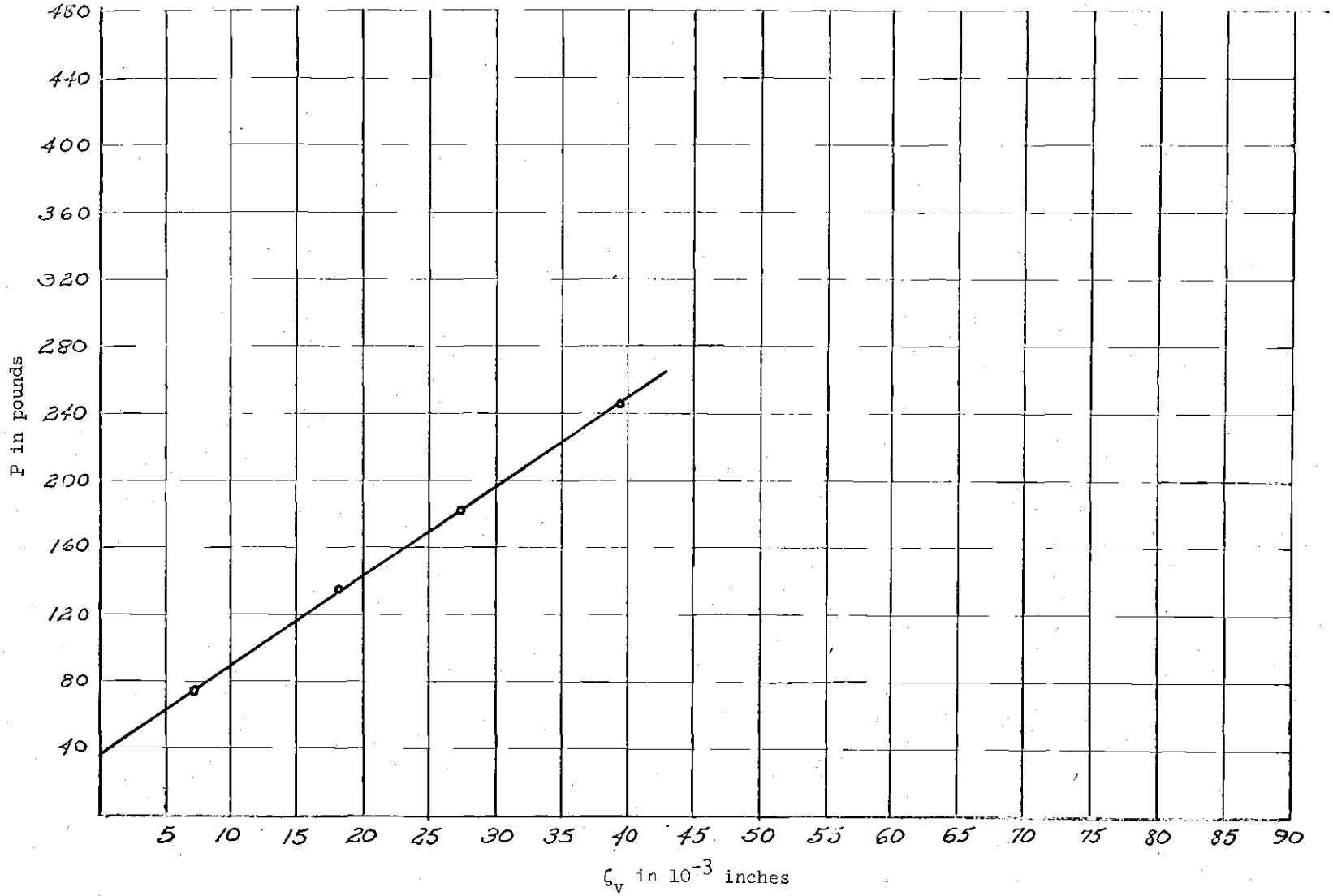

Figure 44. P versus ζ_v Curve for Test II(b)

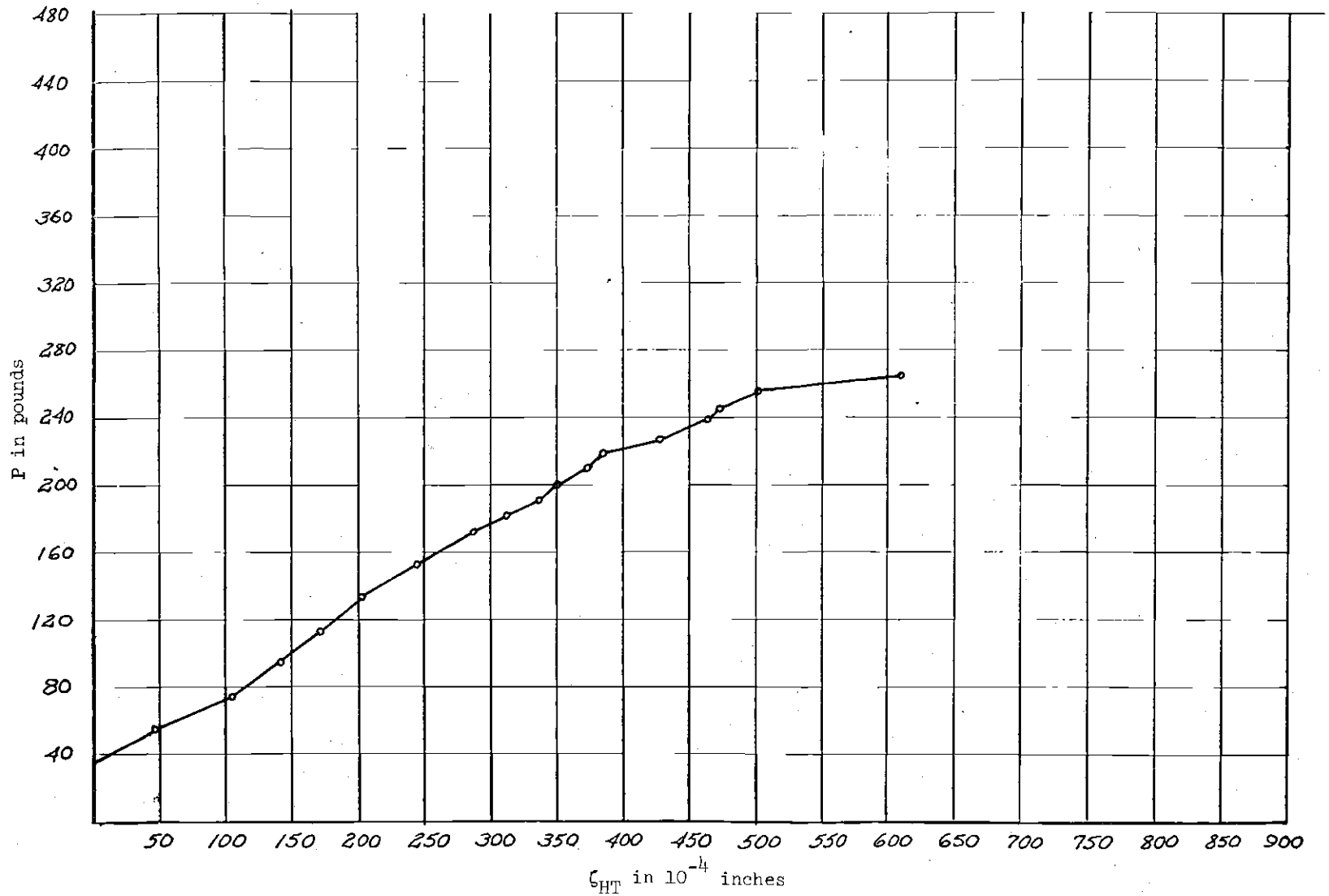

Figure 45. P versus ζ_{HT} Curve for Test II(b)

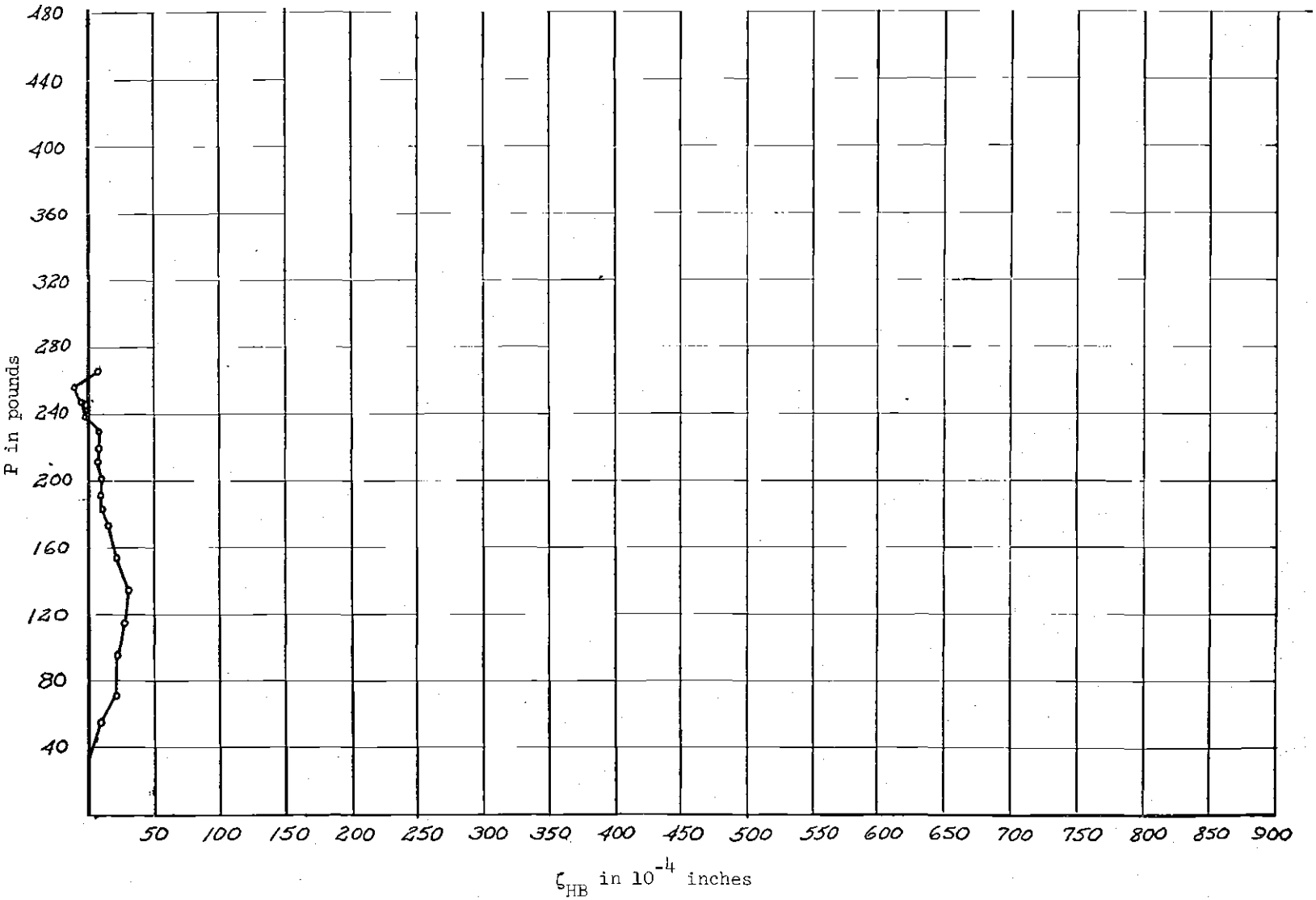

Figure 46. P versus ζ_{HB} Curve for Test II(b)

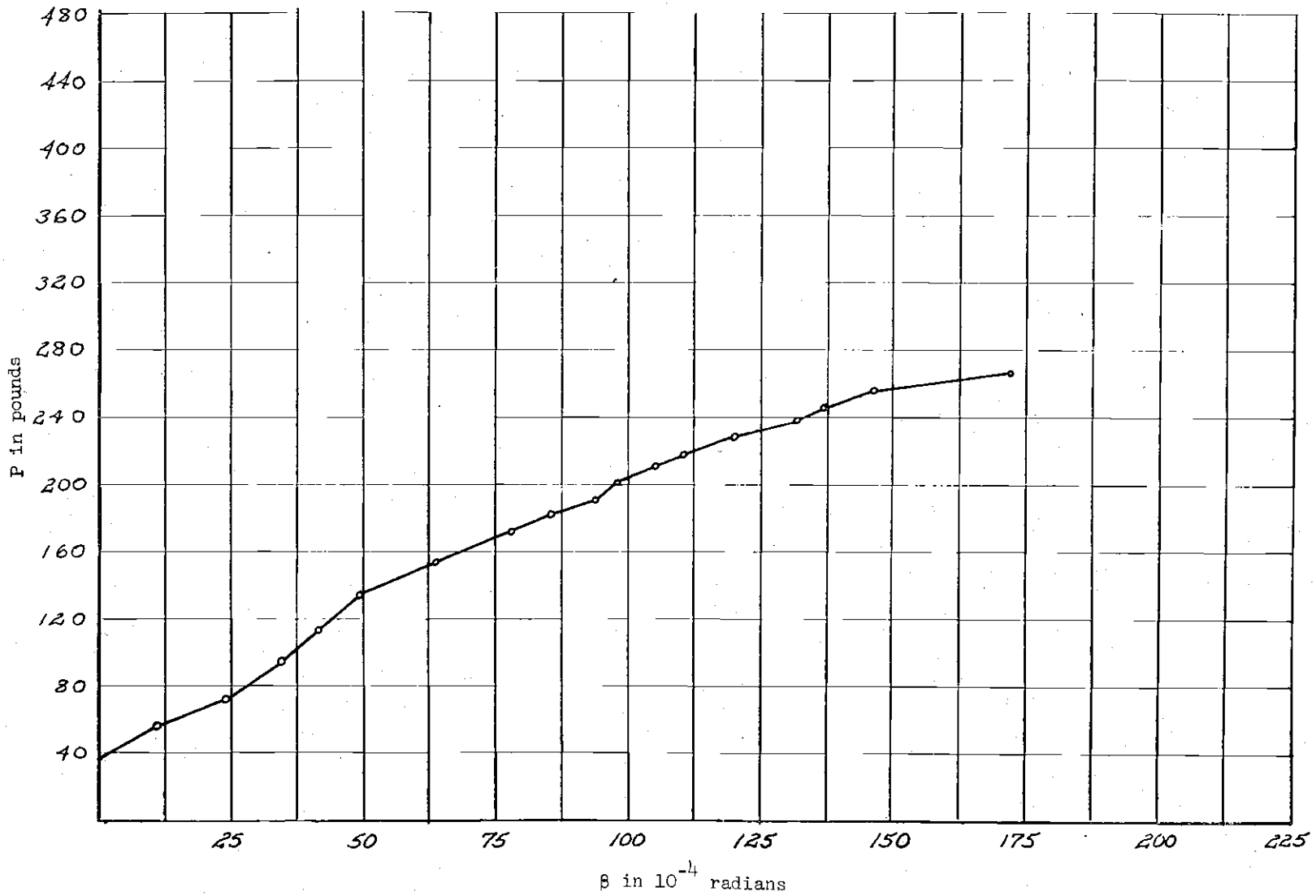

Figure 47. Twist Curve for Test II(b)

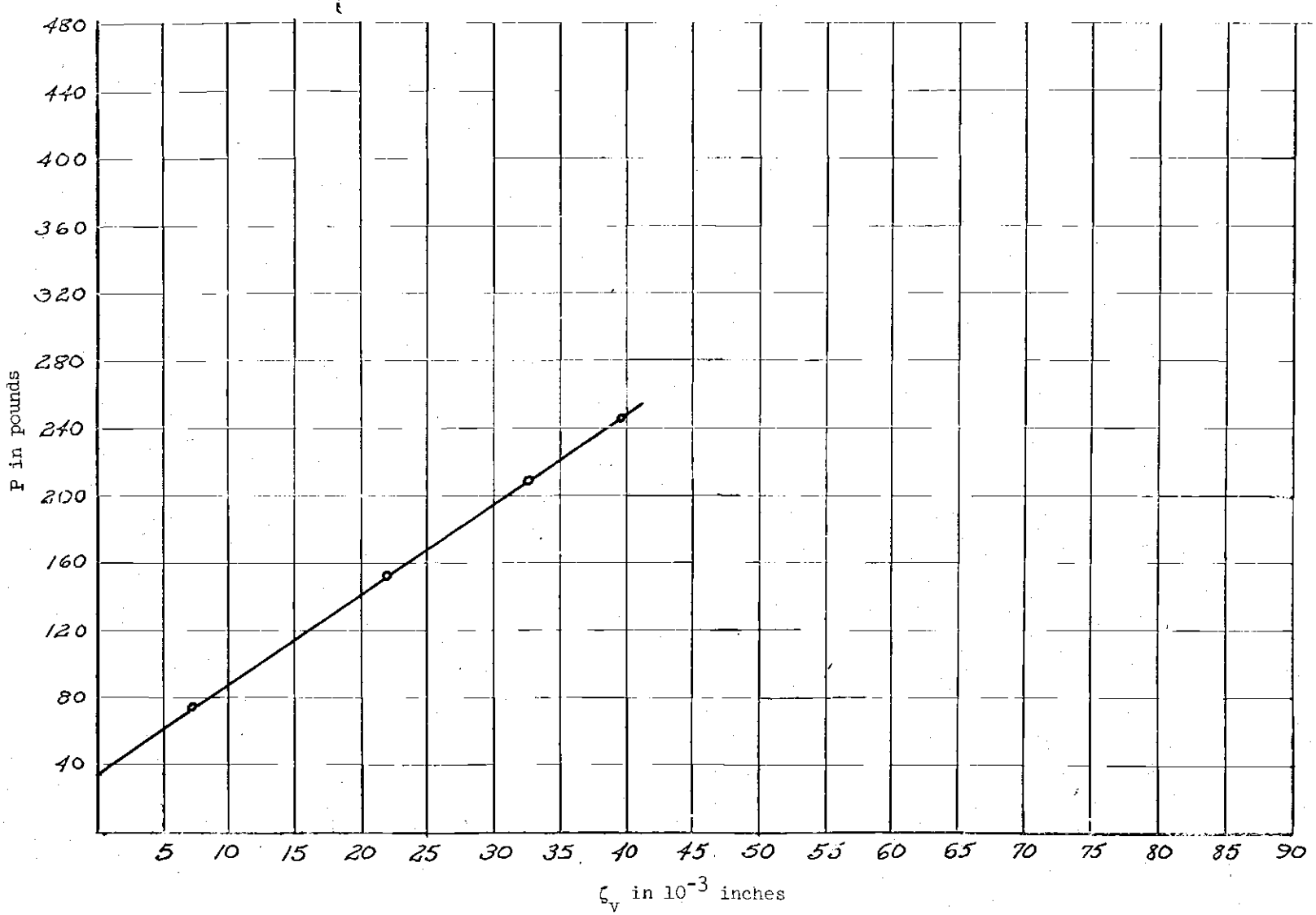

Figure 48. P versus ζ_v Curve for Test III(a)

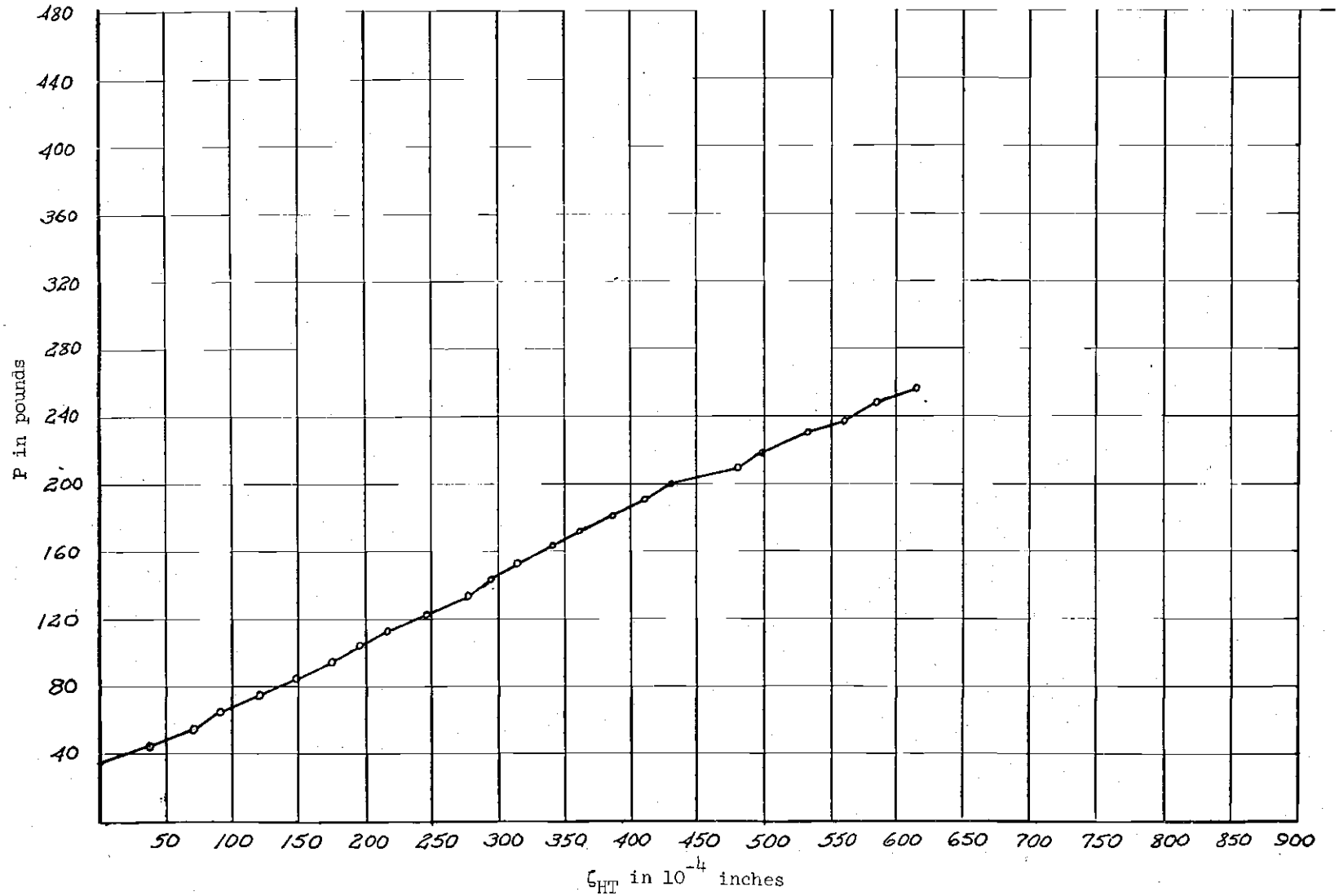

Figure 49. P versus ζ_{HT} Curve for Test III(a)

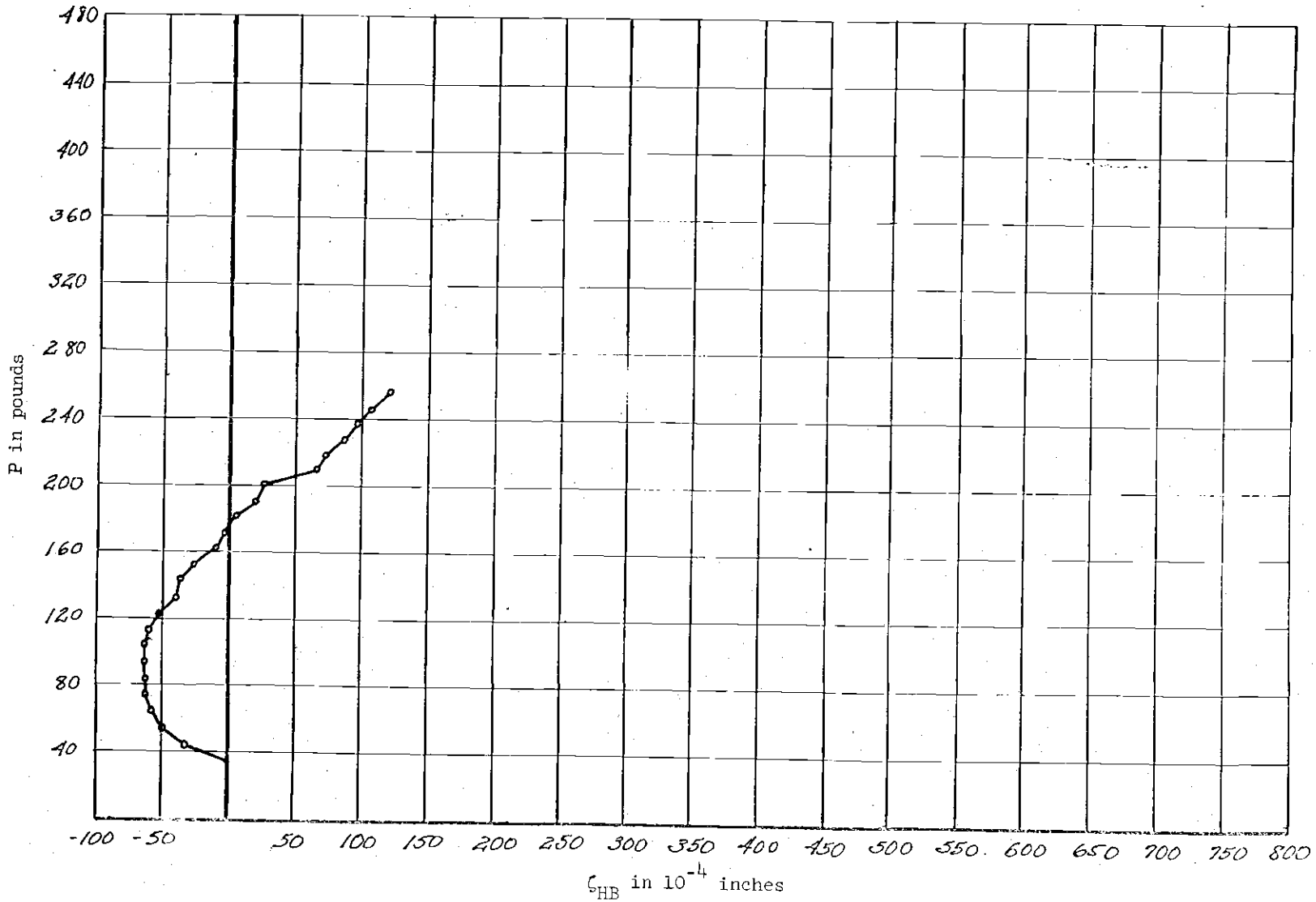

Figure 50. P versus ζ_{HB} Curve for Test III(a)

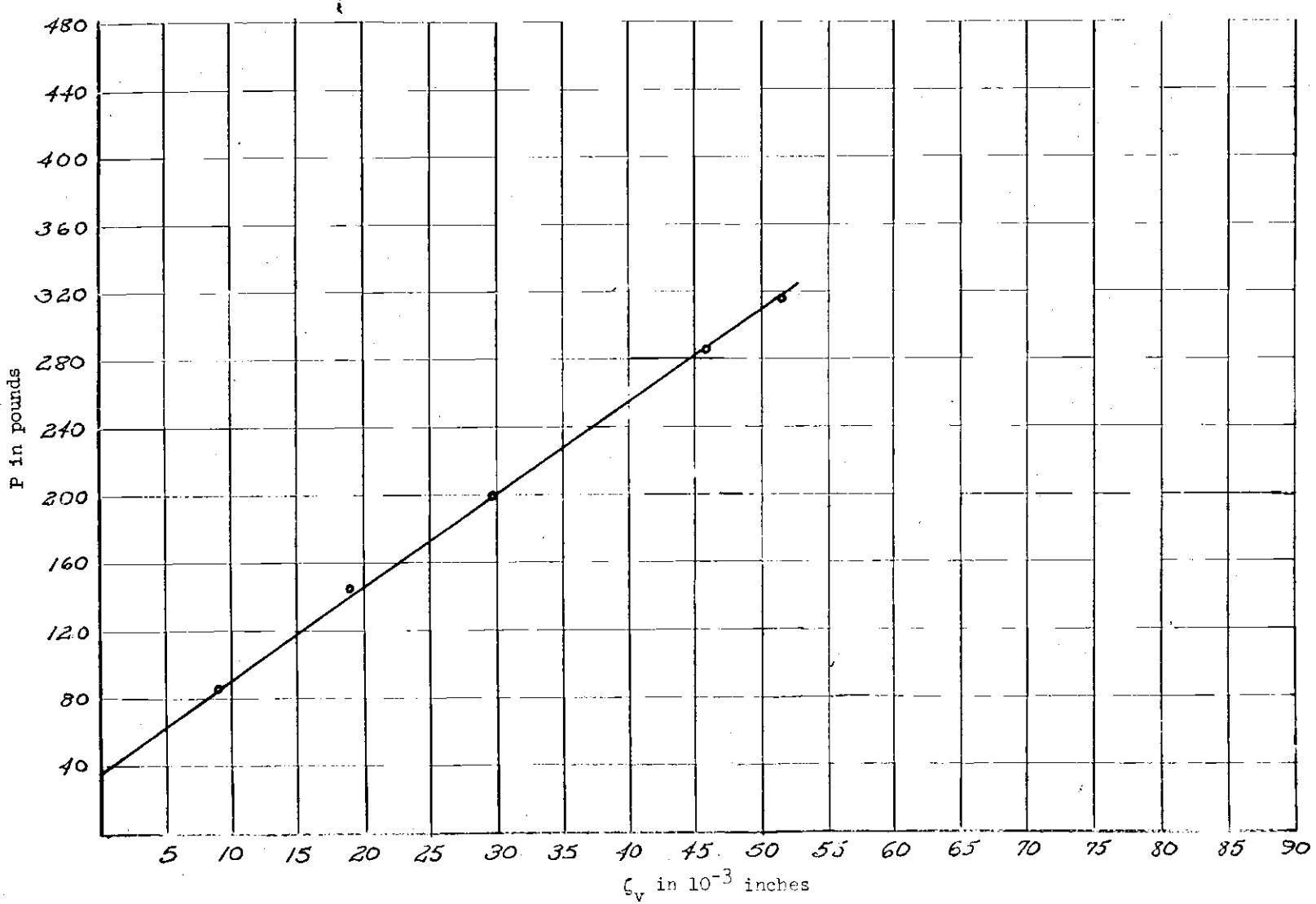

Figure 51. P versus ζ_v Curve for Test III(b)

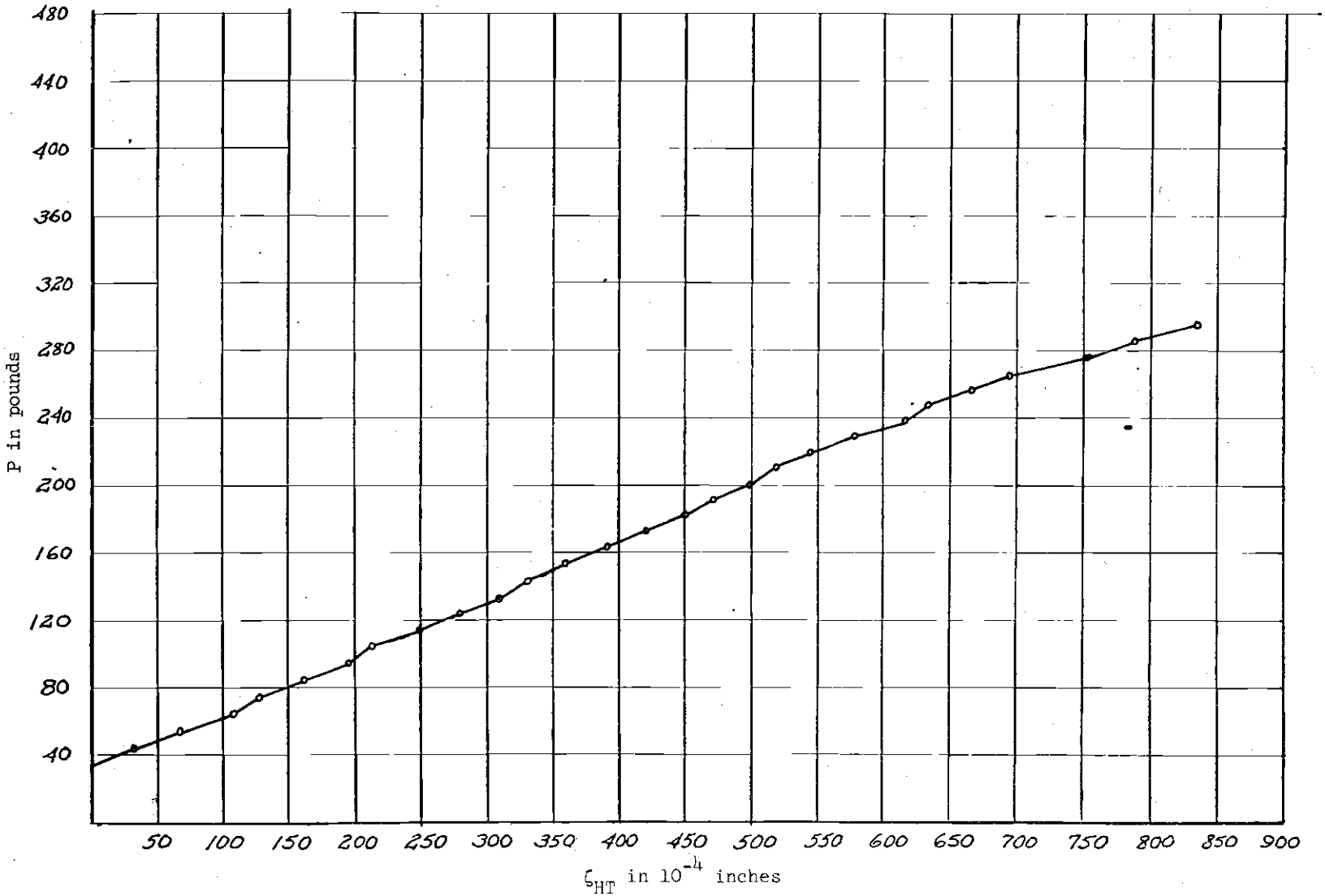

Figure 52. P versus ζ_{HT} Curve for Test III(b)

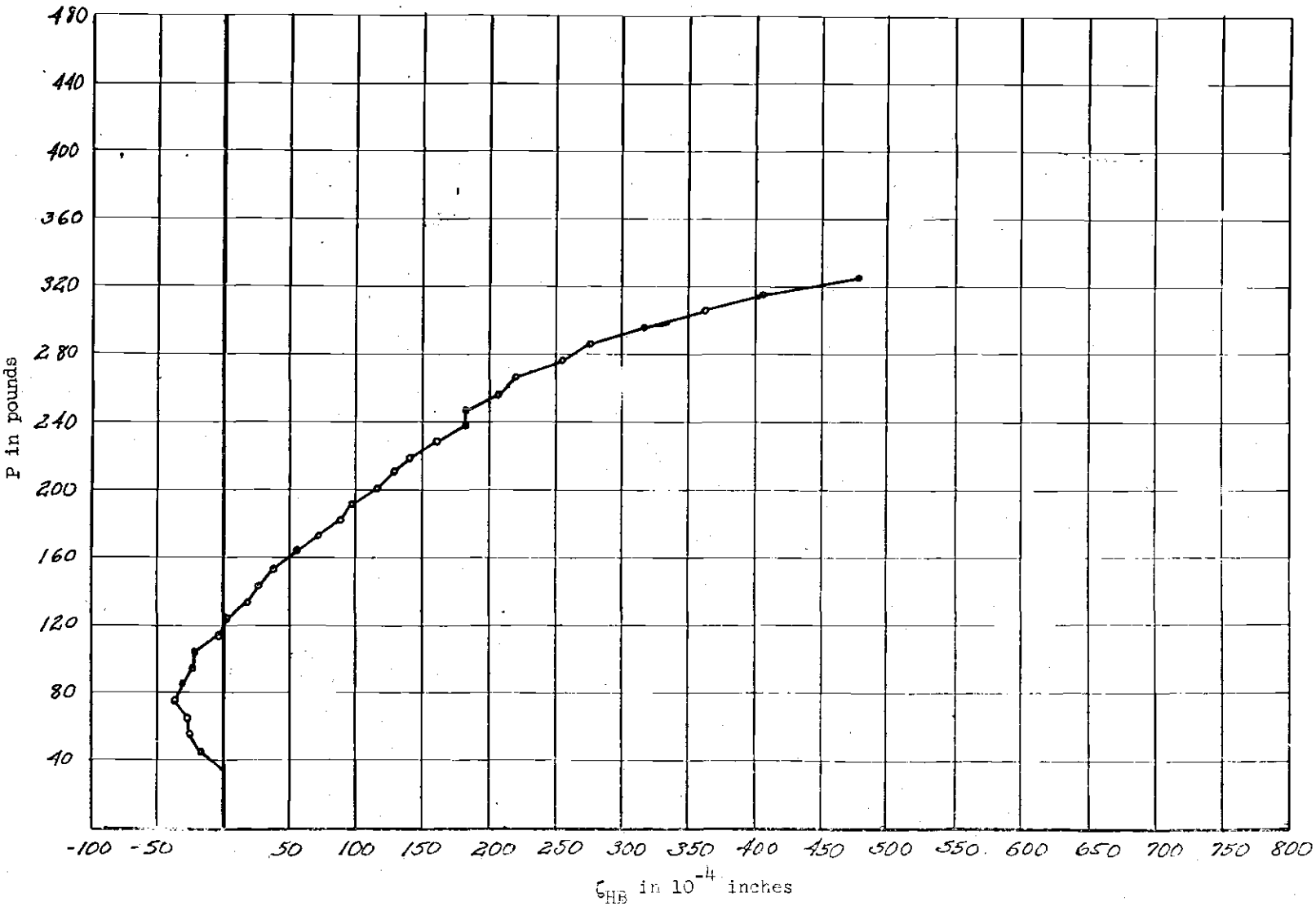

Figure 53. P versus ζ_{HB} Curve for Test III(b)

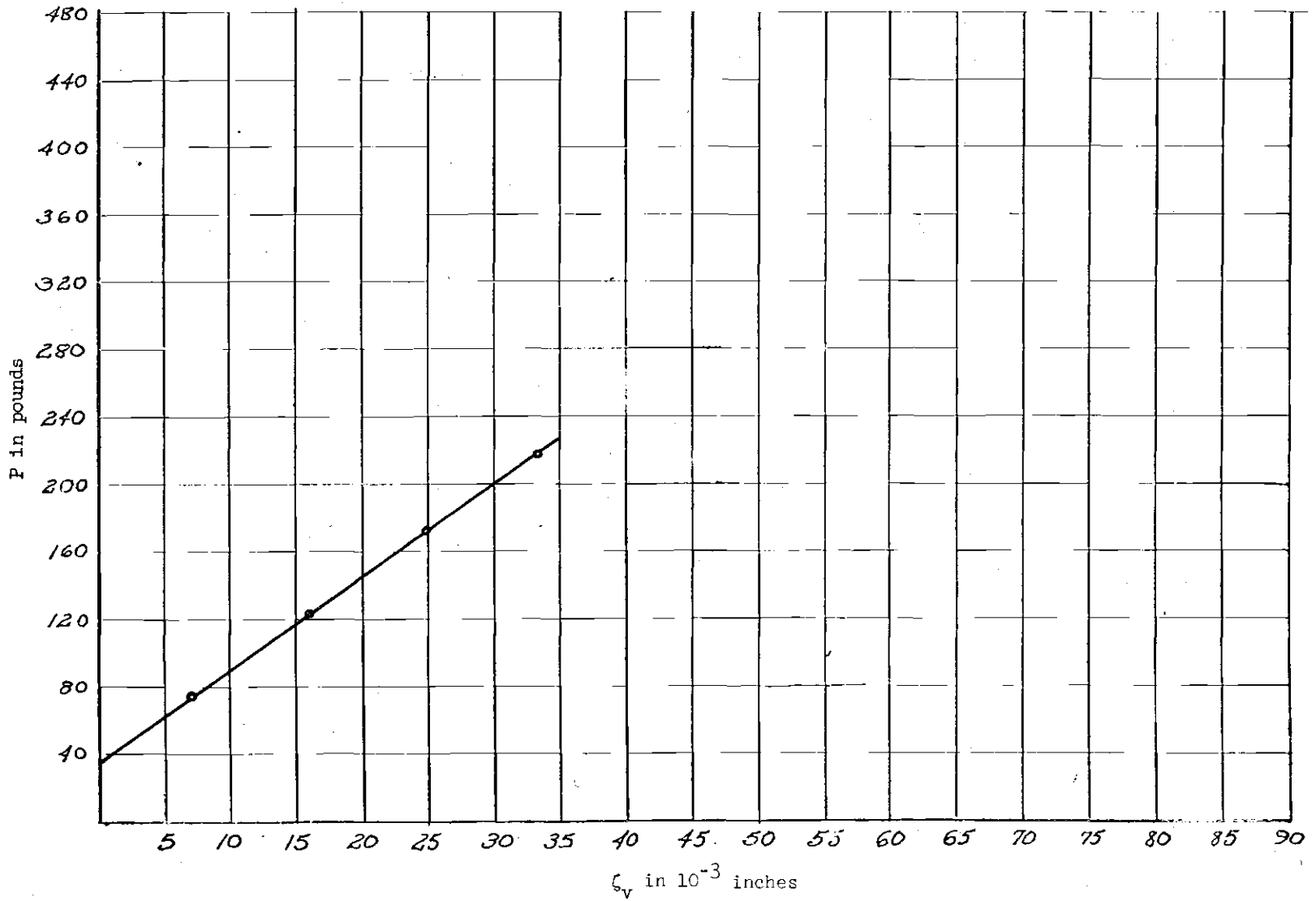

Figure 54. P versus ζ_v Curve for Test III(c)

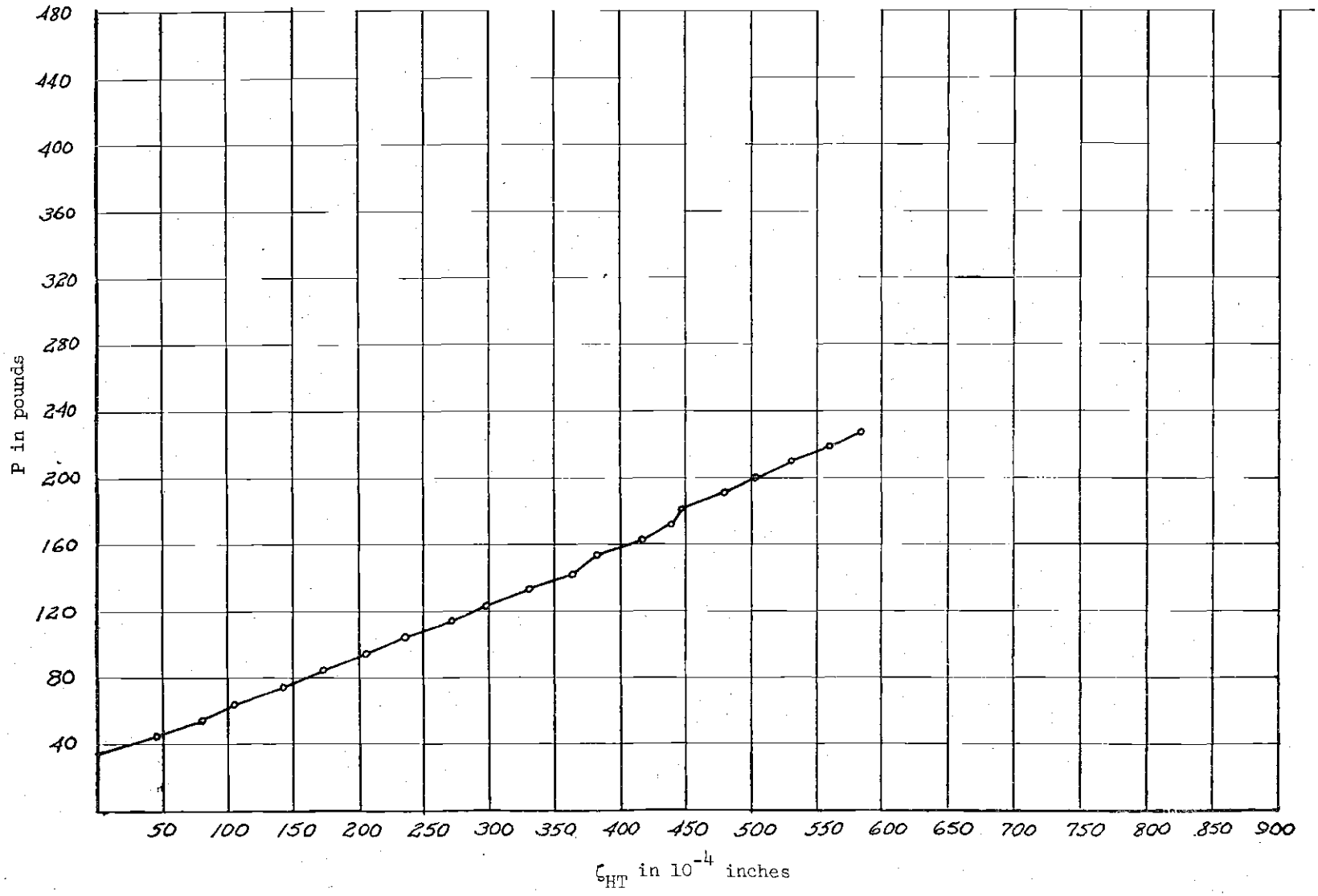

Figure 55. P versus ζ_{HT} Curve for Test III(c)

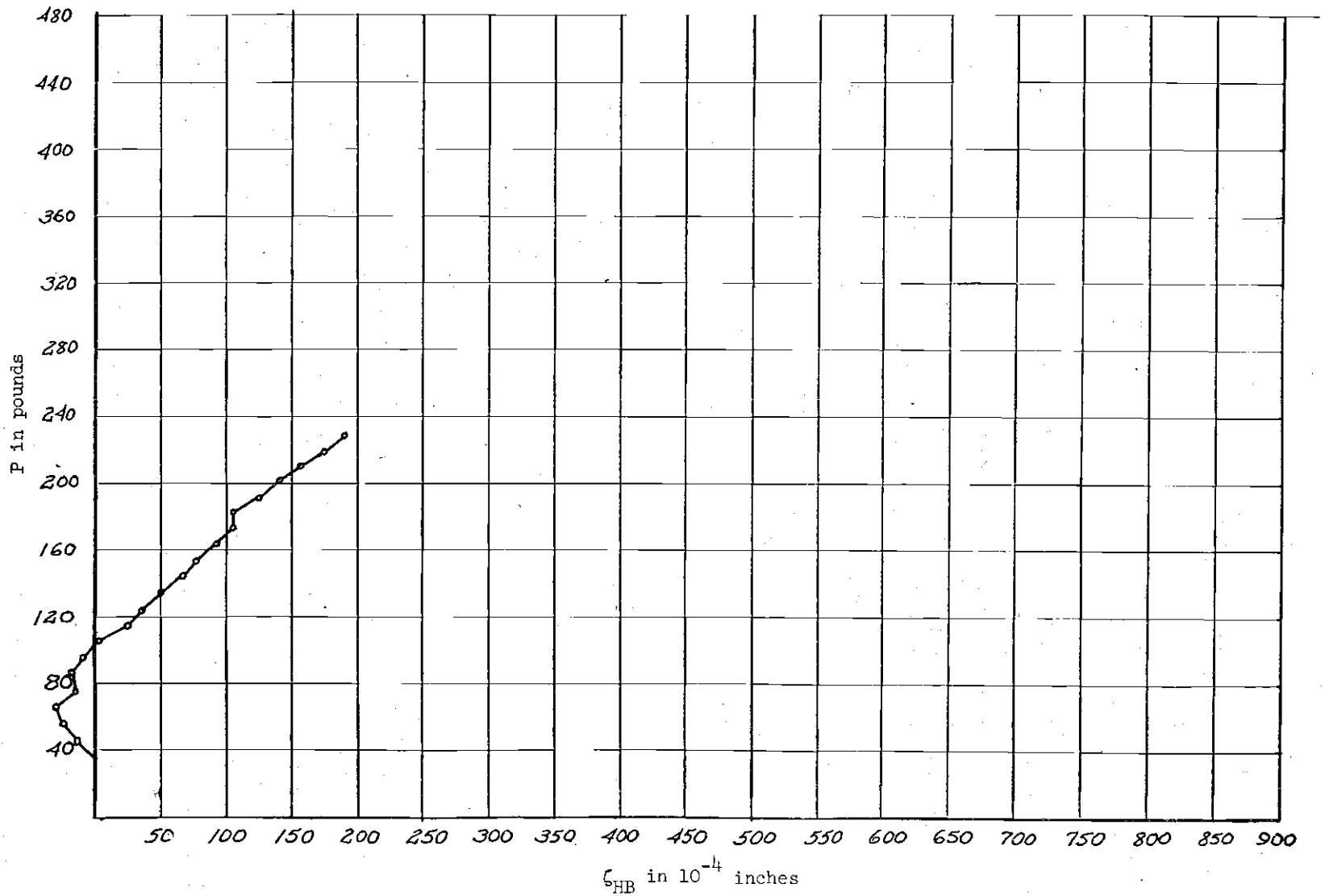

Figure 56. P versus ζ_{HB} Curve for Test III(c)

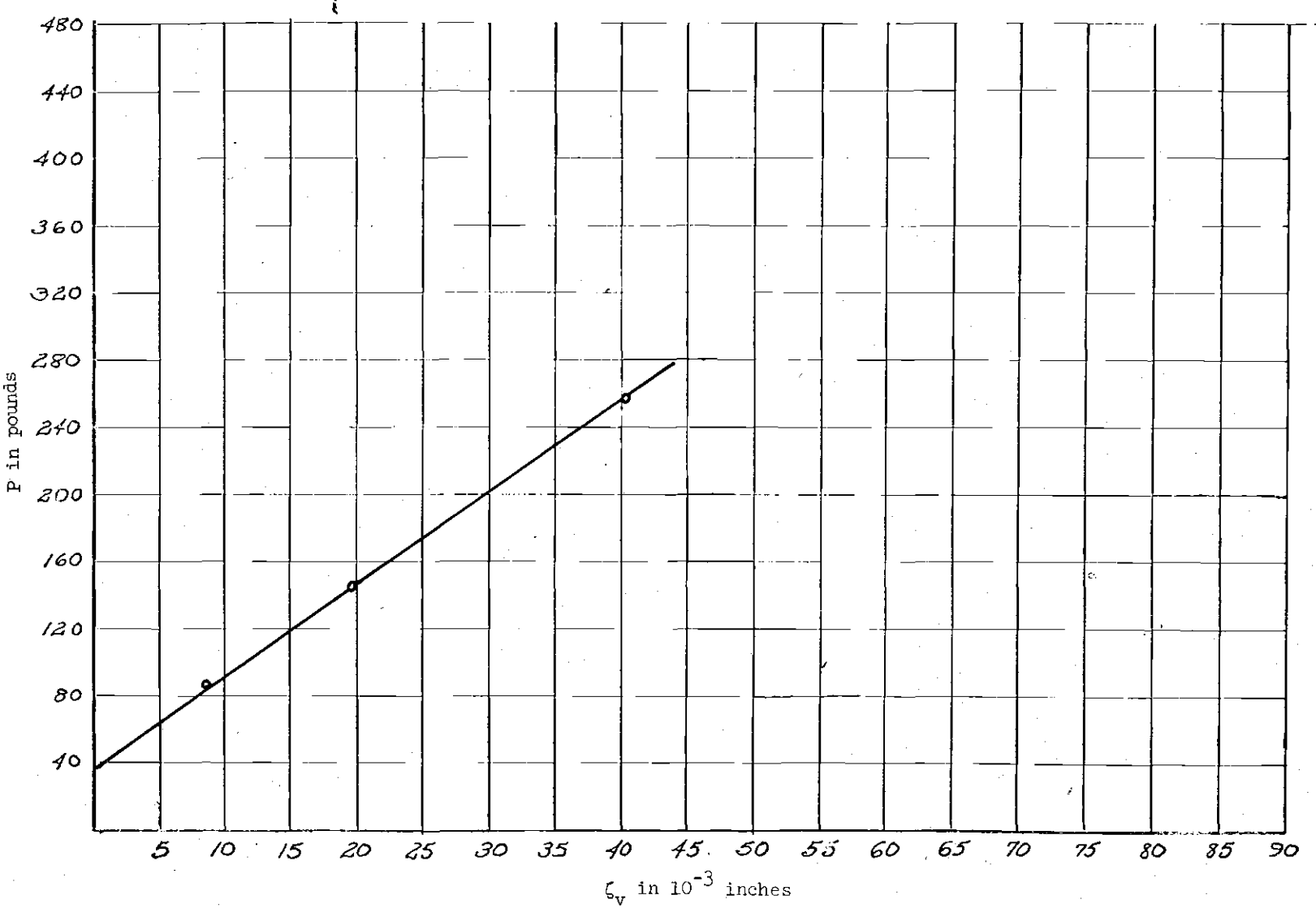

Figure 57. P versus ζ_v Curve for Test III(c)

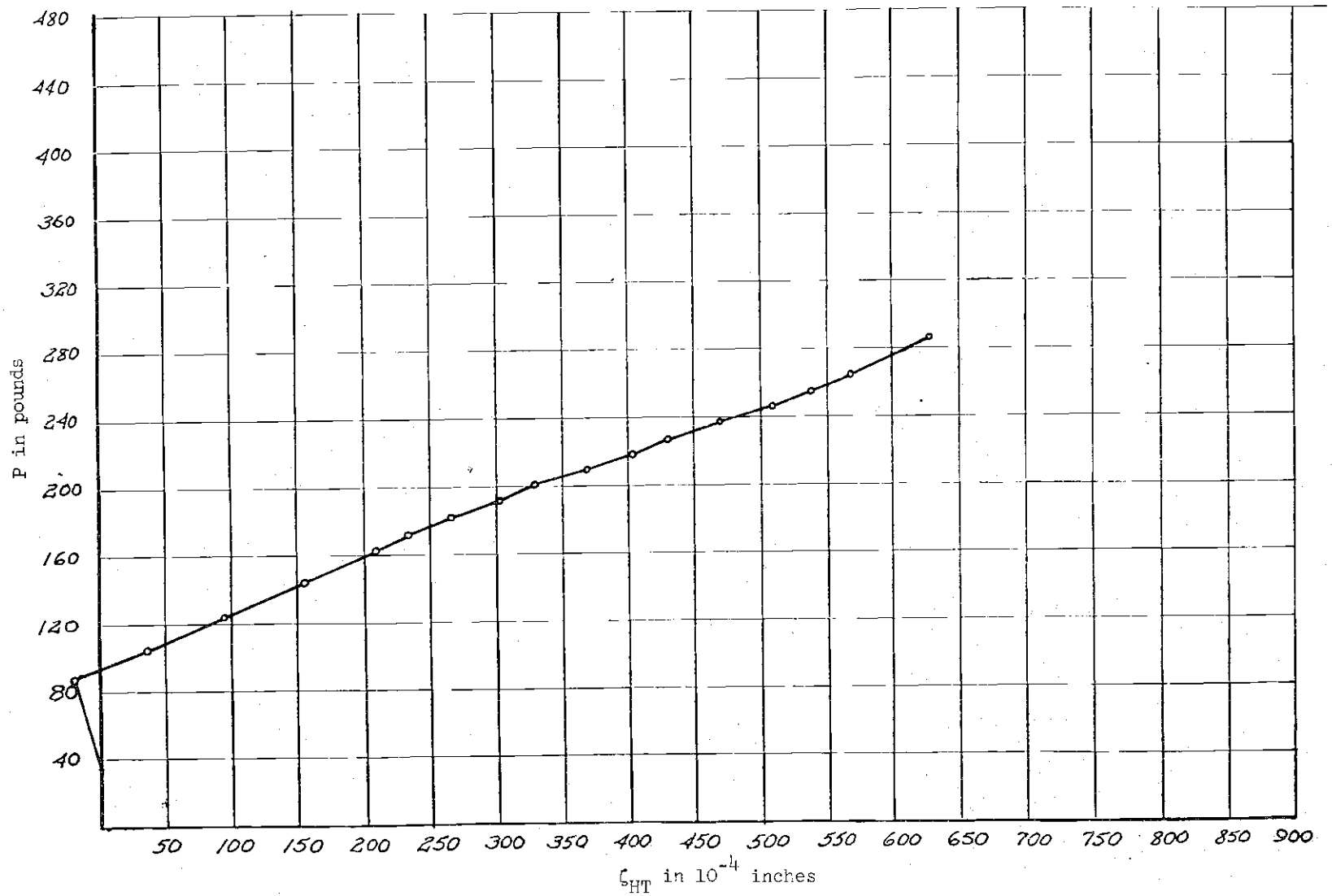

Figure 58. P versus ζ_{HT} Curve for Test III(c)

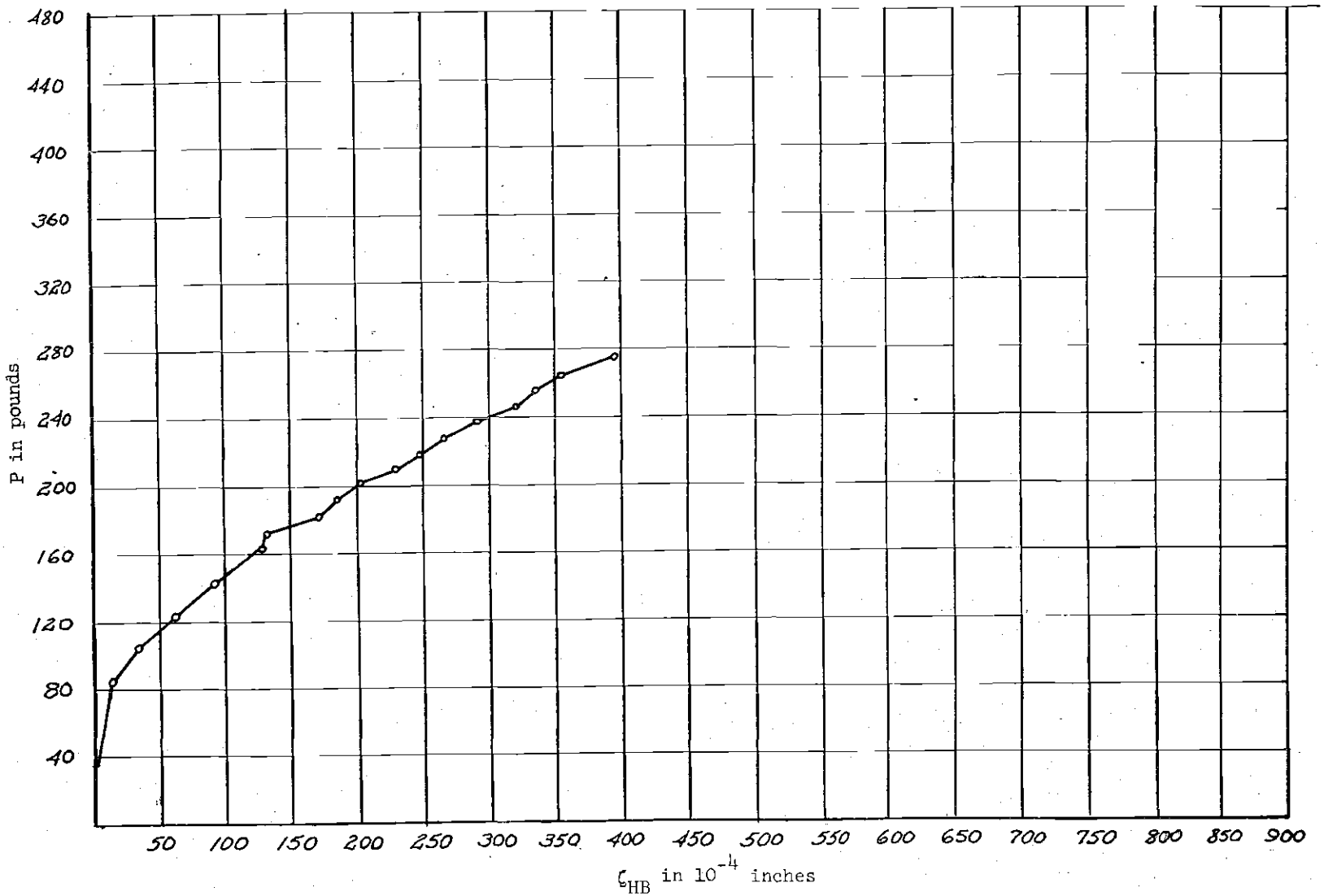

Figure 59. P versus ζ_{HB} Curve for Test III(d)

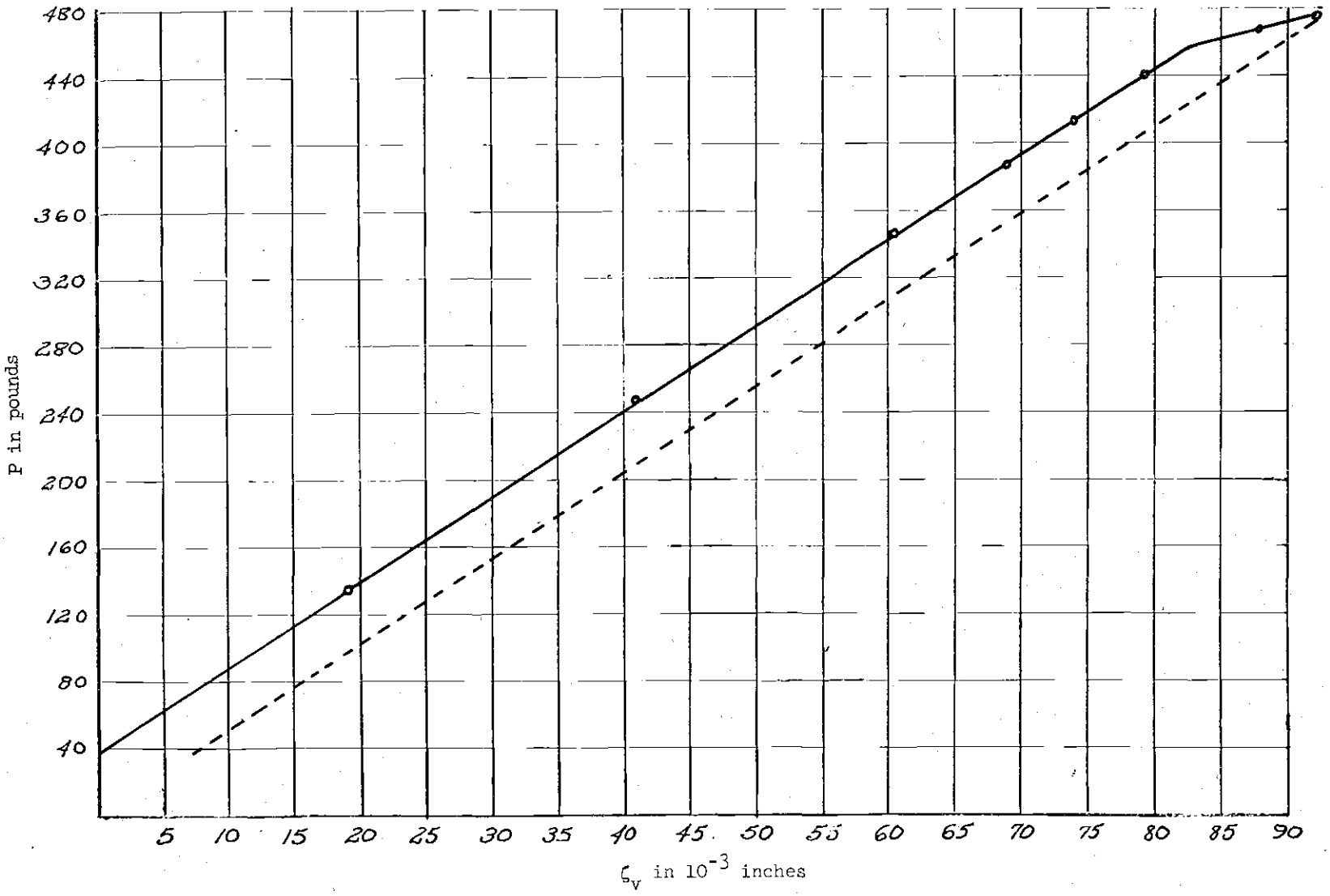

Figure 60. P versus ζ_v Curve for Test III(e)

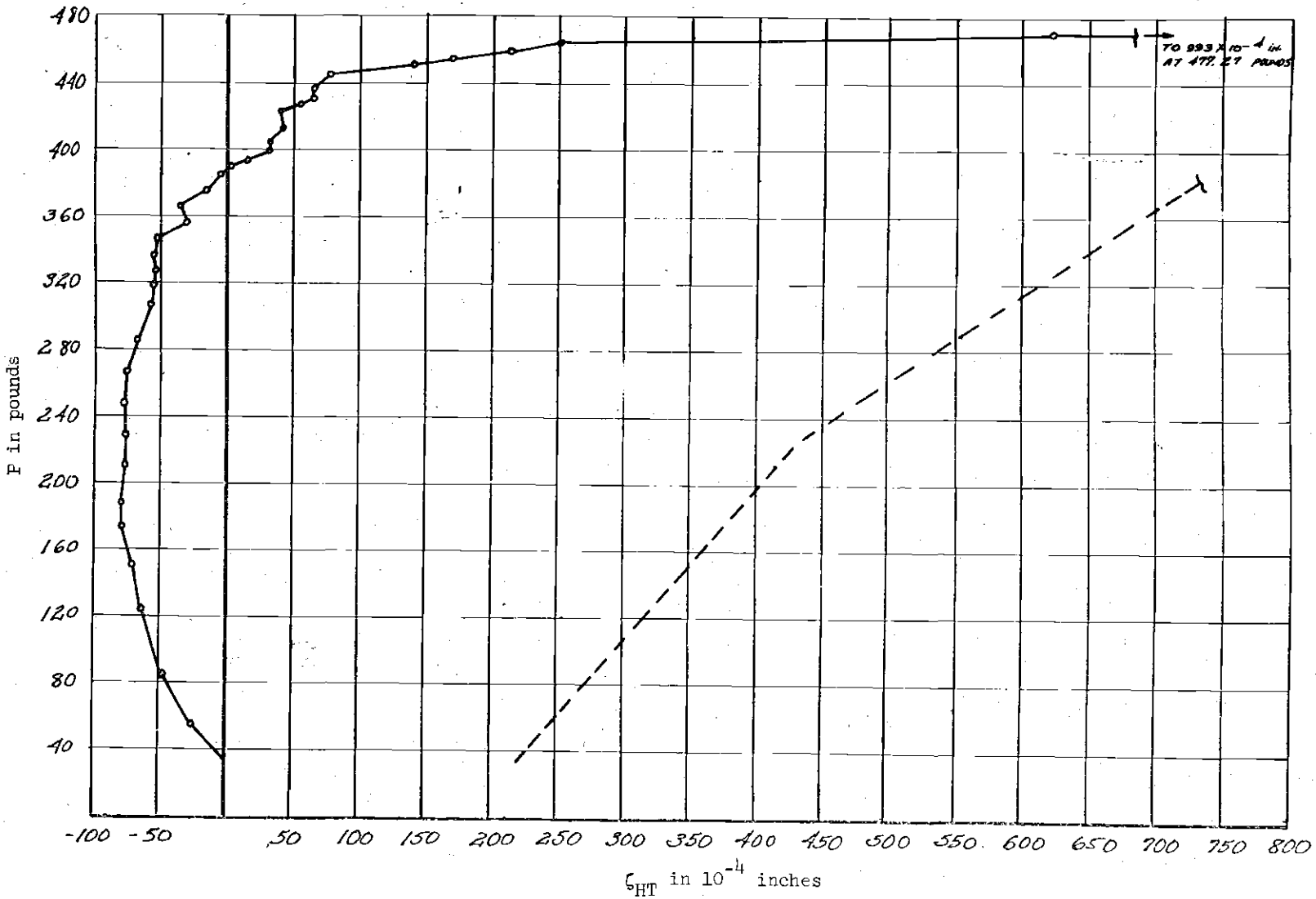

Figure 61. P versus ζ_{HT} Curve for Test III(e)

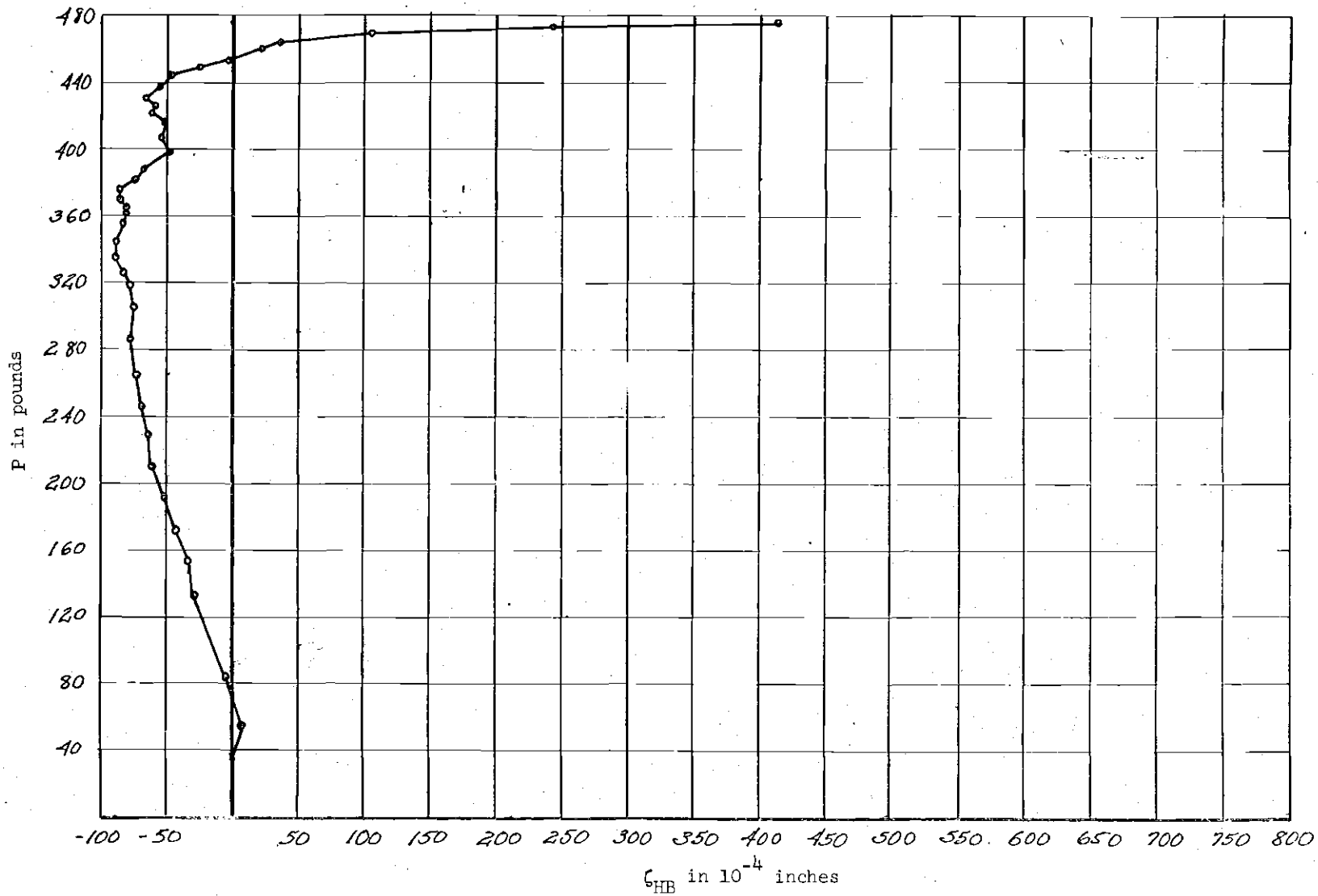

Figure 62. P versus ζ_{HB} Curve for Test III(e)

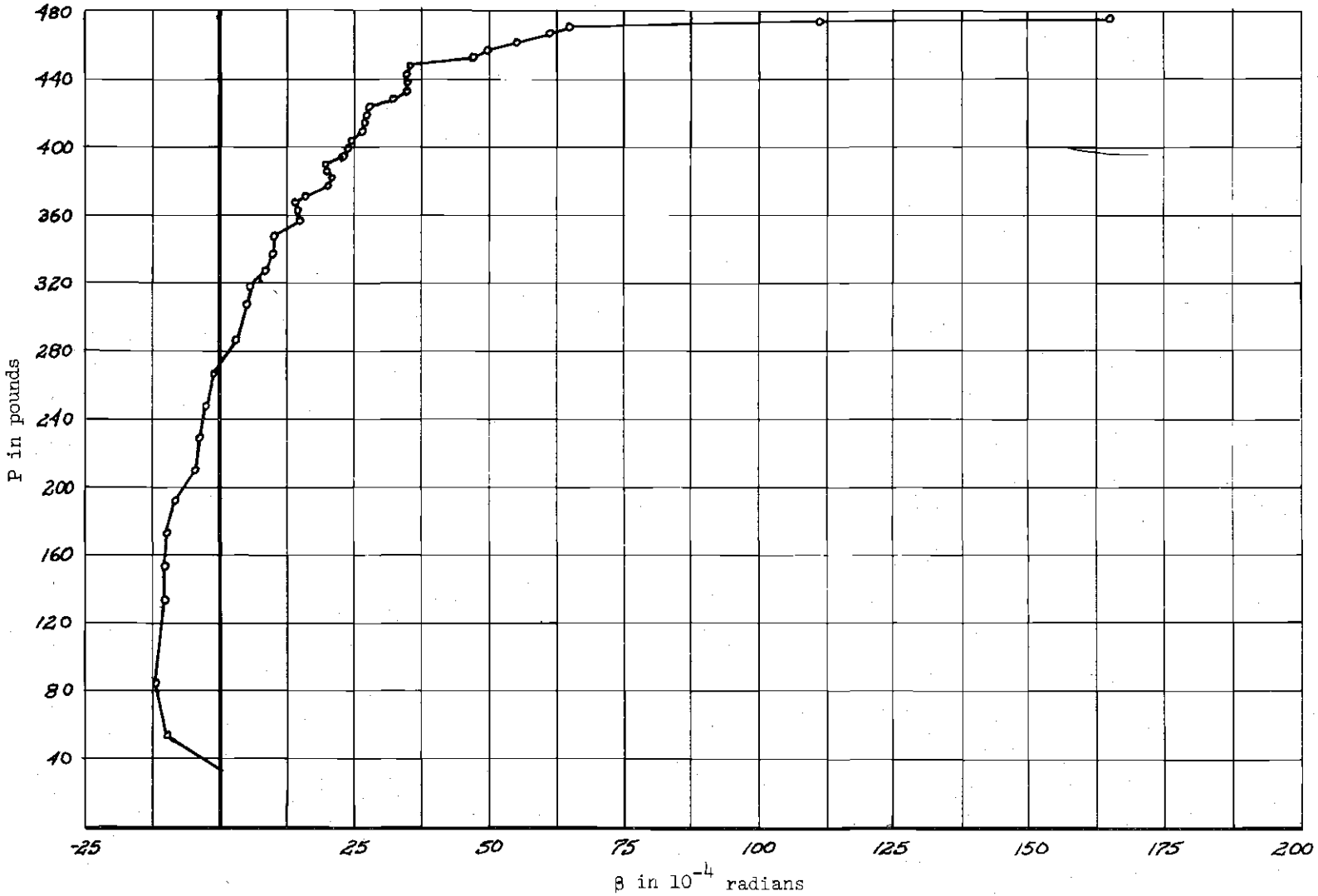

Figure 63. Twist Curve for Test III(e)

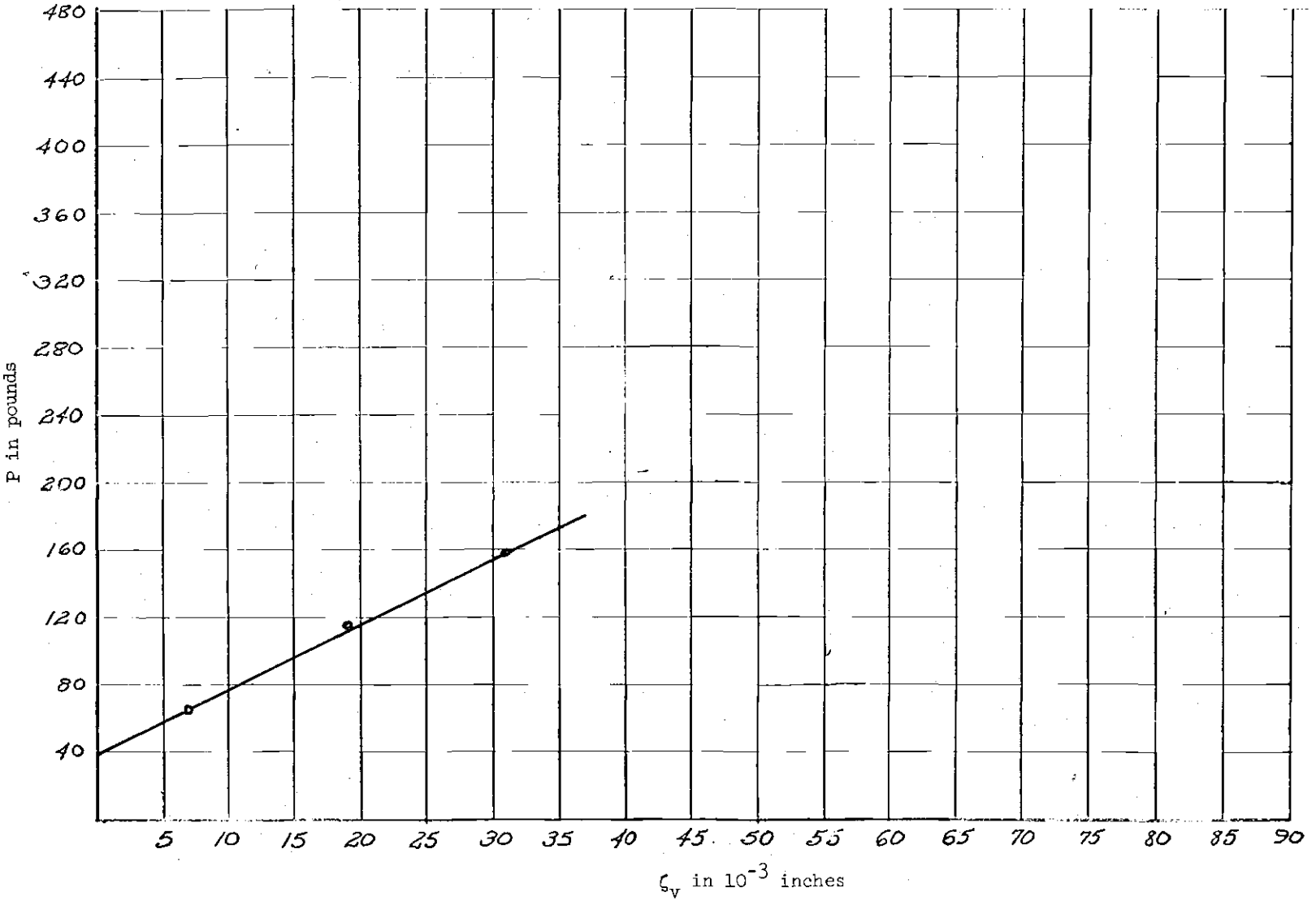

Figure 64. P versus ζ_v for Test IV(a)

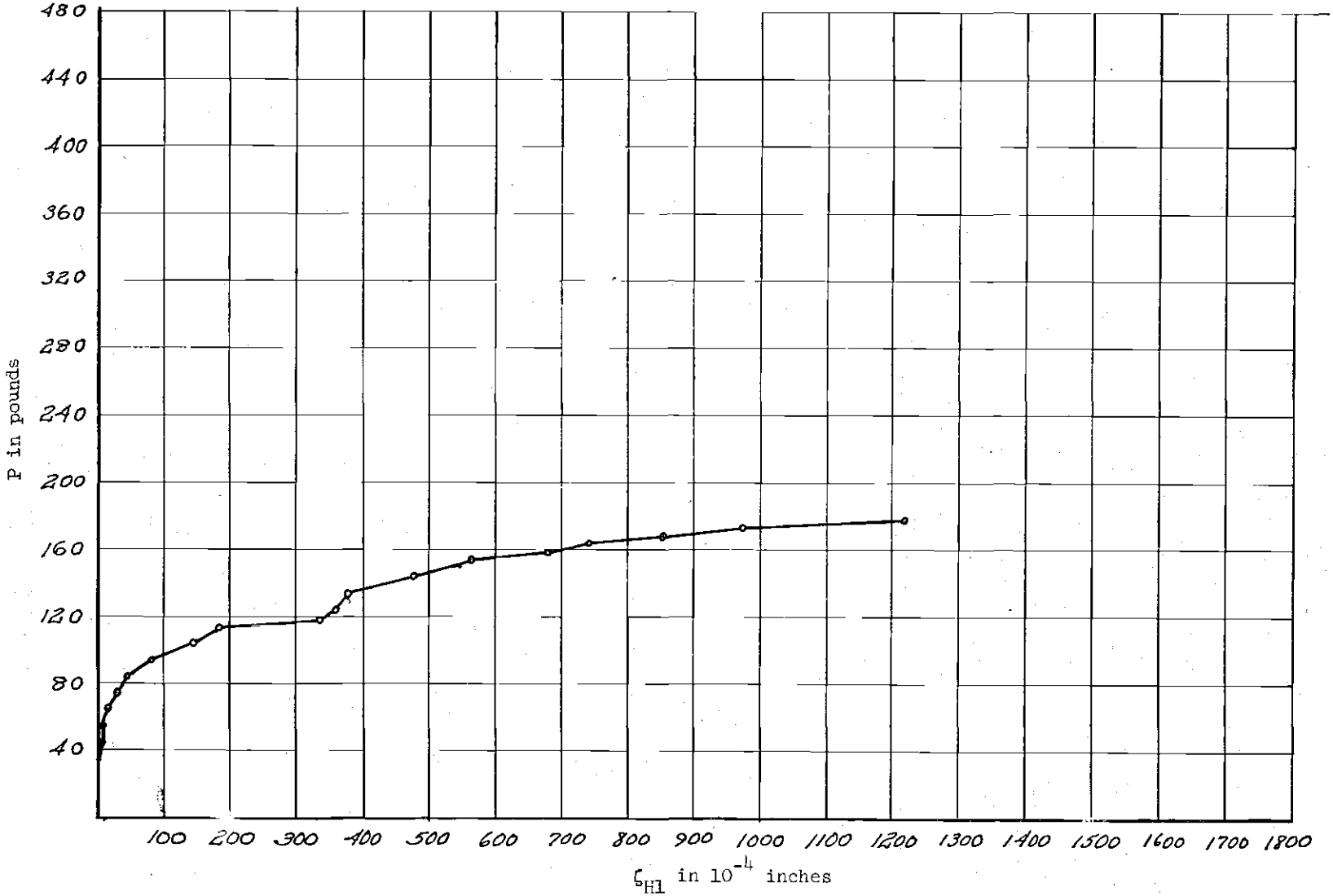

Figure 65. P versus ζ_{H1} for Test IV(a)

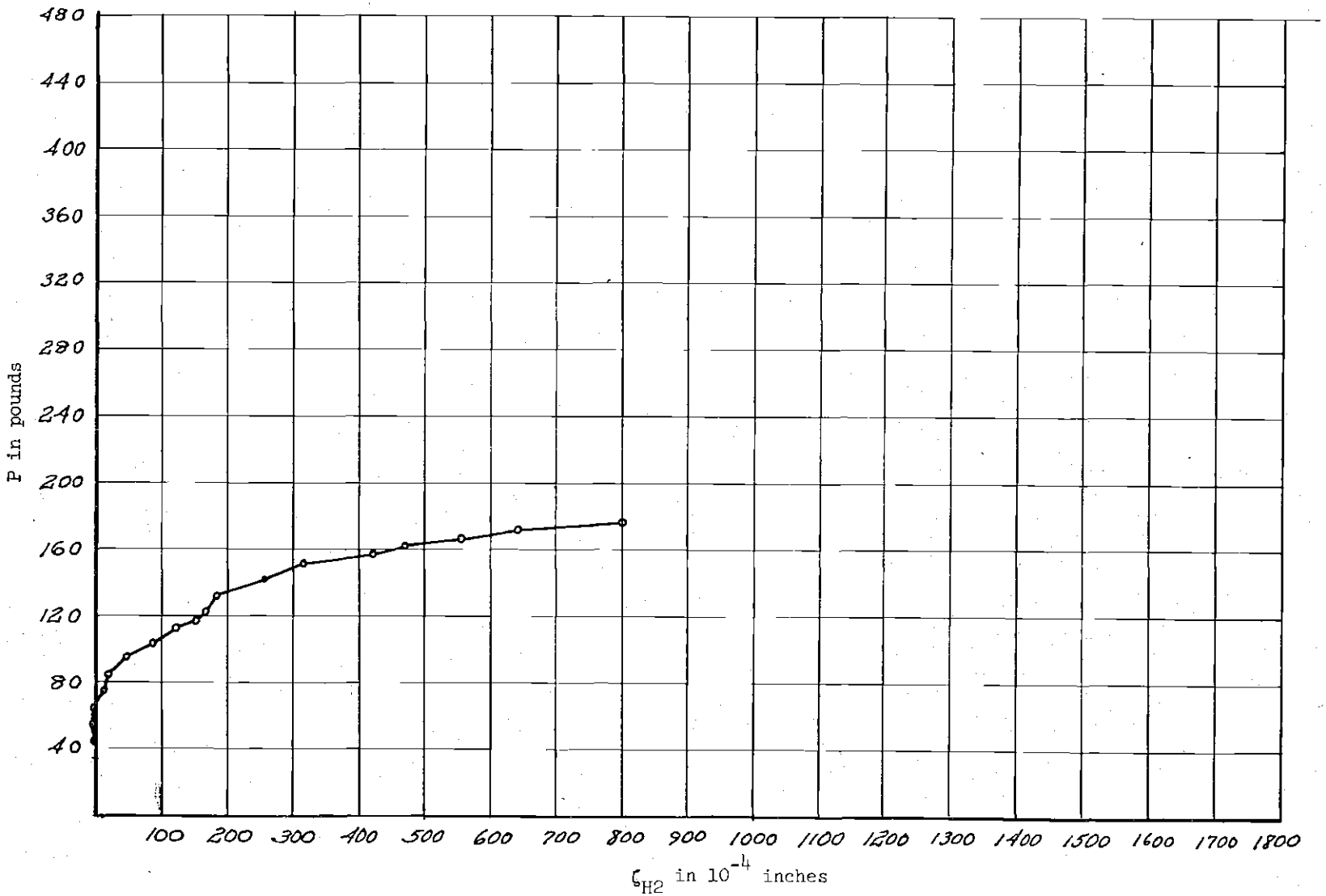

Figure 66. P versus ζ_{H2} for Test IV(a)

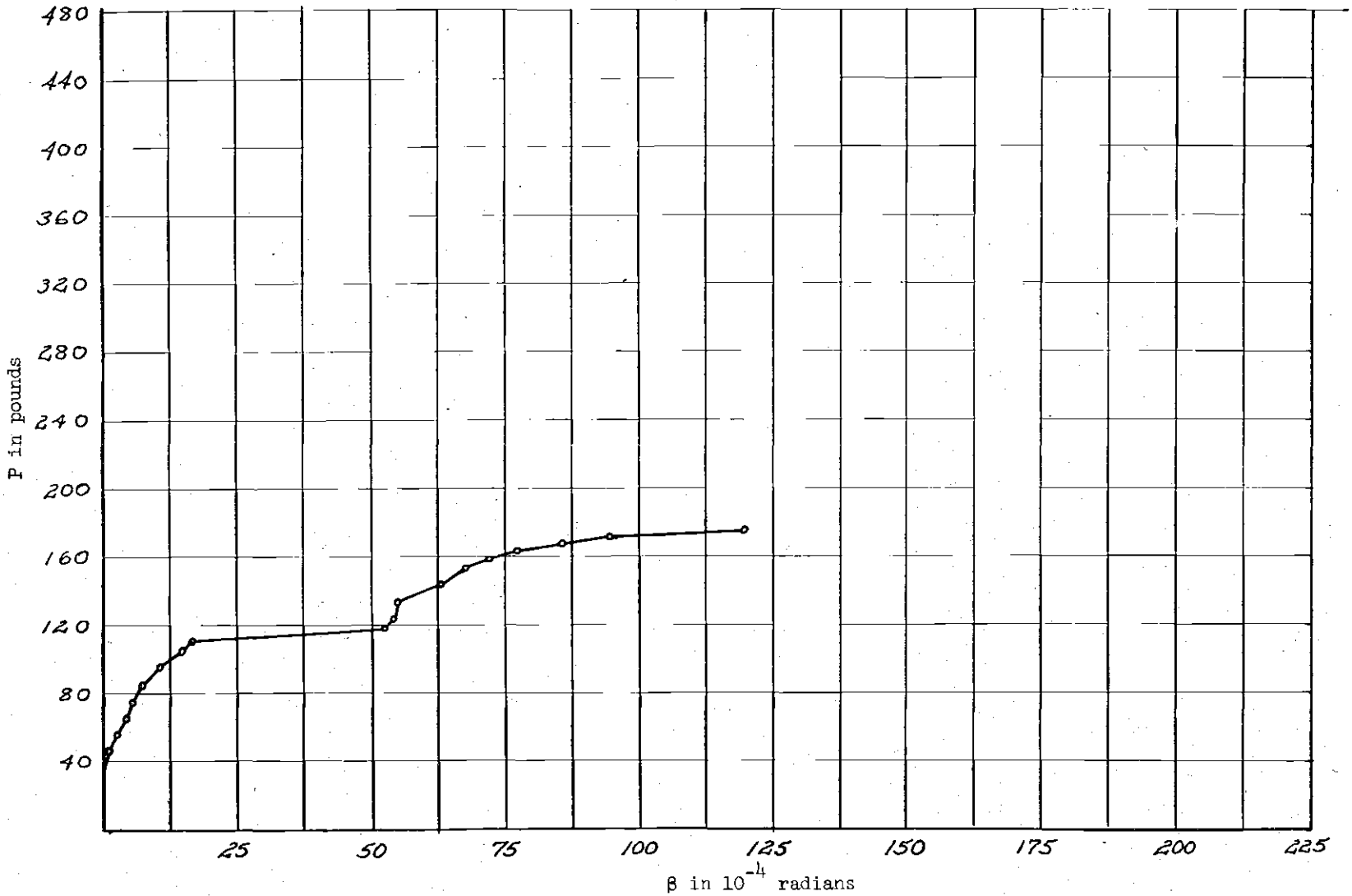

Figure 67. Twist Curve for Test IV(a)

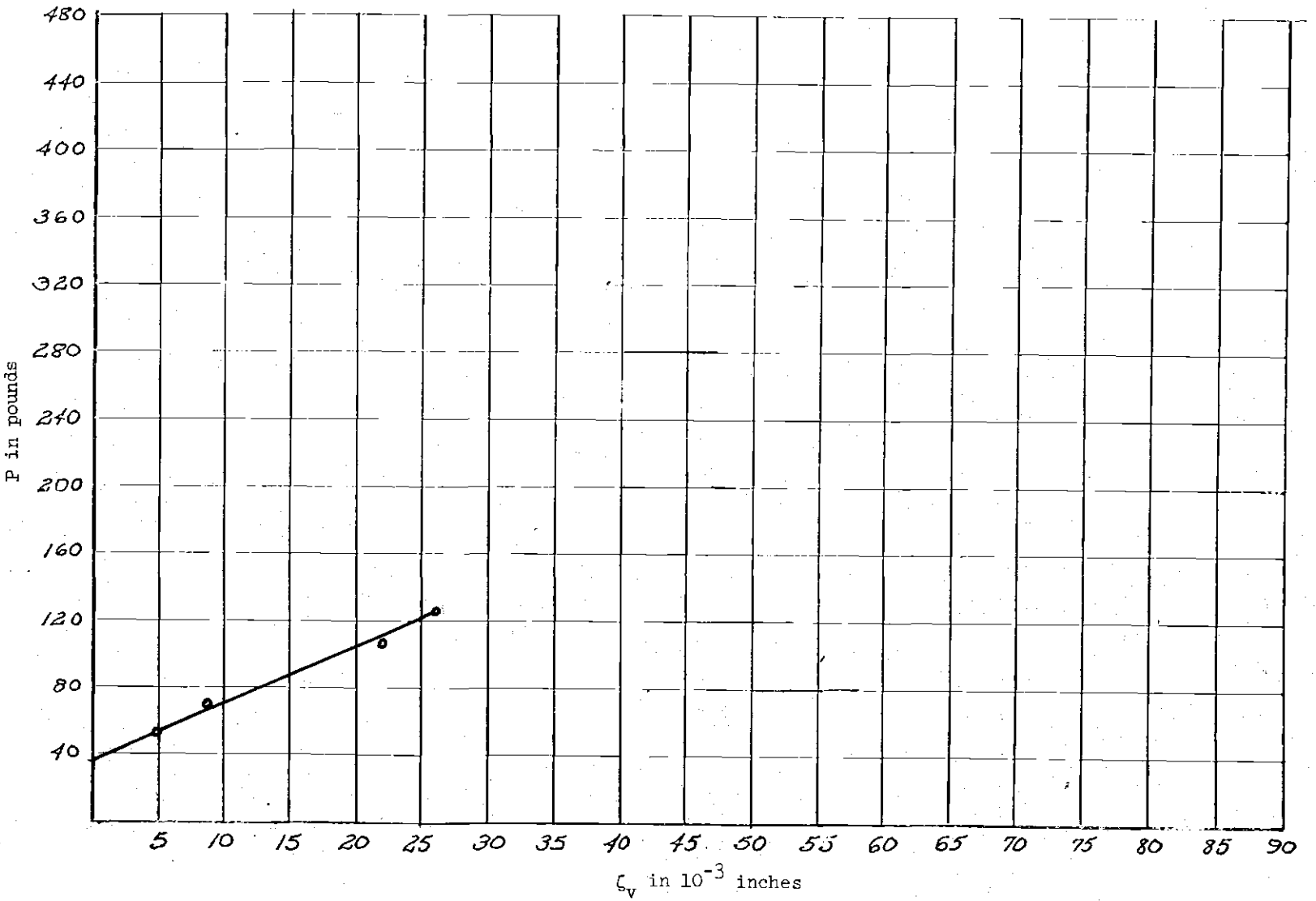

Figure 68. P versus ζ_v Curve for Test IV(b)

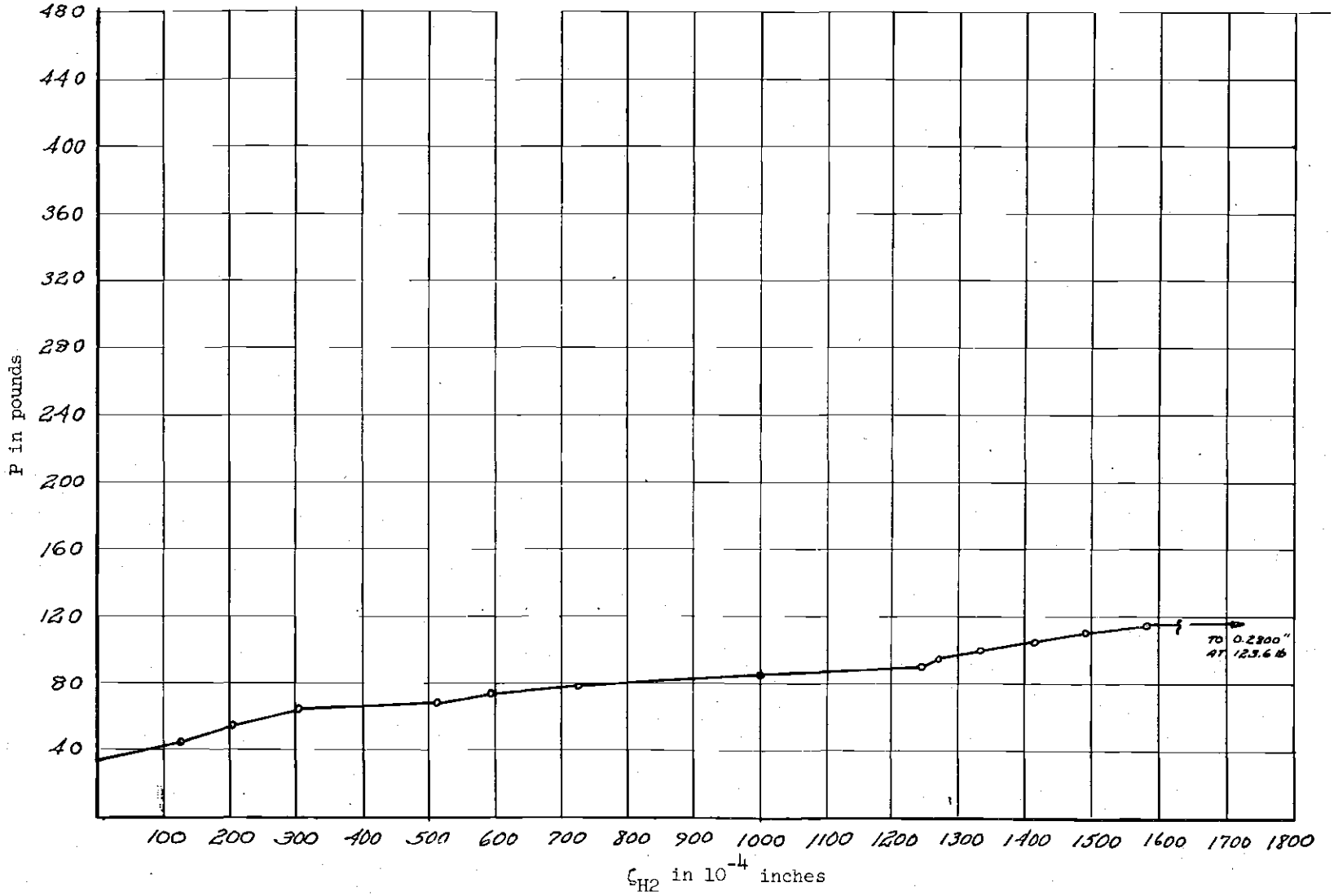

Figure 69. P versus ζ_{H2} Curve for Test IV(b)

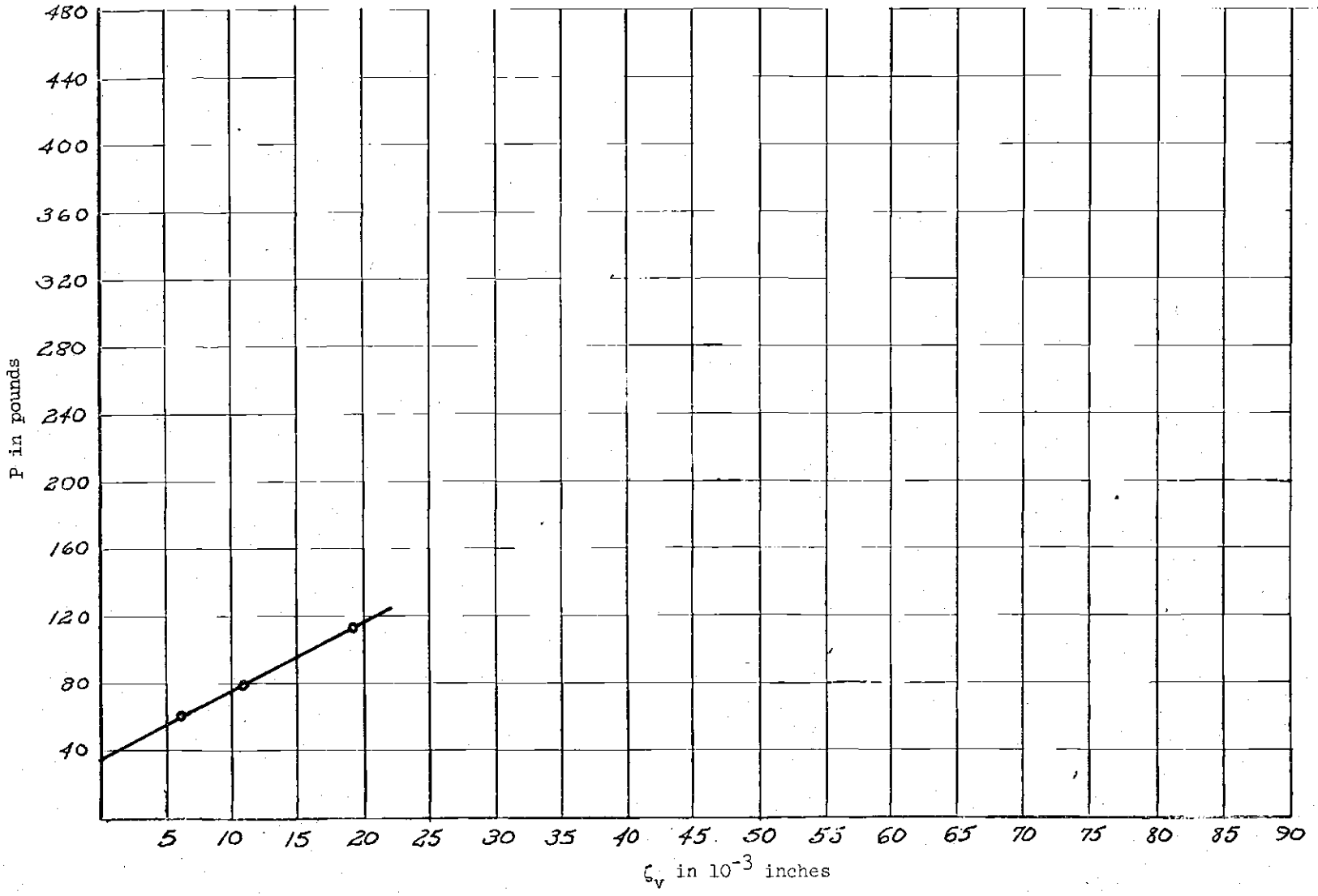

Figure 70. P versus ζ_v Curve for Test IV(c)

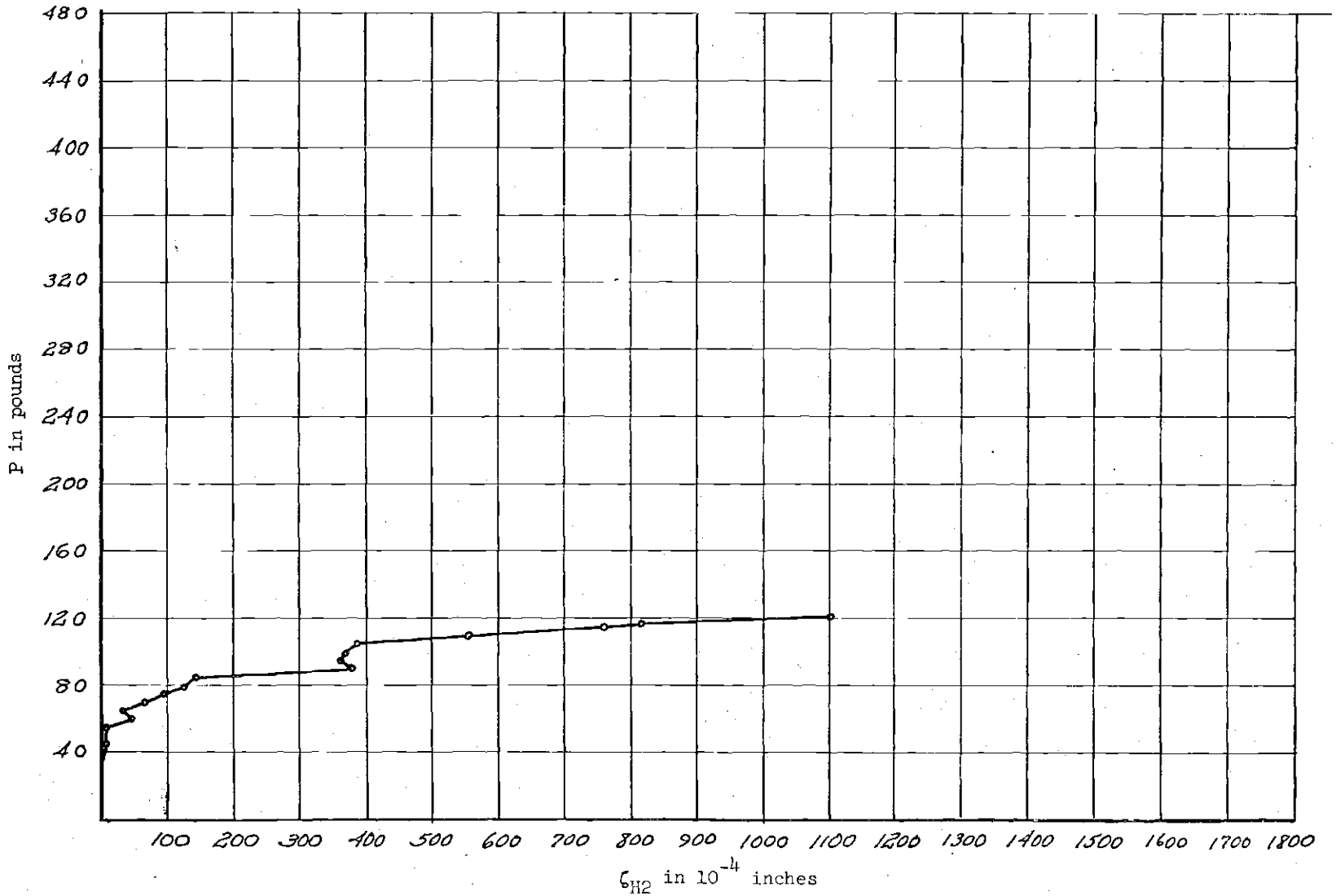

Figure 71. P versus ζ_{H2} Curve for Test IV(c)

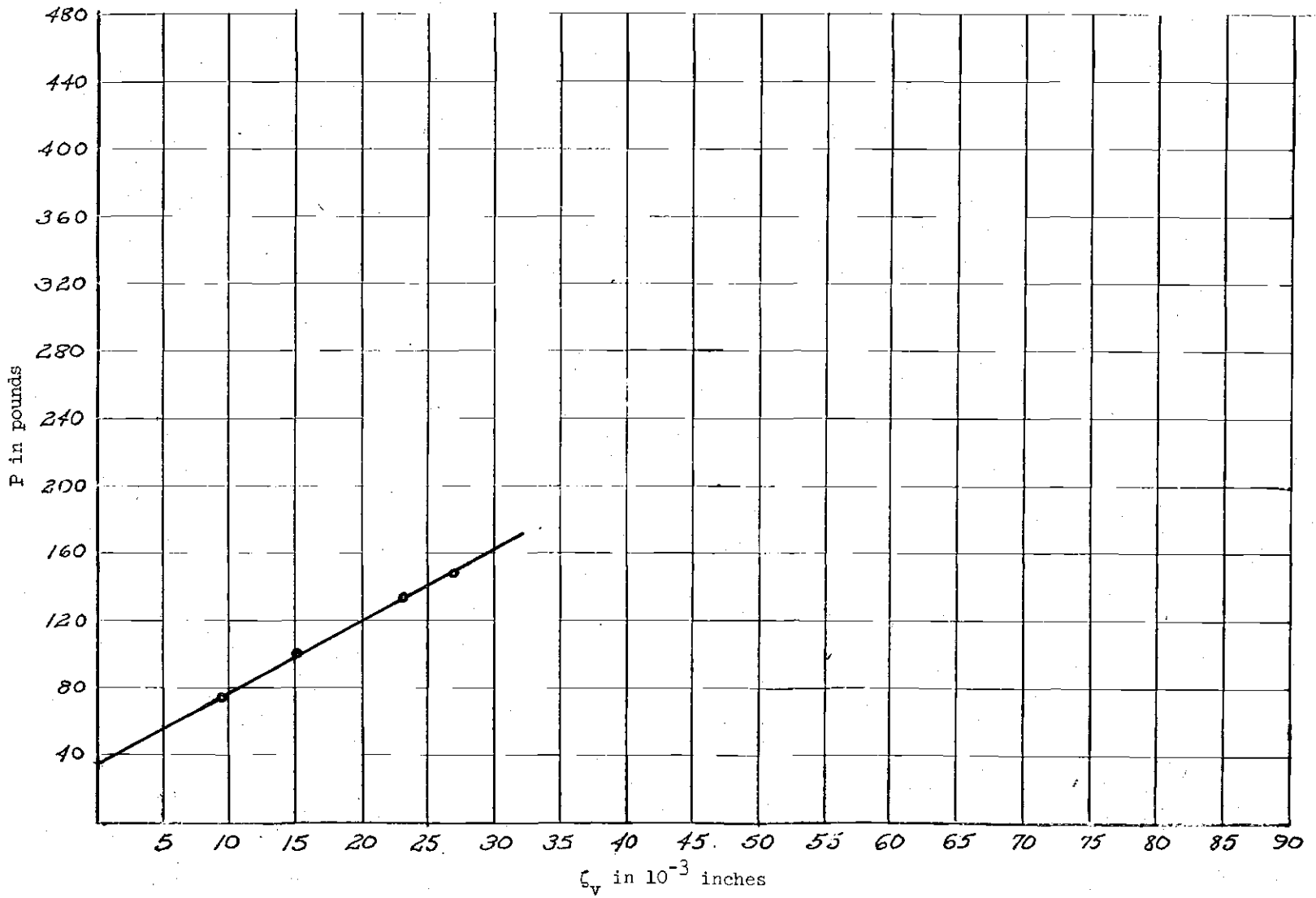

Figure 72. P versus ζ_v Curve for Test IV(d)

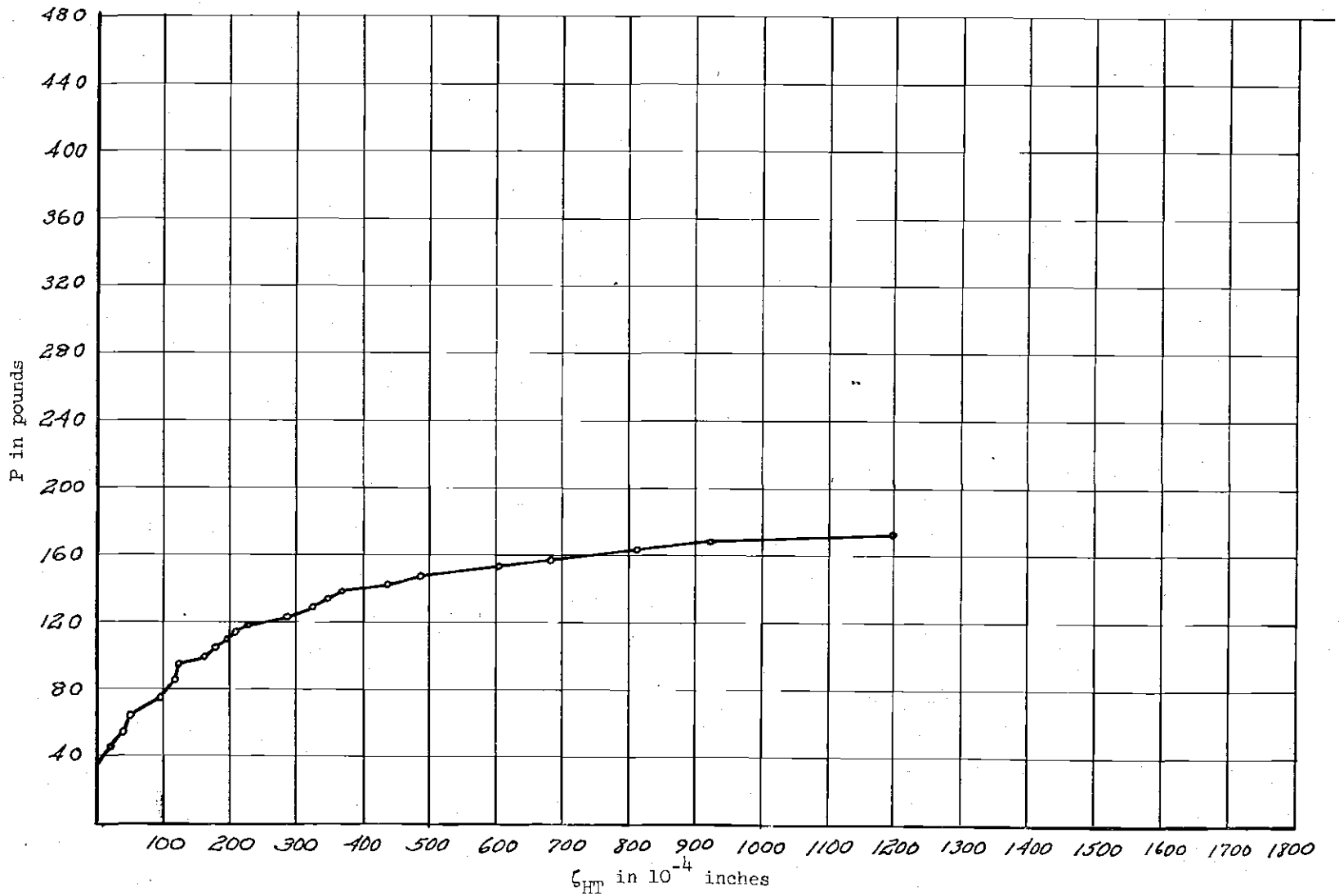

Figure 73. P versus ζ_{H1} Curve for Test IV(d)

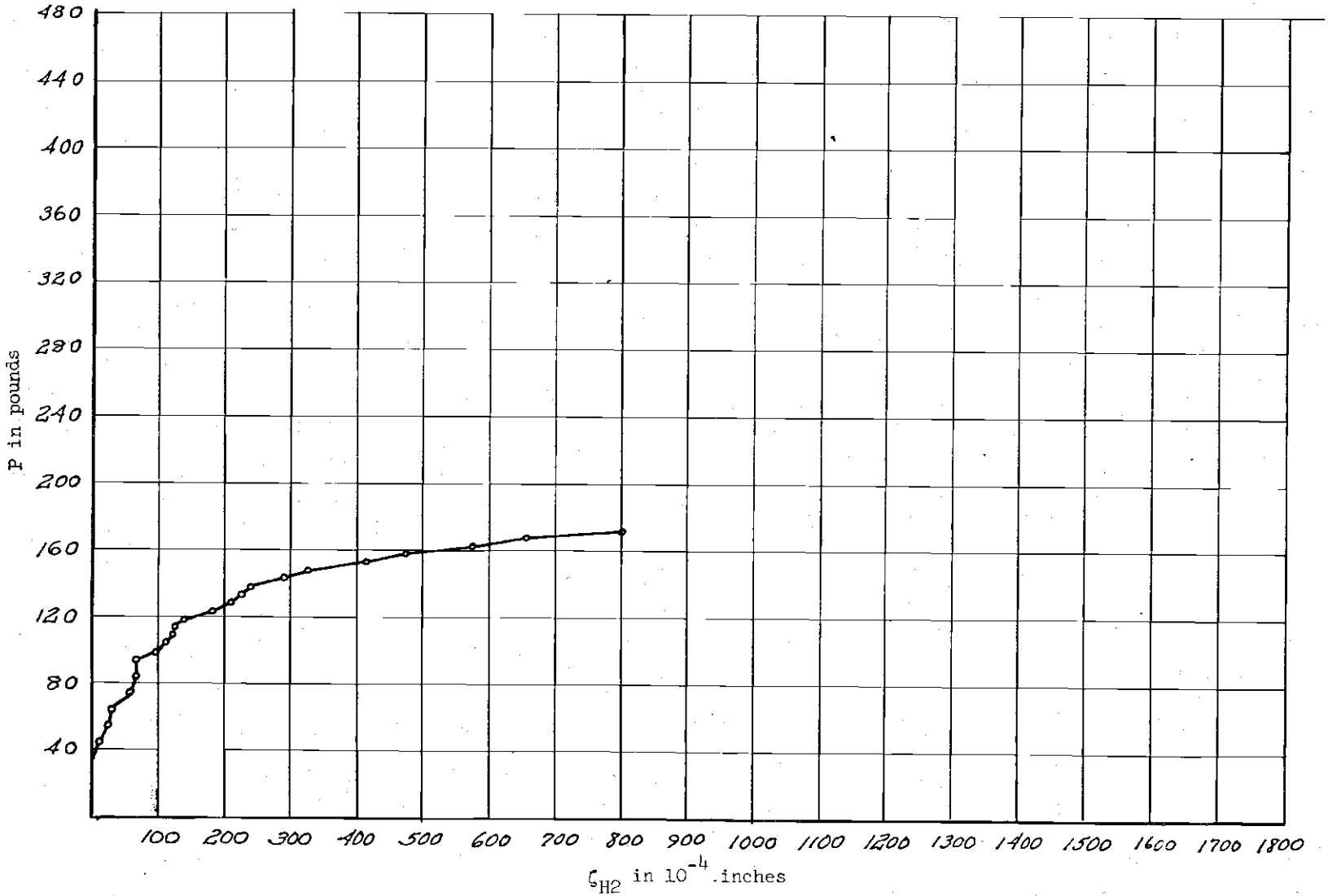

Figure 74. P versus ζ_{H2} Curve for Test IV(d)

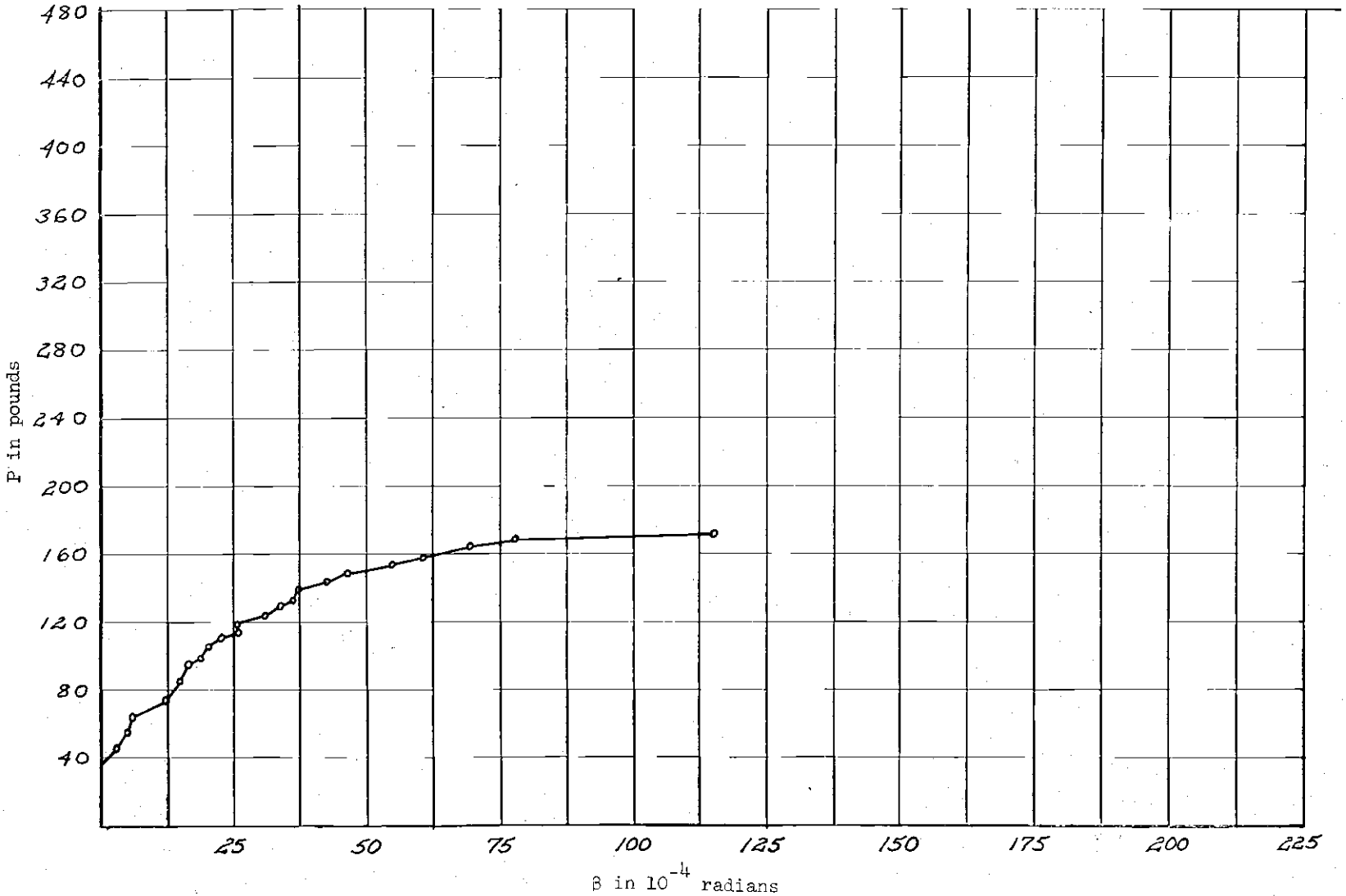

Figure 75. Twist Curve for Test IV(d)

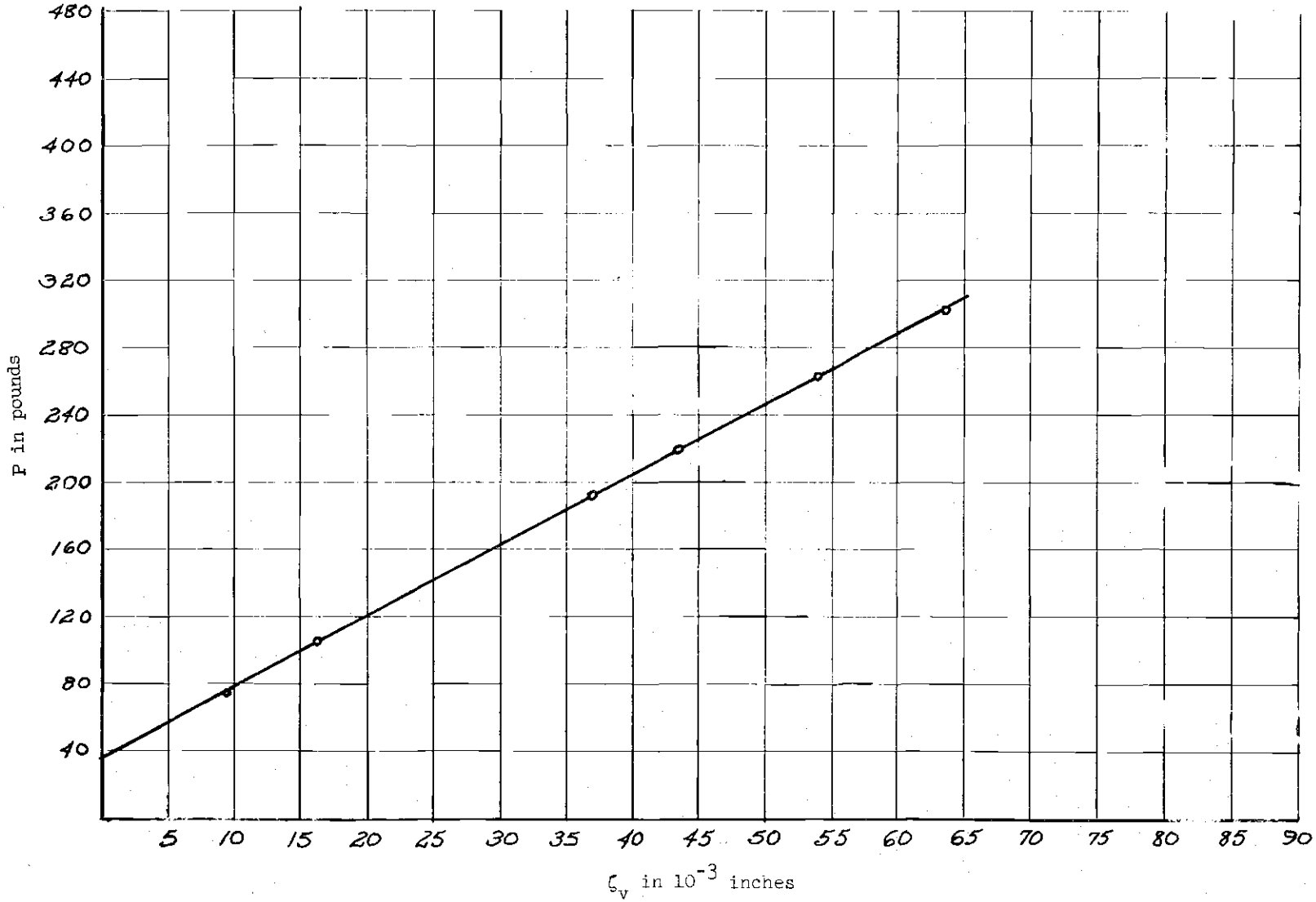

Figure 76. P versus ζ_v Curve for Test V

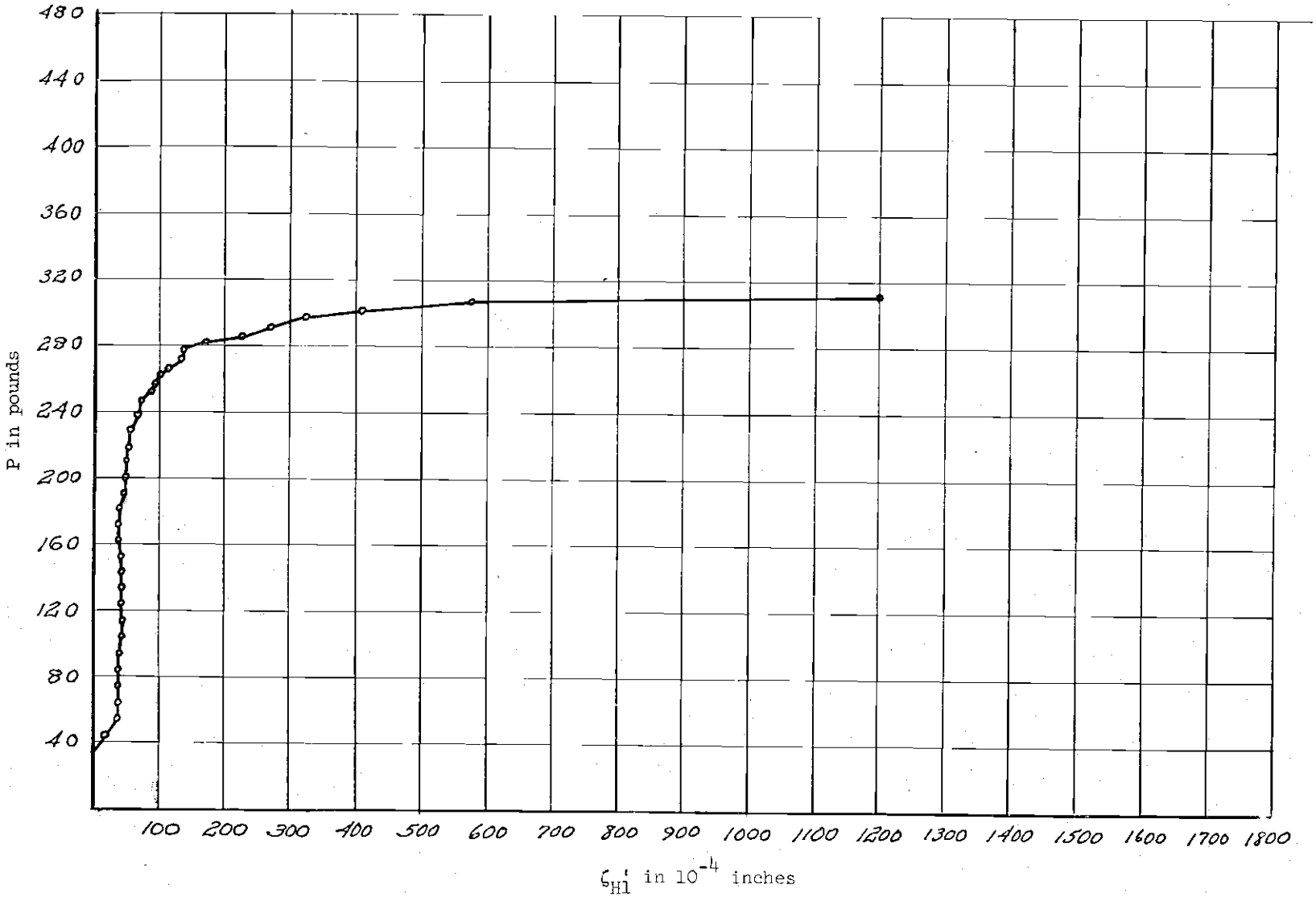

Figure 77. P versus ζ_{H1}' Curve for Test V

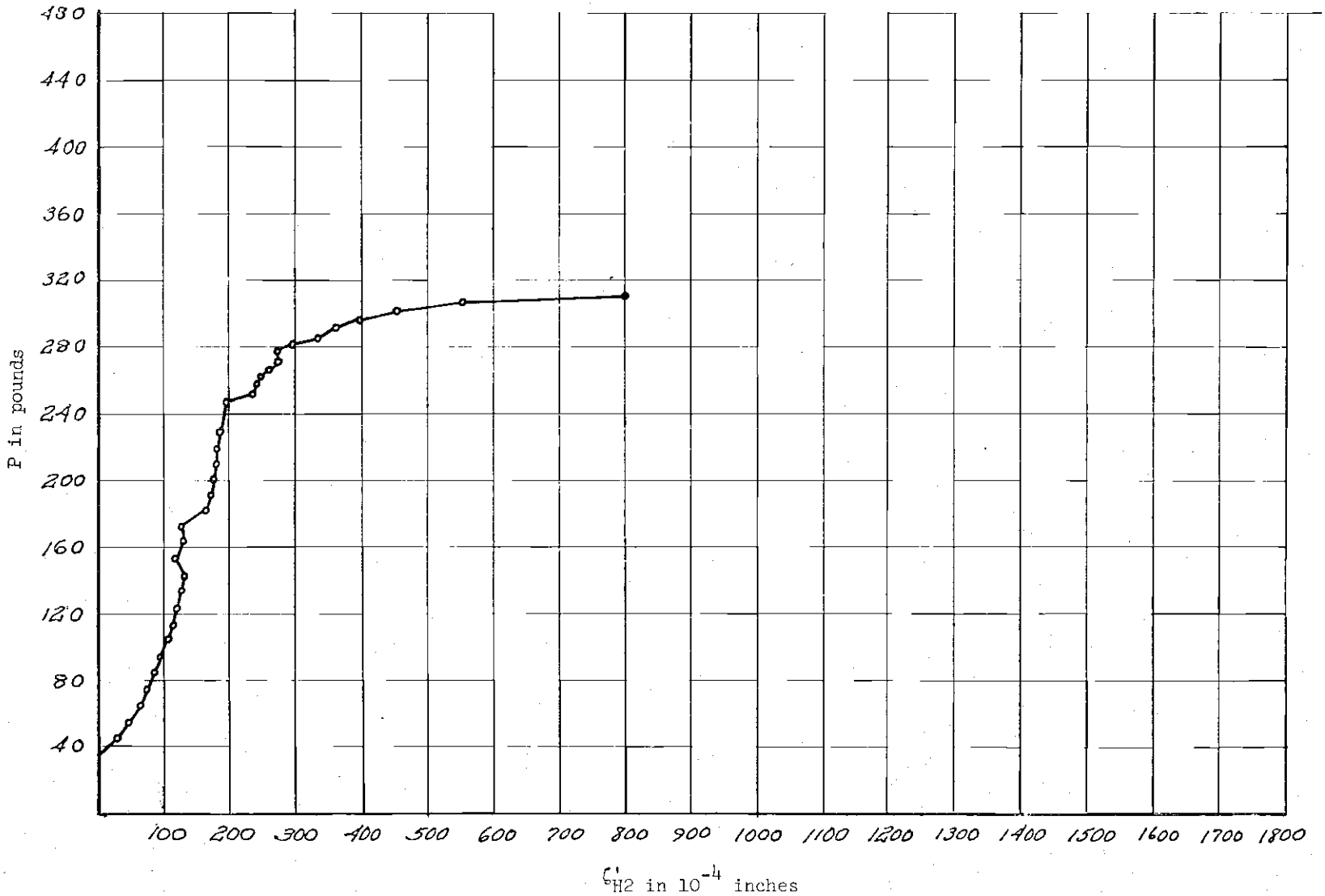

Figure 78. P versus ζ'_{H2} Curve for Test V

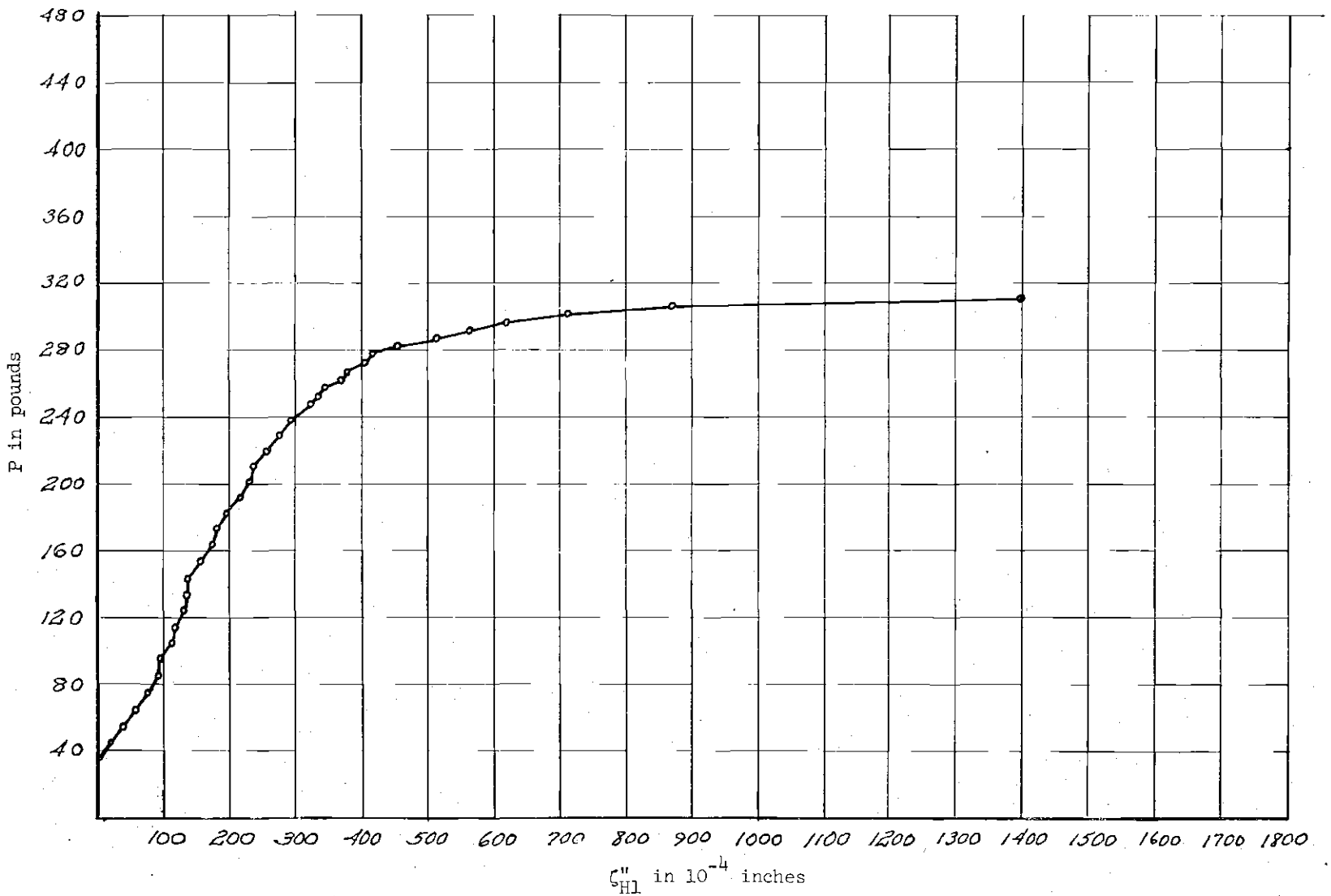

Figure 79. P versus ζ''_{H1} Curve for Test V

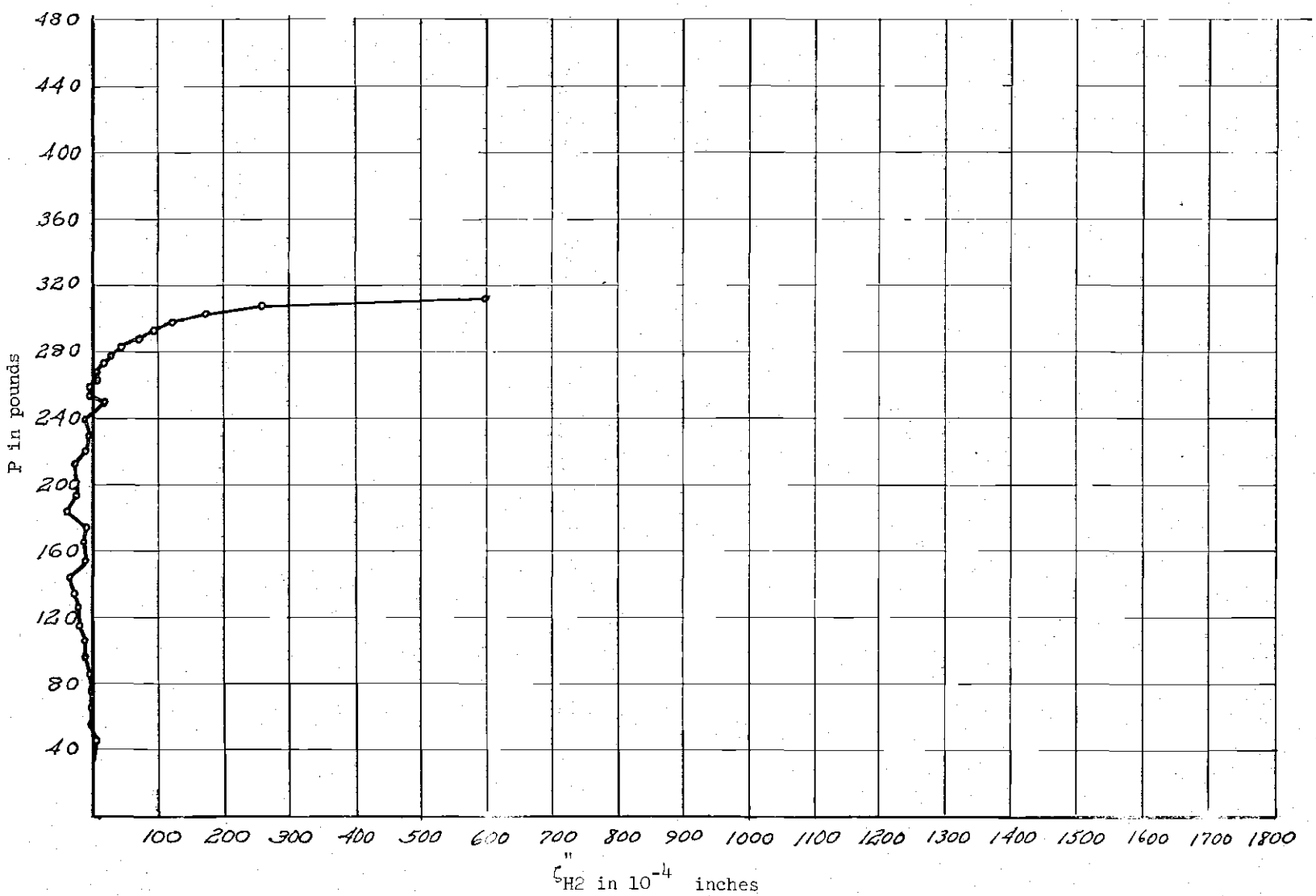

Figure 80. P versus ζ''_{H2} Curve for Test V

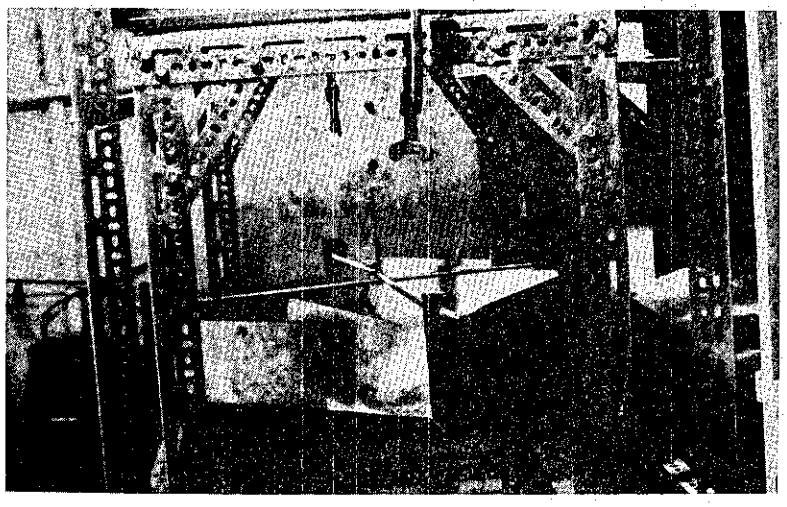

(a) Illustration of Cable Connections in Place

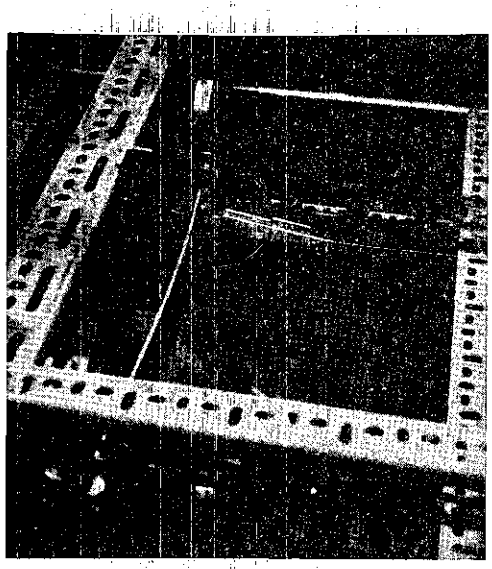

(b) Secondary Mode of Failure Observed in Test V

Figure 81. Model Beam Form (for Phosphorus Bronze)

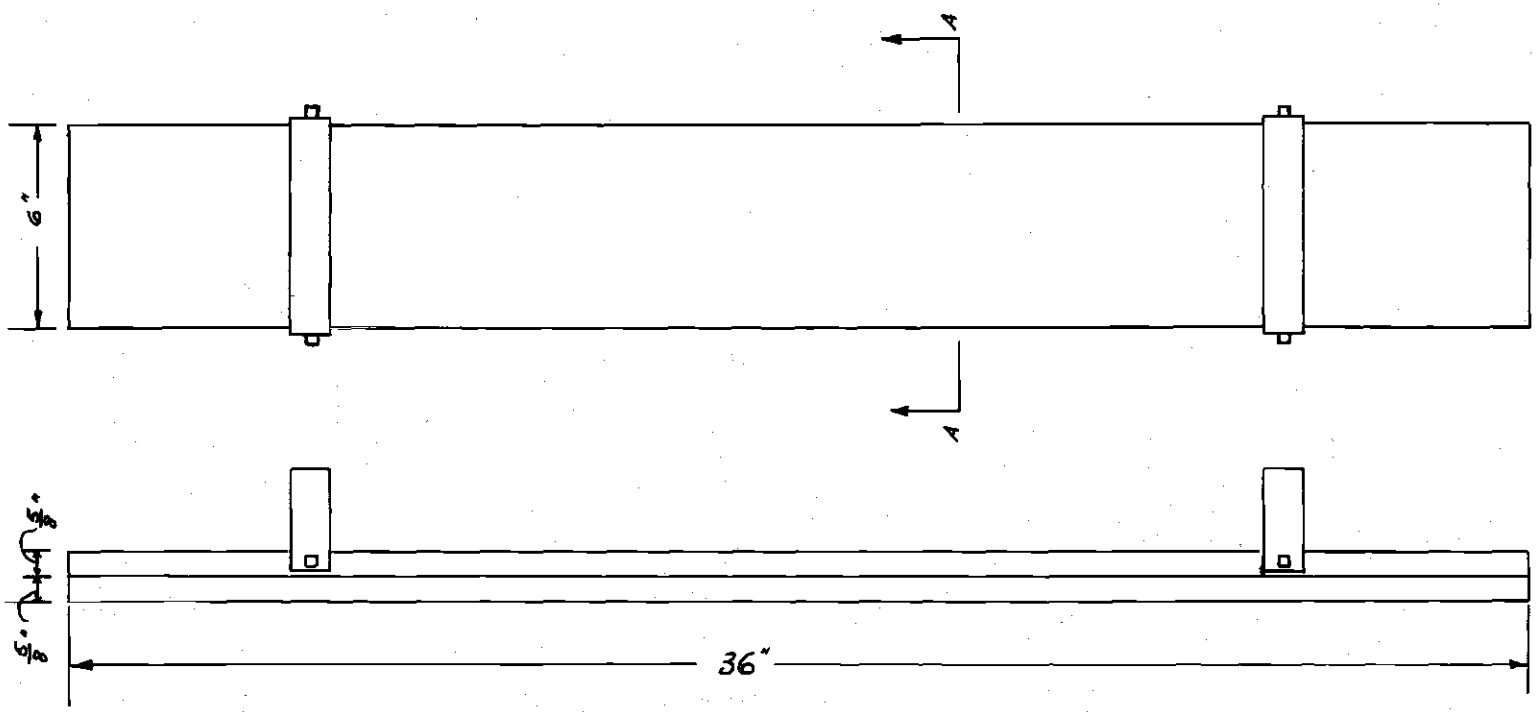

Figure 82. Model Beam Form

APPENDIX C

TABLES

Table 1. Data For Tensile Test 1

Load (Pounds)	Elongation (Inches)
0	0.00000
60	0.0002
80	0.00035
100	0.00048
120	0.00050
140	0.00052
160	0.00075
180	0.0009
220	0.0010
240	0.0012
260	0.0013
280	0.0015
300	0.0016
320	0.00175
340	0.00195
360	0.0021
380	0.0025
390	0.0036
396	0.0083
398	0.0110
400	0.0131
410	0.0169
420	0.0216

Table 2. Data For Tensile Test 2

Load (Pounds)	Elongation (Inches)	Load (Pounds)	Elongation (Inches)
0	0.00000	443	0.0263
20	0.0001	445	0.0271
40	0.00015	447	0.0283
60	0.002	448	0.0290
80	0.0003	450	0.0299
100	0.0004	451	0.0306
120	0.0005	453	0.0315
140	0.0006	454	0.0322
160	0.0007	455	0.0328
180	0.0008	457	0.0337
200	0.0009	460	0.0340
220	0.0010	465	0.0343
240	0.0011	468	0.0348
260	0.00125	470	0.0353
280	0.00135	473	0.0369
300	0.00145	475	0.0381
320	0.0016	478	0.0382
340	0.0017	480	0.0386
360	0.0018	483	0.0390
380	0.0020	485	0.0397
390	0.0024	487	0.0405
400	0.0069	488	0.0412
405	0.0103	490	0.0420
409	0.0119	491	0.0422
415	0.0142	492	0.0430
416	0.0149	493	0.0435
417	0.0155	495	0.0445
418	0.0159	498	0.0453
419	0.0164	499	0.0460
420	0.0169	500	0.0466
423	0.0183	501	0.0472
424	0.0190	502	0.0479
425	0.0195	504	0.0487
426	0.0199	505	0.0494
427	0.0204	507	0.0503
428	0.0210		
430	0.0223		
435	0.0227		
438	0.0235		
440	0.0245		

Table 3. Data For Tensile Test 3

Load (Pounds)	Elongation (Inches)
0	0.00000
20	0.0001
40	0.0015
60	0.0002
80	0.0003
100	0.00035
120	0.00045
140	0.0005
160	0.0006
180	0.0007
200	0.00085
220	0.0010
240	0.0012
260	0.00135
280	0.00155
300	0.00175
320	0.0021
360	0.0029
380	0.0037
390	0.0047
400	0.0066
405	0.0079
410	0.0090
415	0.0103
419	0.0120
425	0.0135
430	0.0147
435	0.0164
440	0.0190
445	0.0207
460	0.0217
465	0.0245
470	0.0270
475	0.0299
479	0.0323
490	0.0351
495	0.0379
500	0.0407
505	0.0413
508	0.0446

Table 4. Other Pertinent Information From The Tensile Tests

	Test 1	Test 2	Test 3
Initial Thickness of Coupon in.	0.0485	0.0502	0.0508
Final Thickness of Coupon (at point of failure) in.	------	0.0328	0.0345
Initial Neck Width of Coupon in.	0.5076	0.5025	0.493
Final Neck Width of Coupon (at point of failure) in.	------	0.3820	0.3780
Yield Load (P_y) Pounds	325	370	330
Yield Stress (f_y) PSI	13,000	15,070	13,800
ζ Yield in.	------	0.00185	------
Gage Length in.	2.00	2.00	2.00
ϵ Yield $\frac{\zeta \text{ Yield in}}{\text{Gage Length in}}$	0.000900	0.000925	0.000935
$E = \frac{\sigma_y}{\epsilon_y}$ PSI	14,450,000	16,300,00	15,200,000
Ultimate Load Pounds	------	1,130	1,150
Breaking Load Pounds	------	1,100	1,080

Table 5. Data For Test I(a)

Load Added (Pounds)	Total Load (Pounds)	ζ_V (Inches)	ζ_{HT} (Inches)	ζ_{HB} (Inches)
Load Pan	29	0.0000	0.0000	-0.0000
10.12	39.12	0.0020	0.0000	-0.0011
9.32	48.44	0.0035	0.0003	-0.0000
9.51	57.95	0.0050	0.0024	-0.0008
10.61	68.56	0.0070	0.0045	-0.0015
10.18	78.74	0.0090	0.0064	-0.0022
10.23	88.97	0.00115	0.0083	-0.0012
9.37	98.34	0.00130	0.0104	-0.0012
9.44	107.78	0.00155	0.0122	-0.0006
9.28	117.06	0.00175	0.0137	0.0003
9.49	126.55	0.00195	0.0183	0.0006
9.25	135.80	0.00215	0.0226	0.0012
10.15	145.95	0.00235	0.0267	0.0017
9.76	156.71	0.00257	0.0322	0.0031
9.55	166.26	0.00280	0.0382	0.0038
9.97	176.23	0.00305	0.0440	0.0048
9.96	186.19*	0.00335	0.0528	0.0097

Notes: 1. The horizontal gauges are 1.5" off the beam.
2. The vertical gauge is 1" off the beam.

* Buckling Load

Table 6. Data For Test I(b)

Load Applied (Pounds)	Total Load (Pounds)	ζ_V (Inches)	ζ_{HT} (Inches)	ζ_{HB} (Inches)
Load Pan	29.0	0.0000	0.0000	0.0000
10.04	39.04	0.0018	0.0008	0.0000
10.06	49.10	0.0034	0.0032	0.0000
10.44	59.54	0.0057	0.0082	0.0004
10.80	70.34	0.0069	0.0124	0.0008
9.33	70.67	0.0097	0.0165	0.0015
9.37	89.04	0.0117	0.0193	0.0020
10.21	99.25	0.0138	0.0256	0.0019
10.53	109.78	0.0158	0.0313	0.0031
10.14	119.92	0.0170	0.0395	0.0042
9.40	129.32	0.0190	0.0471	0.0056
9.43	138.75	0.0208	0.0596	0.0066
10.52	149.27	0.0226	0.0696	0.0073
9.76	158.03*	0.0244	0.0931	0.0093

Notes: 1. The horizontal gauges are 1.5" off the beam.
2. The vertical gauge is 1" off the beam.

* Buckling Load

Table 7. Data For Test I(c)

Load Added (Pounds)	Total Load (Pounds)	ζ_V (Inches)	ζ_{HT} (Inches)	ζ_{HB} (Inches)
Load Pan	29.0	0.0000	0.0000	0.0000
10.25	39.25	0.0012	0.0015	-0.0002
9.96	49.21	0.0030	0.0057	0.0001
9.50	58.71	0.0050	0.0091	0.0013
9.39	68.10	0.0067	0.0140	0.0007
10.08	78.18	0.0086	0.0193	0.0009
9.53	87.71	0.0104	0.0256	0.0019
10.08	97.79	0.0124	0.0306	0.0022
10.67	108.47	0.0150	0.0380	0.0015
10.61	119.07	0.0166	0.0404	0.0020
10.22	129.29	0.0186	0.0482	0.0033
10.04	139.33	0.0206	0.0556	0.0040
9.48	148.81*	0.0224	0.0862	0.0088

Notes: 1. The horizontal gauges are 1.5" off the beam.
2. The vertical gauges are 1" off the beam.

* Buckling Load

Table 8. Data For Test I(e)

Load Added (Pounds)	Total Load (Pounds)	ζ_V (Inches)	ζ_{HT} (Inches)	ζ_{HB} (Inches)
Pan + 4.50	34.50	0.0000	0.0000	0.0000
10.03	44.53	0.0017	0.0024	0.0009
10.01	54.54	0.0036	0.0041	0.0017
9.53	64.07	0.0055	0.0053	0.0025
10.19	74.26	0.0075	0.0081	0.0038
10.08	84.34	0.0095	0.0098	0.0050
9.86	94.20	0.0112	0.0106	0.0049
10.20	104.40	0.0129	0.0137	0.0061
9.23	113.63	0.0144	0.0146	0.0056
10.02	123.65	0.0160	0.0173	0.0050
9.59	133.24	0.0179	0.0193	0.0054
9.70	142.94	0.0195	0.0204	0.0054
10.78	153.22	0.0212	0.0228	0.0062
10.10	163.32	0.0233	0.0244	0.0069
9.32	172.64	0.0250	0.0263	0.0077
9.50	182.14	0.0267	0.0290	0.0113
4.70	186.84*	0.0285	0.0393	0.0170

Notes: 1. The horizontal gauges are 2" off the beam.
2. The vertical gauge is 1" off the beam

* Buckling Load

Table 9. Data For Test II (a)

Total Load (Pounds)	ζ_V (Inches)	ζ_{HT} (Inches)	ζ_{HB} (Inches)
34.50	0.0000	0.0000	0.0000
54.54	0.0047	0.0035	0.0010
74.26	0.0082	0.0068	0.0021
94.20	0.0112	0.0106	0.0033
113.63	0.0137	0.0142	0.0036
133.24	0.0170	0.0180	0.0033
153.22	0.0196	0.0217	0.0029
172.64	0.0216	0.0253	0.0025
182.14	0.0228	0.0270	0.0024
191.44	0.0239	0.0288	0.0021
200.85	0.0248	0.0306	0.0020
210.49	0.0258	0.0325	0.0017
219.49	0.0271	0.0343	0.0013
228.98	0.0278	0.0361	0.0011
233.54	0.0279	0.0371	0.0008
238.19	0.0285	0.0380	0.0004
240.12	0.0286	0.0385	0.0000
245.16	0.0294	0.0395	-0.0001
248.73	0.0291	0.0400	-0.0008
252.85	0.0278	0.0409	-0.0019
257.51	0.0252	------	-0.0030

Table 10. Data For Test II(b)

Total Load (Pounds)	ζ_V (Inches)	ζ_{HT} (Inches)	ζ_{HB} (Inches)
34.50	0.0000	0.0000	0.0000
54.54	0.0033	0.0046	0.0009
74.26	0.0068	0.0103	0.0021
94.20	0.0105	0.0140	0.0022
113.63	0.0142	0.0170	0.0027
133.24	0.0180	0.0201	0.0029
153.22	0.0217	0.0244	0.0021
172.64	0.0253	0.0286	0.0014
182.14	0.0270	0.0312	0.0011
191.44	0.0286	0.0336	0.0009
200.85	0.0304	0.0350	0.0010
210.24	0.0321	0.0372	0.0007
219.49	0.0339	0.0384	0.0007
228.98	0.0357	0.0427	0.0007
238.54	0.0374	0.0463	-0.0001
247.55	0.0393	0.0473	-0.0005
257.39	0.0412	0.0502	-0.0010
266.94	0.0430	0.0611	+0.0007

Table 11. Data For Test III(a)

Load Added (Pounds)	Total Load (Pounds)	ζ_V (Inches)	ζ_{HT} (Inches)	ζ_{HB} (Inches)
Pan + 4.50	34.50	0.0000	0.0000	0.0000
10.03	44.53	0.0018	0.0036	-0.0034
10.01	54.54	0.0038	0.0069	-0.0050
9.53	64.07	0.0055	0.0089	-0.0059
10.19	74.26	0.0072	0.0119	-0.0063
10.08	84.34	0.0090	0.0149	-0.0063
9.86	94.20	0.0108	0.0173	-0.0064
9.20	104.40	0.0129	0.0195	-0.0564
9.23	113.63	0.0145	0.0216	-0.0061
10.02	123.65	0.0165	0.0246	-0.0054
9.70	133.35	0.0185	0.0277	-0.0042
9.59	142.94	0.0200	0.0293	-0.0037
10.28	153.22	0.0220	0.0313	-0.0029
10.10	163.32	0.0240	0.0342	-0.0011
9.32	172.64	0.0255	0.0361	-0.0005
9.50	182.14	0.0273	0.0387	+0.0004
4.70	186.84	0.0281	0.0405	+0.0016
4.60	191.44	0.0290	0.0410	+0.0017
4.57	196.01	0.0299	0.0419	+0.0021
4.84	200.84	0.0309	0.0431	+0.0025
4.67	206.71	0.0315	0.0461	+0.0044
4.58	210.49	0.0325	0.0481	+0.0065
4.67	215.16	0.0330	0.0488	+0.0067
4.58	219.74	0.0340	0.0498	+0.0072
4.73	224.47	0.0350	0.0508	+0.0075
4.76	229.23	0.0360	0.0539	+0.0085
4.65	233.88	0.0368	0.0550	+0.0090
4.56	238.44	0.0378	0.0563	+0.0096
4.67	243.11	0.0381	0.0571	+0.0098
4.74	247.83	0.0395	0.0586	+0.0107
4.69	252.54	0.0405	0.0608	+0.0118
4.61	257.15	0.0415	0.0616	+0.0121

Table 12. Data For Test III(b)

Total Load (Pound)	ζ_V (Inches)	ζ_{HT} (Inches)	ζ_{HB} (Inches)
34.50	0.0000	0.0000	0.0000
44.53	0.0018	0.0032	-0.0018
54.54	0.0036	0.0066	-0.0027
64.07	0.0053	0.0106	-0.0028
74.26	0.0069	0.0127	-0.0038
84.34	0.0088	0.0160	-0.0033
94.20	0.0106	0.0194	-0.0025
104.40	0.0128	0.0213	-0.0024
113.63	0.0142	0.0256	-0.0005
123.65	0.0158	0.0278	+0.0001
133.24	0.0173	0.0308	+0.0016
142.94	0.0188	0.0330	+0.0024
153.22	0.0208	0.0358	+0.0037
163.32	0.0227	0.0391	+0.0054
172.64	0.0244	0.0421	0.0070
182.14	0.0262	0.0450	0.0087
191.44	0.0278	0.0472	0.0097
200.85	0.0276	0.0499	0.0114
210.24	0.0312	0.0520	0.0127
219.49	0.0328	0.0546	0.0138
228.98	0.0348	0.0581	0.0158
238.54	0.0358	0.0619	0.0182
247.55	0.0378	0.0637	0.0182
257.39	0.0398	0.0668	0.0207
266.94	0.0418	0.0694	0.0218
277.68	0.0438	0.0755	0.0254
287.00	0.0458	0.0791	0.0275
297.00	0.0478	0.0867	0.0317
307.04	0.0494	0.0936	0.0361
317.56	0.0516	0.1009	0.0406
326.09	0.0526	0.1022	0.0476

Table 13. Data For Test III(c)

Total Load	ζ_V (Inches)	ζ_{HT} (Inches)	ζ_{HB} (Inches)
34.50	0.0000	0.0000	0.0000
44.53	0.0017	0.0044	-0.0014
54.54	0.0035	0.0079	-0.0025
64.07	0.0053	0.0103	-0.0031
74.26	0.0071	0.0143	-0.0015
84.34	0.0089	0.0172	-0.0019
94.20	0.0105	0.0204	-0.0009
104.40	0.0125	0.0235	+0.0003
113.63	0.0145	0.0271	0.0025
123.65	0.0160	0.0298	0.0034
133.24	0.0177	0.0330	0.0050
142.94	0.0194	0.0363	0.0067
153.22	0.0213	0.0382	0.0076
163.32	0.0231	0.0416	0.0092
172.64	0.0248	0.0438	0.0104
182.14	0.0265	0.0447	0.0104
191.44	0.0282	0.0479	0.0124
200.85	0.0297	0.0504	0.0139
210.24	0.0316	0.0530	0.0156
219.49	0.0333	0.0562	0.0174
228.98	0.0350	0.0586	0.0188

Table 14. Data For Test IV(d)

Total Load	ζ_v (Inches)	ζ_{HT} (Inches)	ζ_{HB} (Inches)	ζ_{v1} (Inches)	ζ_{v2} (Inches)
34.50	0.0000	0.0000	0.0000	0.0000	0.0000
84.34	0.0087	-0.0020	0.0013	0.0024	0.0018
104.40	0.0123	+0.0036	0.0033	0.0036	0.0030
123.65	0.0157	0.0094	0.0061	0.0062	0.0048
142.94	0.0196	0.0155	0.0092	0.0065	0.0058
163.32	0.0234	0.0209	0.0128	0.0082	0.0068
172.64	0.0250	0.0233	0.0132	0.0083	0.0076
182.14	0.0268	0.0267	0.0172	0.0089	0.0080
191.44	0.0285	0.0302	0.0184	0.0092	0.0088
200.85	0.0303	0.0329	0.0201	0.0069	0.0090
210.24	0.0318	0.0369	0.0228	0.0112	0.0098
219.49	0.0335	0.0403	0.0249	0.0112	0.0106
228.98	0.0353	0.0431	0.0266	0.0122	0.0108
238.54	0.0367	0.0470	0.0291	0.0137	0.0118
247.55	0.0386	0.0512	0.0320	0.0159	0.0127
257.39	0.0405	0.0539	0.0335	0.0159	0.0130
266.94	0.0424	0.0570	0.0355	0.0160	0.0138
277.68	0.0443	0.0630	0.0395	0.0172	0.0150

Table 15. Data For Test III(e)

Total Load	ζ_v (Inches)	ζ_{HT} (Inches)	ζ_{HB} (Inches)	ζ_{v1} (Inches)	ζ_{v2} (Inches)
34.50	0.0000	0.0000	0.0000	0.0000	0.0000
54.54	0.0037	-0.0026	+0.0006	0.0016	0.0007
84.34	0.0096	-0.0048	-0.0006	0.0028	0.0026
133.24	0.0190	-0.0065	-0.0028	0.0050	0.0059
153.22	0.0230	-0.0072	-0.0035	0.0062	0.0074
172.64	0.0266	-0.0080	-0.0044	0.0074	0.0085
191.44	0.0301	-0.0080	-0.0051	0.0084	0.0092
210.24	0.0337	-0.0077	-0.0061	0.0093	0.0105
228.98	0.0373	-0.0077	-0.0063	0.0104	0.0127
247.55	0.0409	-0.0078	-0.0069	0.0112	0.0141
266.94	0.0445	-0.0077	-0.0073	0.0126	0.0153
286.98	0.0485	-0.0068	-0.0078	0.0142	0.0170
307.60	0.0527	-0.0058	-0.0075	0.0161	0.0185
318.12	0.0547	-0.0056	-0.0078	0.0169	0.0193
327.65	0.0565	0.0054	-0.0083	0.0176	0.0211
337.64	0.0585	-0.0055	-0.0088	0.0192	0.0218
347.84	0.0605	-0.0054	-0.0088	0.0202	0.0224
357.51	0.0625	0.0031	-0.0083	0.0222	0.0235
362.35	0.0632	-0.0030	-0.0081	0.0225	0.0240
367.03	0.0643	-0.0035	-0.0081	0.0227	0.0243
371.82	0.0652	-0.0031	-0.0087	0.0232	0.0245
376.49	0.0662	-0.0016	-0.0087	0.0235	0.0253
381.20	0.0672	-0.0012	-0.0084	0.0237	0.0255
385.78	0.0682	-0.0005	-0.0074	0.0247	0.0259
390.49	0.0692	+0.0001	-0.0067	0.0246	0.0262
395.25	0.0703	+0.0015	-0.0064	0.0251	0.0265
399.93	0.0712	+0.0032	-0.0049	0.0258	0.0269
404.74	0.0722	+0.0032	-0.0051	0.0261	0.0273
409.49	0.0732	+0.0037	-0.0055	0.0261	0.0278
414.25	0.0742	+0.0042	-0.0051	0.0266	0.0282
418.99	0.0752	+0.0041	-0.0053	0.0266	0.0288
424.29	0.0763	+0.0039	-0.0061	0.0269	0.0294
428.83	0.0773	+0.0055	-0.0058	0.0276	0.0298
433.57	0.0783	+0.0065	-0.0066	0.0277	0.0302
438.12	0.0793	+0.0065	-0.0055	0.0280	0.0305
442.46	0.0803	+0.0070	-0.0051	0.0283	0.0310
447.35	0.0814	+0.0076	-0.0048	0.0287	0.0311
452.47	0.0826	+0.0141	-0.0025	0.0290	0.0321
456.70	0.0836	+0.0171	-0.0003	0.0287	0.0327
461.11	0.0849	+0.0213	+0.0021	0.0295	0.0335
465.74	0.0863	+0.0250	+0.0036	0.0300	0.0341
470.53	0.0885	+0.0350	+0.0106	0.0310	0.0362
475.04	0.0904	+0.0624	+0.0244	0.0322	0.0375
477.27	0.0924	+0.0988	+0.0413	0.0322	0.0381

Table 16. Data For Test IV(a)

Load Added	Total Load	ζ_v (Inches)	ζ_{H1} (Inches)	ζ_{H2} (Inches)	ζ_{v1} (Inches)	ζ_{v2} (Inches)
Pan + 4.50	34.50	0.0000	0.0000	0.0000	0.0000	0.0000
10.03	44.53	0.0020	0.0003	-0.0001	0.0004	0.0001
10.01	54.54	0.0044	0.0002	-0.0007	0.0010	0.0006
9.53	64.07	0.0068	0.0013	-0.0001	0.0016	0.00011
10.19	74.26	0.0094	0.0027	+0.0008	0.0024	0.0014
10.08	84.34	0.0019	0.0040	0.0014	0.0031	0.0021
9.86	94.20	0.0144	0.0079	0.0042	0.0038	0.0023
10.20	104.40	0.0169	0.0141	0.0089	0.0045	0.0029
9.23	113.63	0.0190	0.0181	0.0123	0.0052	0.0032
5.33	118.96	0.0204	0.0335	0.0153	0.0056	0.0033
4.69	123.65	0.0216	0.0353	0.0166	0.0060	0.0036
9.59	133.24	0.0242	0.0375	0.0181	0.0067	0.0041
9.70	142.94	0.0277	0.0475	0.0255	0.0084	0.0043
10.28	153.22	0.0303	0.0560	0.0315	0.0091	0.0049
5.43	158.65	0.0313	0.0679	0.0420	0.0093	0.0050
4.67	163.32	0.0331	0.0739	0.0468	0.0097	0.0051
4.53	167.85	0.0341	0.0853	0.0553	0.0098	0.0052
4.79	172.64	0.0351	0.0973	0.0641	0.0101	0.0062
4.67	177.31*	0.0371	0.1220	0.0800	------	0.0063

* Buckling Load

Table 17. Data For Test IV(b)

Load Added	Total Load	ζ_v (Inches)	ζ_{H1} (Inches)	ζ_{H2} (Inches)	ζ_{v1} (Inches)	ζ_{v2} (Inches)
Pan + 4.50	34.50	0.0000	0.0000	0.0000	0.0000	0.0000
10.03	44.53	0.0022	0.0124	0.0125	0.0003	0.0002
10.01	54.54	0.0048	0.0240	0.0201	0.0012	0.0009
9.53	64.07	0.0079	0.0380	0.0301	0.0021	0.0012
5.40	69.47	0.0085	0.0581	0.0514	0.0025	0.0019
4.79	74.26	0.0099	0.0705	0.0595	0.0029	0.0020
5.51	79.77	0.0111	0.0980	0.0727	0.0033	0.0021
4.58	84.34	0.0129	0.1278	0.1000	0.0038	0.0030
5.23	89.57	0.0149	0.1603	0.1245	0.0042	0.0031
4.63	94.20	0.0168	0.1645	0.1274	0.0050	0.0033
5.50	99.70	0.0193	0.1756	0.1338	0.0052	0.0038
4.70	104.40	0.0218	0.1819	0.1416	0.0060	0.0039
4.71	109.11	0.0238	0.1954	0.1494	0.0067	0.0040
4.52	113.63	0.0247	0.2069	0.1587	0.0070	0.0041
4.69	118.32	0.0260	0.2387	0.1810	0.0072	0.0041
5.33	123.65*	------	0.3675	0.280	0.0075	0.0045

* Buckling Load

Table 18. Data For Test IV(c)

Load Added	Total Load	ζ_v (Inches)	ζ_{H1} (Inches)	ζ_{H2} (Inches)	ζ_{v1} (Inches)	ζ_{v2} (Inches)
Pan + 4.50	34.50	0.0000	0.0000	0.0000	0.0000	0.0000
10.03	44.53	0.0021	0.0017	0.0009	0.0008	0.0002
10.01	54.54	0.0043	0.0020	0.0009	0.0016	0.0008
4.74	59.28	0.0060	0.0065	0.0047	0.0020	0.0010
4.79	64.07	0.0067	0.0058	0.0032	0.0023	0.0011
4.79	68.86	0.0082	0.0086	0.0066	0.0028	0.0015
5.40	74.26	0.0092	0.0141	0.0095	0.0033	0.0018
5.51	79.77	0.0107	0.0186	0.0125	0.0038	0.0020
4.57	84.34	0.0113	0.0206	0.0142	0.0041	0.0021
5.23	89.57	0.0128	0.0531	0.0379	0.0045	0.0027
4.63	94.20	0.0137	0.0534	0.0361	0.0050	0.0030
4.70	98.90	0.0148	0.0542	0.0367	0.0053	0.0030
4.50	104.40	0.0162	0.0568	0.0387	0.0058	0.0035
4.52	108.92	0.0178	0.0953	0.0558	0.0062	0.0040
4.71	113.63	0.0192	0.1227	0.0762	0.0068	0.0041
2.23	115.86	0.0207	0.1305	0.0817	0.0070	0.0041
4.69	120.55*	0.0227	0.1992	0.1100	0.0075	0.0045

* Buckling Load

Table 19. Data For Test IV(d)

Load Applied	Total Load	ζ_v (Inches)	ζ_{H1} (Inches)	ζ_{H2} (Inches)	ζ_{v1} (Inches)	ζ_{v2} (Inches
Pan + 4.50	34.50	0.0000	0.0000	0.0000	0.0000	0.0000
10.03	44.53	0.0021	0.0020	0.0011	0.0007	0.0002
10.01	54.54	0.0044	0.0040	0.0023	0.0014	0.0005
9.53	64.07	0.0069	0.0050	0.0029	0.0018	0.0011
10.19	74.26	0.0094	0.0097	0.0055	0.0025	0.0014
10.08	84.34	0.0119	0.0118	0.0066	0.0033	0.0022
9.86	94.20	0.0141	0.0122	0.0066	0.0040	0.0024
4.70	98.90	0.0151	0.0161	0.0097	0.0043	0.0027
5.50	104.40	0.0166	0.0178	0.0109	0.0047	0.0031
4.71	109.11	0.0177	0.0198	0.0120	0.0050	0.0035
4.52	113.63	0.0187	0.0203	0.0122	0.0052	0.0038
4.69	118.32	0.0197	0.0225	0.0136	0.0055	0.0039
5.33	123.65	0.0207	0.0286	0.0179	0.0060	0.0040
4.81	128.46	0.0219	0.0324	0.0208	0.0062	0.0042
4.78	133.24	0.0232	0.0347	0.0222	0.0065	0.0045
4.85	138.09	0.0244	0.0367	0.0226	0.0070	0.0049
4.85	142.94	0.0258	0.0437	0.0289	0.0072	0.0050
4.74	147.68	0.0271	0.0485	0.0323	0.0075	0.0052
5.54	153.22	0.0286	0.0602	0.0411	0.0081	0.0057
4.67	157.89	0.0295	0.0682	0.0471	0.0083	0.0060
5.43	163.32	0.0308	0.0813	0.0572	0.0089	0.0061
4.79	168.11	0.0315	0.0923	0.0652	0.0093	0.0063
4.53	172.64	------	0.1200	0.0800	------	------

* Buckling Load

Table 20. Data For Test V

Load Applied	Total Load	ζ_v (Inches)	ζ_{HT} (Inches)	ζ_{HB} (Inches)	ζ_{v1} (Inches)	ζ_{v2} (Inches)	ζ_{HT} (Inches)	ζ_{HB} (Inches)
Pan + 4.50	34.50	0.0000	0.0000	0.0000	0.0000	0.0000	0.0000	0.0000
10.03	44.53	0.0024	0.0019	0.0026	0.0009	0.0002	0.0019	0.0001
10.01	54.54	0.0050	0.0038	0.0044	0.0018	0.0002	0.0037	-0.0003
9.53	64.07	0.0072	0.0038	0.0061	0.0026	0.0010	0.0056	-0.0003
10.19	74.26	0.0094	0.0038	0.0072	0.0036	0.0012	0.0073	-0.0004
10.08	84.34	0.0117	0.0039	0.0084	0.0045	0.00157	0.0090	-0.0007
9.86	94.20	0.0140	0.0040	0.0092	0.0055	0.00202	0.0094	-0.0015
10.20	104.40	0.0162	0.0042	0.0104	0.0061	0.00246	0.0111	-0.0015
9.23	113.63	0.0183	0.0042	0.0111	0.0070	0.00302	0.0117	-0.0022
10.02	123.65	0.0204	0.0040	0.0117	0.0078	0.00313	0.0130	-0.0025
9.59	133.24	0.0231	0.0041	0.0124	0.0088	0.0039	0.0133	-0.0030
9.70	142.94	0.0252	0.0041	0.0129	0.0097	0.0041	0.0135	-0.0039
10.28	153.22	0.0273	0.0039	0.0115	0.0109	0.0048	0.0153	-0.0015
10.10	163.32	0.0300	0.0036	0.0128	0.0117	0.0052	0.0174	-0.0018
9.32	172.64	0.0320	0.0037	0.0125	0.0126	0.0057	0.0179	-0.0011
9.50	182.14	0.0342	0.0038	0.0162	0.0136	0.0062	0.0194	-0.0043
9.30	191.44	0.0369	0.0044	0.0166	0.0146	0.0068	0.0215	-0.0029
9.45	200.85	0.0391	0.0047	0.0173	0.0155	0.0072	0.0229	-0.0029
9.39	210.24	0.0413	0.0047	0.0177	0.0163	0.0077	0.0234	-0.0031

Table 20. Continued

Load Applied	Total Load	ζ_V (Inches)	ζ_{HT} (Inches)	ζ_{HB} (Inches)	ζ_{V1} (Inches)	ζ_{V2} (Inches)	ζ_{HT} (Inches)	ζ_{HB} (Inches)
9.25	219.49	0.0434	0.0051	0.0179	0.0170	0.0077	0.0256	-0.0017
9.49	228.98	0.0457	0.0055	0.0183	0.0180	0.0086	0.0273	-0.0009
9.21	238.54	0.0480	0.0063	0.0201	0.0188	0.0091	0.0292	-0.0014
9.36	247.55	0.0503	0.0070	0.0195	0.0197	0.0093	0.0320	+0.0016
5.18	252.73	0.0517	0.0086	0.0232	0.0203	0.0098	0.0334	-0.0005
4.66	257.39	0.0528	0.0091	0.0238	0.0208	0.0100	0.0343	-0.0006
4.78	262.17	0.0540	0.0098	0.0245	0.0215	0.0162	0.0366	+0.0005
4.77	266.94	0.0552	0.0112	0.0258	0.0218	0.0102	0.0376	+0.0005
5.45	272.39	0.0564	0.0130	0.0271	0.0223	0.0105	0.0403	+0.0016
5.29	277.68	0.0576	0.0134	0.0270	0.0227	0.0107	0.0416	+0.0026
4.69	282.37	0.0588	0.0170	0.0297	0.0233	0.0111	0.0454	+0.0041
4.61	286.98	0.0600	0.0225	0.0334	0.0238	0.0112	0.0513	+0.0070
5.21	292.19	0.0611	0.0266	0.0359	0.0243	0.00112	0.0561	0.0094
5.37	297.56	0.0623	0.0321	0.0398	0.0248	0.00114	0.0617	0.0121
4.83	302.39	0.0638	0.0406	0.0452	0.0254	0.00117	0.0712	0.0171
5.21	307.60	0.0653	0.0575	0.0552	0.0259	0.00119	0.0868	0.0255
4.78	312.38	------	0.1200	0.0800	------	------	0.1200	0.0600

BIBLIOGRAPHY

LITERATURE CITED

(1) Timoshenko, S., Elastic Stability, Chapter V, Mcgraw - Hill Book Co., Inc., 1936.

(2) Lyse, I., and Johnson, B. G., "Structural Beams in Torsion," Transactions American Society of Civil Engineers, pp 857-944, 1936.

(3) Goodier, J. N., "Torsional and Flexural Buckling of Bars of Thin Walled Opened Section Under Compressive and Pending Loads." Journal of Aeronautical Science, 2, A-35, 1944

(4) Winter, G., "Strength of Slender Beams," Transactions American Society of Civil Engineers, pp. 109, 1321, 1944

(5) Nylander, H. "Lateral Buckling of I-Beams of Monosymmetrical Cross Section," (in Swedish), Tekniska Skrifter, p. 111 Stockholar, 1944

(6) Pelterson, O., "Combined Bending and Torsion of Simply Supported Beams of Bisymmetrical Cross Section," Transactions, Royal Institute of Technology, p. 29, Stockholar, Sweden.

(7) Flint, A. R., "The Influence of Restraints on the Stability of Beam," The Structural Engineer, September, 1951 pp. 235-246

(8) Sergev, S. and Moore, P. J., "Effect of Elastic Lateral Support Upon the Buckling Load on Beams," Trend, January, 1963

(9) Schmidt, L. C., "Restraints Against Elastic Lateral Buckling," Proceedings, American Society of Civil Engineers EM6, 4561, December, 1965.

(10) Biggs, J. M., "Buckling Considerations in the Design of Steel Beams and Plate Girders," Journal, Boston Society of Civil Engineers, Volume 41, 1954.

(11) Clark, J. W., and Hill, H. N., "Lateral Buckling of Beams," Proceed A.S.C.E., ST 7, July 1960.

(12) Clark, J. W., and Jombock, J. R., Jr., "Lateral Buckling of I-Beams Subjected to Unequal End Moments," Proceedings A.S.C.E. EM3, July, 1957.